THE UNIVERSITY OF MICHIGAN

COLLEGE OF ENGINEERING

Department of Naval Architecture and Marine Engineering

Final Report

# PROJECT MOHOLE PERFORMANCE TESTS:

## Wake Surveys and Flow Studies
## Main Propulsion Propeller Open Water Tests

J. C. Gebhardt
F. C. Michelsen

ORA Project 07833

under contract with:

BROWN AND ROOT, INC.
HOUSTON, TEXAS

administered through:

OFFICE OF RESEARCH ADMINISTRATION ANN ARBOR

July 1966

Engm
UMR
1526

TABLE OF CONTENTS

## LIST OF FIGURES

# 1. INTRODUCTION

The following is a documentation of various performance tests carried out on a scale model (scale ratio, 27.5) of one hull of the Mohole Drilling Platform. The model was built to Brown and Root Inc. Drawing Number 1-T-10004 (Figure 1.1). Details of construction are described in Reference 1.

Also included in this report are the results of comprehensive open water tests of the main propulsion propellers for the Mohole vehicle. The model propeller was built in accordance with Robert Taggart Inc. Drawing Number RT-14503 to the same scale ratio as that of the platform.

The test program completed to date and discussed in more detail below may be described in outline as follows:

1.1 Three Dimensional Wake Surveys.

a) At the 29' draft (transit condition) at a full scale speed of 10 knots, five hole pitot tube measurements were taken in a transverse plane coinciding with the propeller plane of the starboard hull. From the pressure measurements the cartesian components of the velocity were calculated at selected points in and about the propeller disc.

b) At the 65' draft and a ship speed of 4 knots, attempts were made to obtain conventional wake survey data as in (a) above, but due to the large scale fluctuations of velocity in the area of the propeller plane meaningful data was unobtainable. However, some data was obtained which gives an indication of the magnitude of the large scale variations encountered.

1.2 Open Water Propeller Tests.

Open water tests were performed with the five bladed main propulsion propeller. The performance of the propeller was completely characterized by measuring both the torque and thrust at various RPM's, both positive and negative, while running the propeller at different speeds ahead and astern.

1.3 Flow Studies.

Both movies and still pictures were taken of the flow around the stern of the starboard hull. The streamlines close to the hull were made visible by using cellulose streamers and yarn tufts cemented to the hull surface. The pictures and movies disclosed large areas of disturbed, time dependent flow behind the aft vertical cylinder and near the free surface.

1.4 Resistance and Propulsion Tests.

Unsuccessful attempts were made to measure the forces acting on the starboard hull with and without the propeller running. It was found that due to large, low frequency variations in the hydrodynamic forces on the hull, it would be necessary to measure these forces as a function of time. However, the dynamometry, which had been assembled for the testing program, proving inadequate in recording these forces with a sufficient degree of confidence. The main reason for this was the deflections of dynamometer components when subjected to the loads. These deflections were not large in themselves but still did allow the model to assume oscillatory motions in several degrees of freedom of sufficient magnitude to be suspect of influencing the force measurements. The dynamometers have been re-designed to adequately handle the problem, but new tests have not been made as yet.

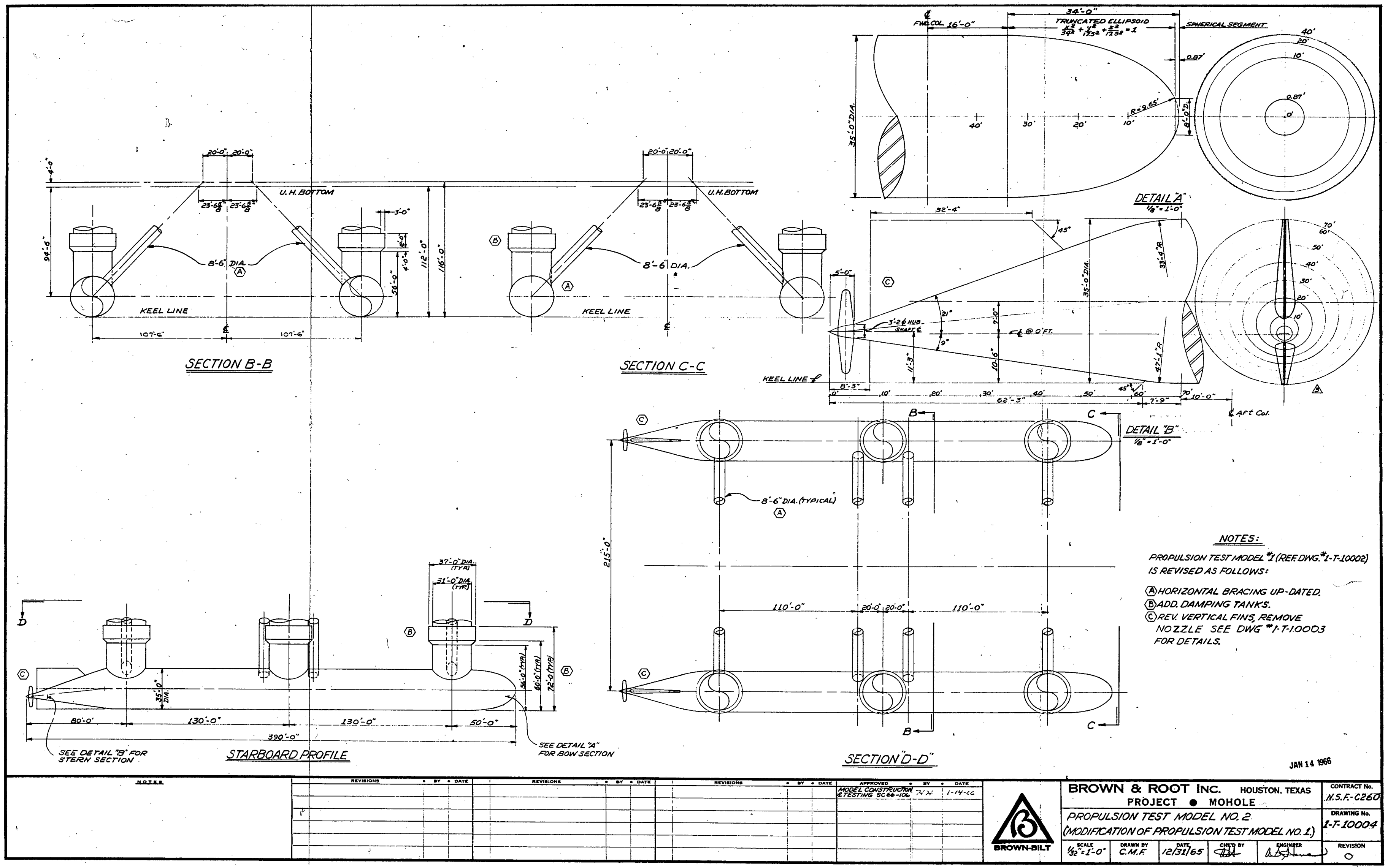


Figure 1.1
Project Mohole Drilling Platform.

## 2. THREE DIMENSIONAL WAKE SURVEYS

### 2.1 Instrumentation and Analysis.

The three dimensional wake velocity surveys were performed on the starboard hull of the Mohole vehicle utilizing a five hole spherical pitot tube with four electronic pressure transducers as pressure sensing elements. The spherical tip of the pitot tube was positioned in a transverse vertical plane corresponding to the plane of the propeller. During each data run the tube was moved horizontally at a slow steady speed at a fixed depth and the pressures were recorded continuously on magnetic tape. A voltage proportional to the distance of the pitot tube from the centerline of the hull was also recorded. From the recorded pressures, together with the calibration curves for the pitot tube the velocity components in the propeller plane were calculated. Details on the pitot tube and its use are given in Reference (2). A wake survey at the drilling depth of 65' and a ship speed of 6 knots was attempted but was for the most part abandoned because the time variations of the pressures were too large. In the majority of test runs they were measured to be at least as large as the mean pressure. However, the pressures at one location were recorded as a function of time and digitized electronically at a sampling rate of 20 data points per second. The velocity components at each sampled point were calculated and plotted versus time. Reference (3) describes the recording and digitizing techniques which were used.

### 2.2 Wake Survey Results; 29' Draft, 10 Knots Ship Speed.

In Figures 2.2.1, 2.2.2 and 2.2.3 the u, v and w components of the velocity are plotted nondimensionally as a fraction of the ship speed versus y, with z as a parameter. The coordinate y is measured horizontally from the centerline of the model with positive y to starboard while z is measured vertically downward from the free surface. The sign conventions for u, v and w are shown in Figure 2.2.7. Figures 2.2.4, 2.2.5 and 2.2.6 are essentially the same as Figures 2.2.1, 2.2.2 and 2.2.3 except that the curves have been separated vertically such that the origin of each curve corresponds to the depth below the free surface which it represents.

Note that the data points are connected by straight lines. This was done because it would be virtually impossible and not even desirable to draw fair curves through the data. Since both time and space velocity variations are present in the wake the only way to completely characterize the wake would be to record data with the pitot tube fixed in space at many points behind the model so that the time variations could be analyzed statistically at each spatial point. This would be very time consuming and costly and probably no more informative than the data presented here which was taken with the tube moving in both space and time simultaneously. By moving in both space and time together the "noise" in the data, while it appears to be due to space variations alone, is actually a combination of space and time fluctuations. Recognized as such the "noise" in the wake data as presented herein is meaningful as an indicator of the time variations which are present.

### 2.3 Wake Survey Results; 65' Draft, 0 Degrees Heading, 6 Knot Ship Speed.

As mentioned earlier, a complete wake survey at 65' draft was not practical due to the large velocity fluctuations present in the wake. Figure 2.3.1 shows the results of the one specific test which was completed. The pitot tube was positioned 2.70" to port of the centerline and 1.60" below the propeller shaft of the model, and the time variations in the velocities were determined. Figure 2.3.1 shows u, v and w plotted against time. Since the time variations are much greater than mean values, a conventional wake survey would be of little value and virtually impossible to accomplish.

As a last attempt to obtain reliable wake data in the drilling condition, the propeller was replaced by low inertia wake wheels of various radii. The results of this study only confirmed the original conclusion that a wake survey in the normal sense is meaningless. The movie which is a part of this report shows that the wake wheels actually reversed direction on occasion, and rotated very irregularly. In fact, their motion was so irregular that no reliable mean values or angular speed could be obtained.

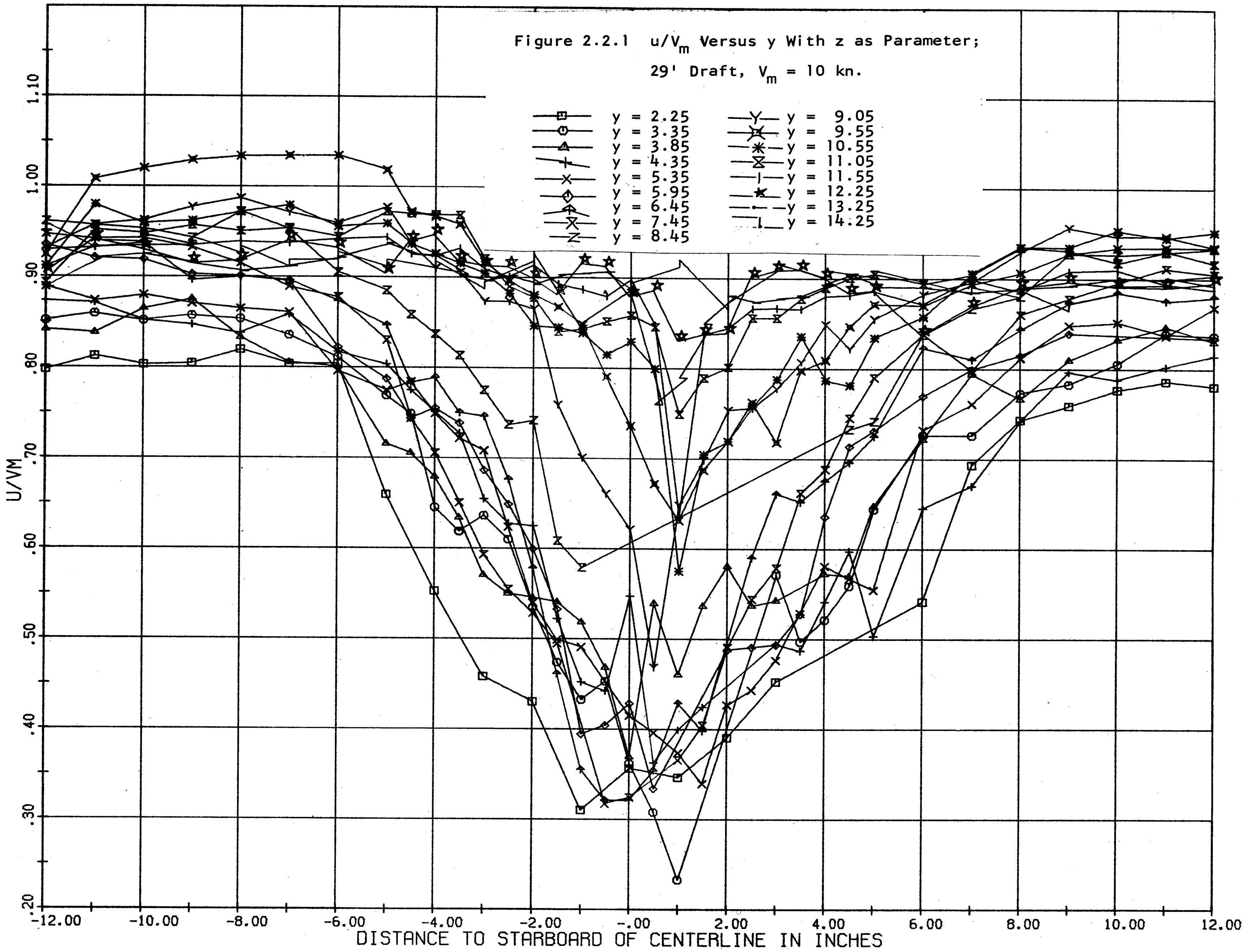


Figure 2.2.1 $u/V_m$ Versus y With z as Parameter; 29' Draft, $V_m$ = 10 kn.

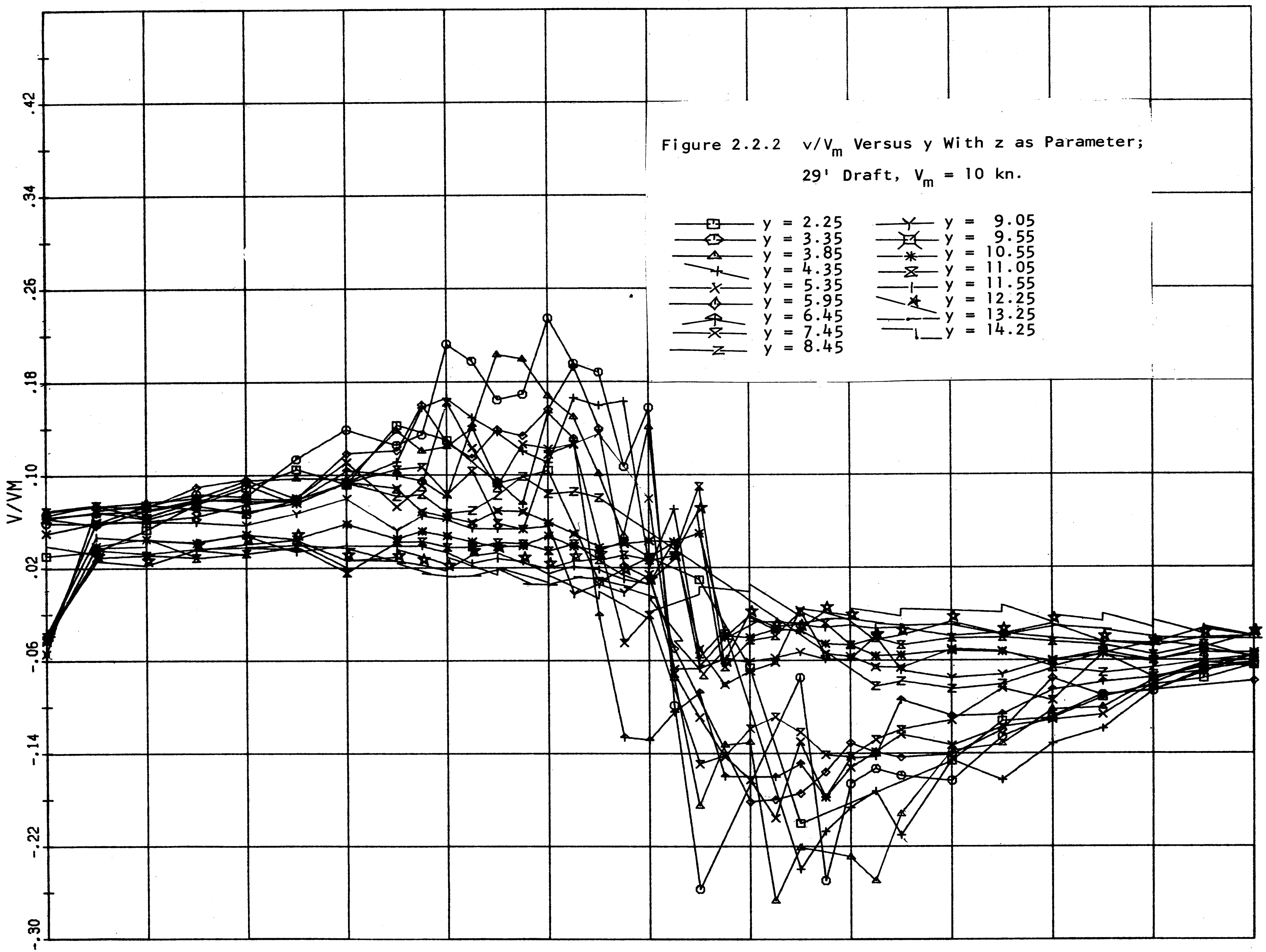


Figure 2.2.2 $v/V_m$ Versus y With z as Parameter; 29' Draft, $V_m$ = 10 kn.

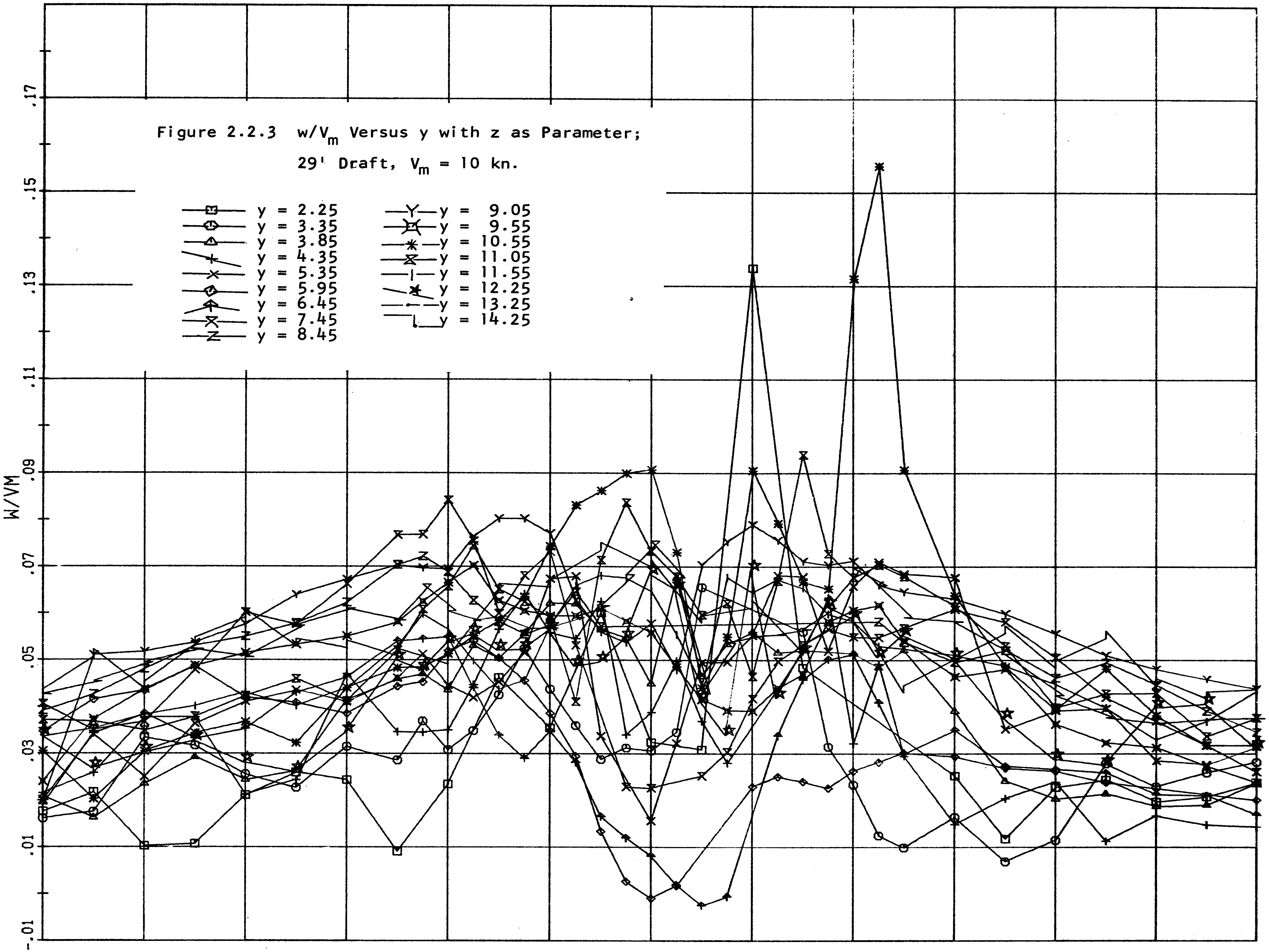


Figure 2.2.3 $w/V_m$ Versus y with z as Parameter; 29' Draft, $V_m$ = 10 kn.

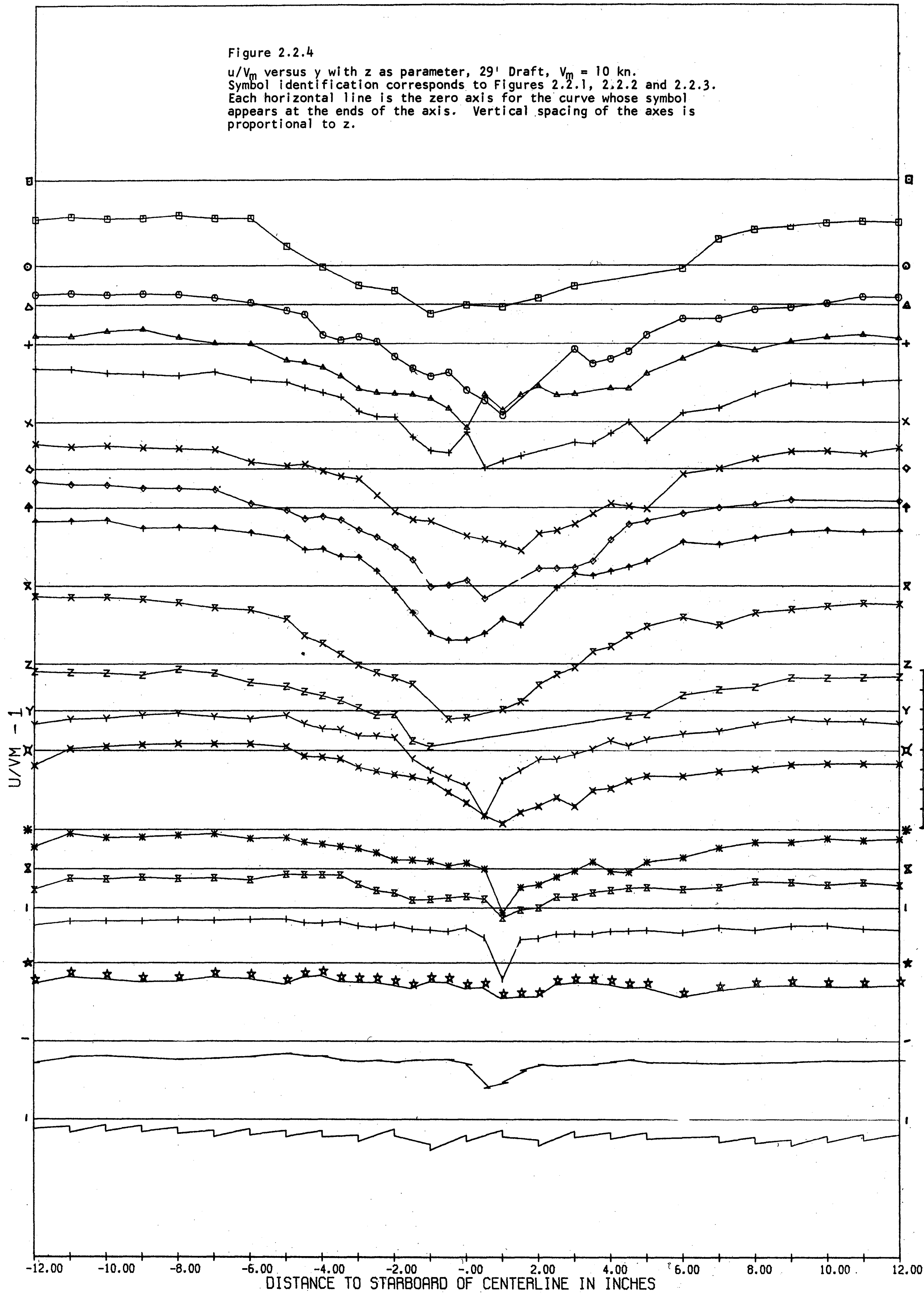
Figure 2.2.4
u/$V_m$ versus y with z as parameter, 29' Draft, $V_m$ = 10 kn.
Symbol identification corresponds to Figures 2.2.1, 2.2.2 and 2.2.3.
Each horizontal line is the zero axis for the curve whose symbol appears at the ends of the axis. Vertical spacing of the axes is proportional to z.
U/VM - 1
0 .1 .2 .3 .4 .5 .6 .7 .8
-12.00 -10.00 -8.00 -6.00 -4.00 -2.00 -.00 2.00 4.00 6.00 8.00 10.00 12.00
DISTANCE TO STARBOARD OF CENTERLINE IN INCHES

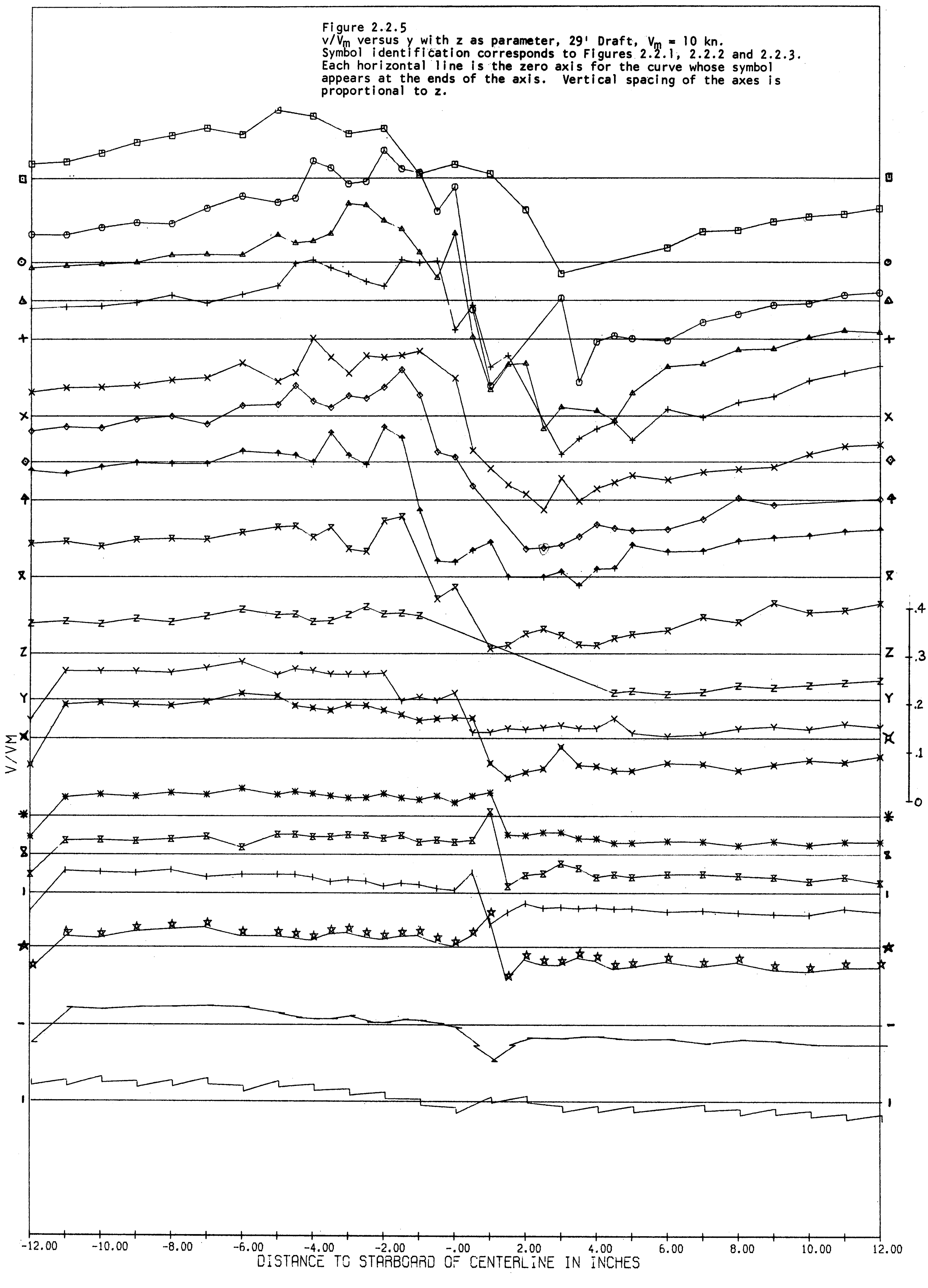
Figure 2.2.5
v/Vm versus y with z as parameter, 29' Draft, Vm = 10 kn.
Symbol identification corresponds to Figures 2.2.1, 2.2.2 and 2.2.3.
Each horizontal line is the zero axis for the curve whose symbol appears at the ends of the axis. Vertical spacing of the axes is proportional to z.
V/VM
.4
.3
.2
.1
0
-12.00
-10.00
-8.00
-6.00
-4.00
-2.00
-.00
2.00
4.00
6.00
8.00
10.00
12.00
DISTANCE TO STARBOARD OF CENTERLINE IN INCHES

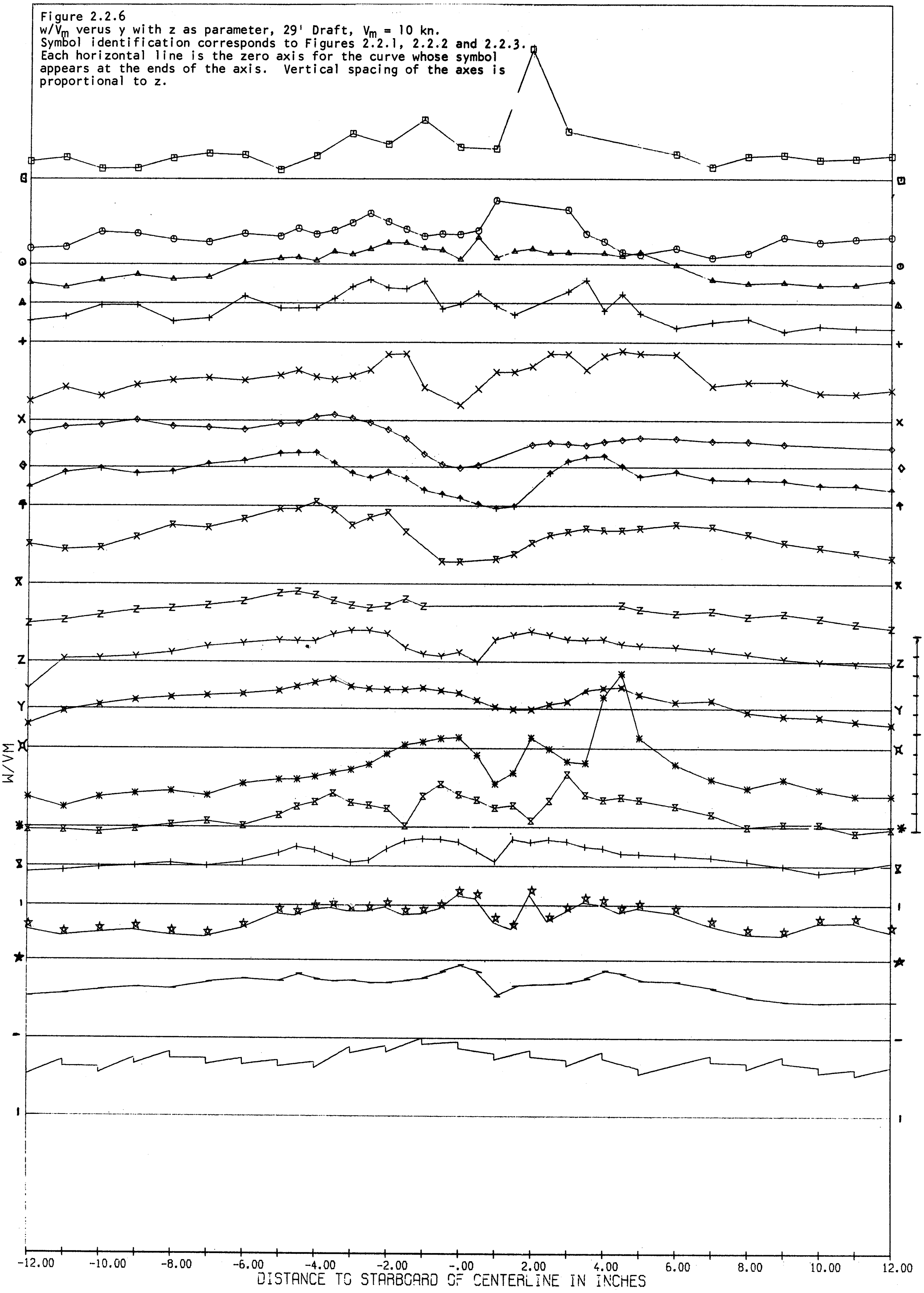

Figure 2.2.6
w/V_m verus y with z as parameter, 29' Draft, V_m = 10 kn.
Symbol identification corresponds to Figures 2.2.1, 2.2.2 and 2.2.3.
Each horizontal line is the zero axis for the curve whose symbol appears at the ends of the axis. Vertical spacing of the axes is proportional to z.
W/VM
0
.1
.2
-12.00
-10.00
-8.00
-6.00
-4.00
-2.00
-.00
2.00
4.00
6.00
8.00
10.00
12.00
DISTANCE TO STARBOARD OF CENTERLINE IN INCHES

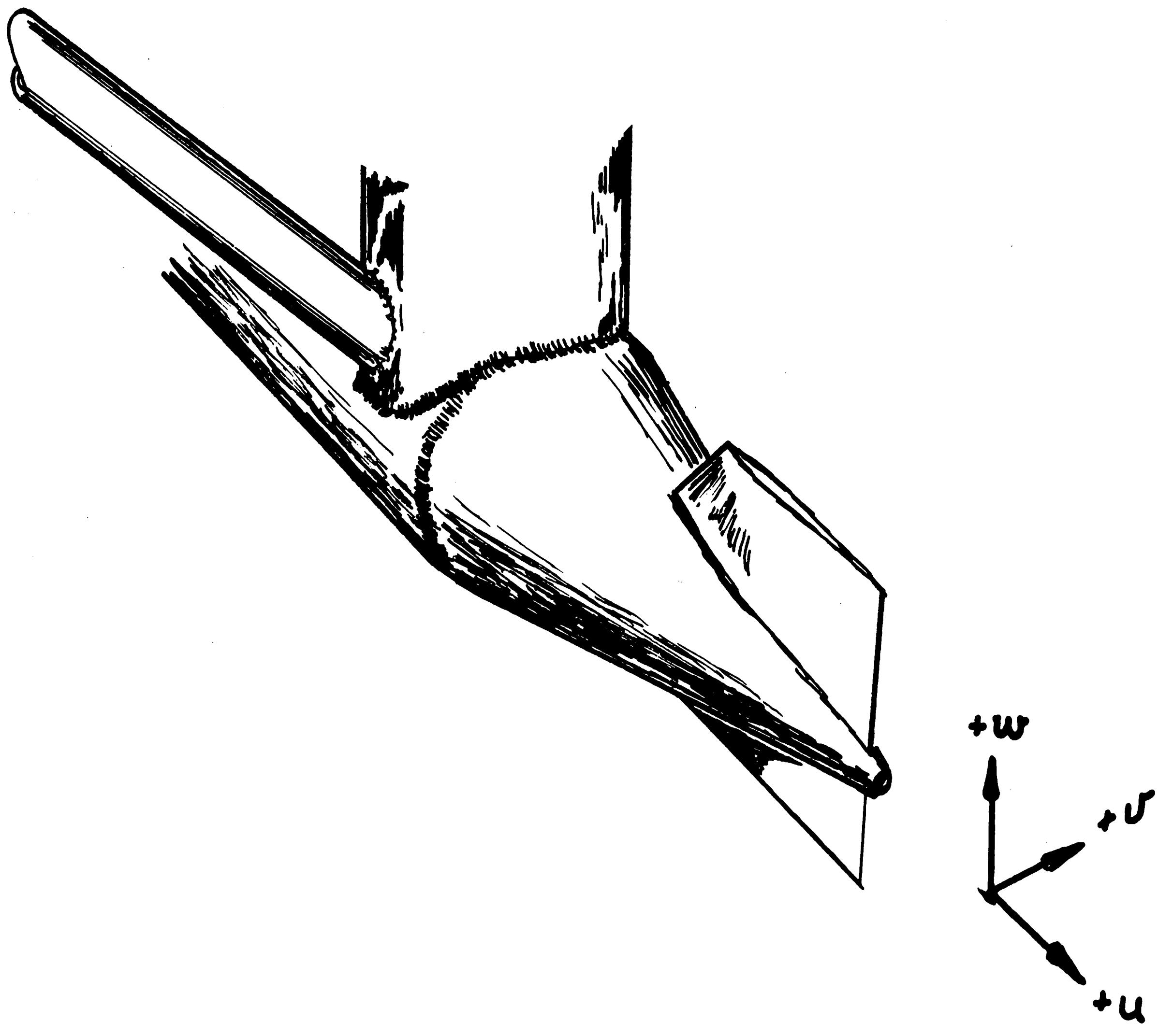


Figure 2.2.7
Wake Survey Sign Conventions.

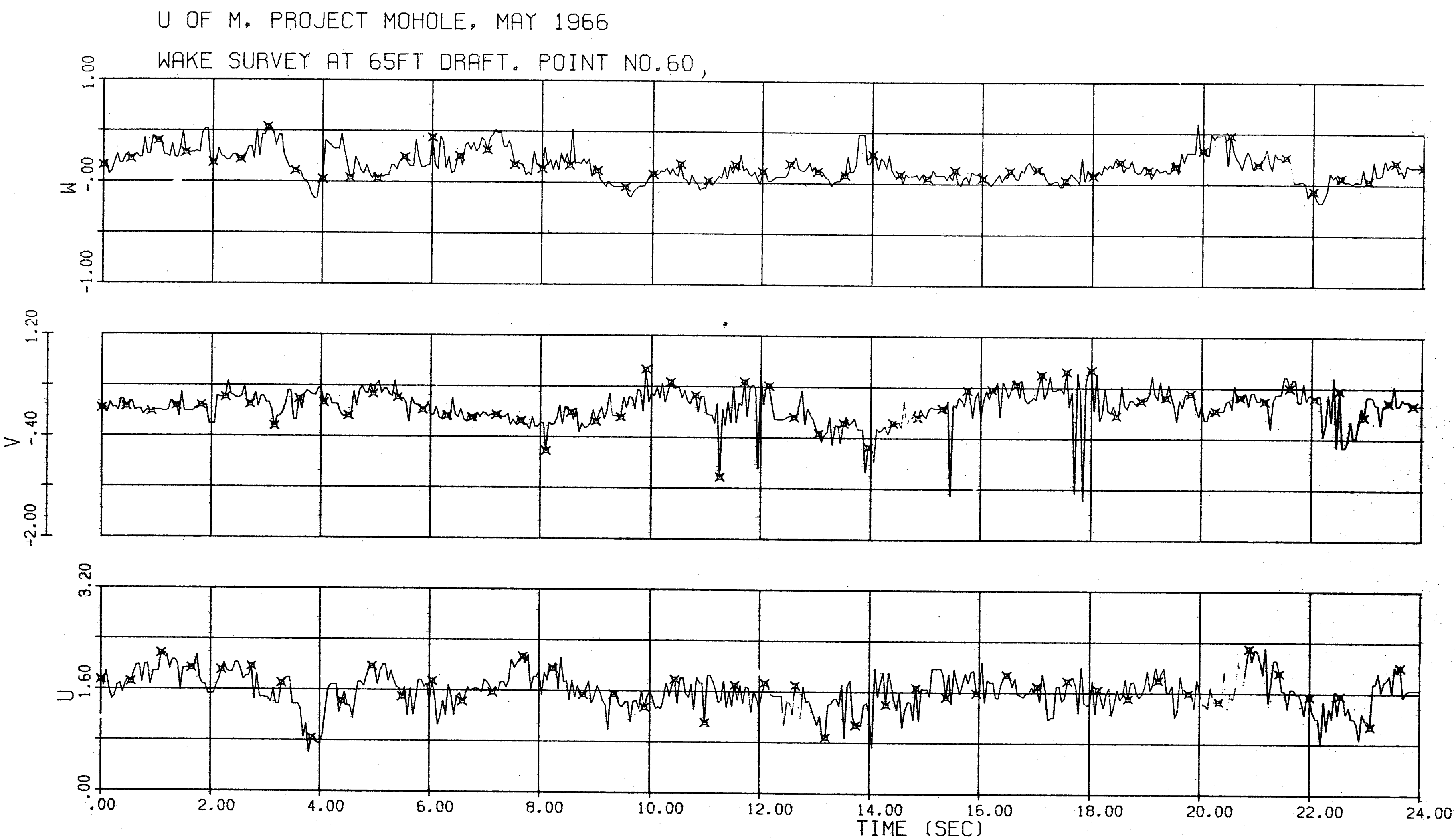


Figure 2.3.1
u, v and w versus time,
pitot tube positioned 1.60" below and 2.70"
to port of the propeller shaft of the model.
$V_m$ = 1.92 ft/sec.

## 3. OPEN WATER TESTS OF MAIN PROPELLER

Propeller performance characteristics of the 5 bladed main propulsion propeller were evaluated from data obtained during open water tests. These tests were performed in a conventional manner with a propeller boat.

The original propeller drawings were redrawn to a large scale and photographically reduced to model size on metal templates. Propeller parameters are shown in Figure 3.1. The model propeller, shown in Figure 3.2, was made from one piece of rolled aluminum alloy.

A constant RPM procedure was used throughout, i.e. during one set of test runs the RPM was kept constant whereas the carriage velocity was varied from run to run. The propeller was tested at 200, 400, 600, 700 and 750 RPM. If no scale effects are present non-dimensional coefficients of performance parameters should be independent of RPM. From results obtained it can be concluded that only at 200 RPM was the scale effect significant.

In addition to the propeller being driven in the ahead direction, three other conditions were investigated:

a. the propeller was moved ahead and the propeller rotated in reverse (positive velocity of advance, negative RPM)

b. the propeller was moved astern (backing) and the propeller rotation was reversed (negative velocity of advance, negative RPM)

c. the propeller was moved astern and the propeller rotation was left as in the ahead propulsion test (negative velocity of advance, positive RPM).

In figures where plots of more than one conditon appear, the following sign convention has been used. The thrust coefficient is positive if thrust is acting in the ahead direction, i.e. with the propeller under installed working conditions the thrust force vector is pointing towards the bow. The torque coefficient, on the other hand, follows the sign of the propeller rotation for the test conditions investigated. To be able to extend results to a locked propeller and also include cases where the propeller is driving the propulsion machinery it is preferable to adopt the right handed vector convention such that torque is positive if the torque vector, as applied to the propeller fitted on the propeller shaft of the drilling platform, is pointing towards the bow. Note that the advance coefficient is negative if the velocity of advance and rotation are of opposite signs.

The tests where the propeller was being moved against its thrust force exhibited some unusual features. In the low speed range the torque and thrust were decreasing slightly in magnitude with increasing velocity. At a certain speed of advance, however, a complete stalling of the propeller blades took place which was associated with a sudden drop-off in propeller forces. As the speed was further increased the flow was apparently completely separated along the edges of the propeller blades and it is expected to be similar in character to the flow created by a plate placed approximately normal to a uniform stream. The torque and thrust coefficients for the locked propeller were estimated on the basis of this hypothesis. It was argued that the flow around a locked propeller is also fully separated along the edge of the blades. If, therefore, we add the zero thrust velocity of advance to the carriage velocity used for the individual test runs which were made above stalling conditions, we shall arrive at hypothetical speeds of advance for the locked propeller where torque and thrust are identical to those measured during the tests. From actual test data it was found that deviations of the coefficients from a mean value for the locked propeller, applying the procedure as outlined above, were well within experimental accuracy. Should the propeller under some operating conditions be driving the propulsion machinery an estimate of torque and thrust should be possible if the no thrust velocity of advance is subtracted instead of added to the platform velocity.

Prior to stalling, the propeller will be moving into its own slipstream, as a result producing an extremely confused flow condition. Large variations in torque and thrust are associated with the formation and shedding of these eddies. It was therefore found necessary to provide a feed-back dynamometer speed control. A commercially available unit proved to be capable of maintaining the rotation speed of the propeller within $\pm$ 1%. Maximum variations in torque under these running conditions were approximately $\pm$ 12%. A typical test record is shown in Figure 3.31. For purposes of calculating propeller performance coefficients an estimated mean value of torque and thrust was used.

The data read from test records are given in Table 3-1.

Torque and thrust coefficients, $K_Q = \frac{Q}{\rho n^2 D^5}$ and $K_T = \frac{T}{\rho n^2 D^4}$ , have been calculated from the data of this table and plotted in

## TABLE 3-1 TEST DATA

| Test No. | Propeller RPM | Carriage Speed Ft/Sec | Torque Ft-LBS | Thrust LBS |
|---|---|---|---|---|
| 1 | +750 | 0 | .731 | 12.90 |
| | | 1.054 | .673 | 10.90 |
| | | 2.030 | .593 | 8.80 |
| | | 3.03 | .488 | 6.22 |
| | | 4.52 | .283 | 1.93 |
| | | 5.21 | .158 | −.24 |
| 2 | −750 | 0 | .463 | 5.57 |
| | | .51 | .483 | 5.30 |
| | | 1.54 | .453 | 5.00 |
| | | 1.49 | .443 | 5.20 |
| | | 2.12 | .453 | 4.25 |
| | | 2.52 | .393 | 4.50 |
| | | 3.49 | .408 | 6.60 |
| | | 4.22 | .498 | 8.50 |
| 3 | +600 | 0 | .480 | 8.25 |
| | | 1.32 | .408 | 5.90 |
| | | 1.63 | .382 | 5.21 |
| | | 2.26 | .335 | 4.19 |
| | | 3.05 | .245 | 2.46 |
| | | 3.53 | .184 | 1.10 |
| 4 | −600 | 2.52 | .303 | 3.50 |
| | | 3.07 | .348 | 4.60 |
| | | 0 | .328 | 3.48 |

TABLE 3-1 Continued.

| Test No. | Propeller RPM | Carriage Speed Ft/Sec | Torque Ft-LBS | Thrust LBS |
|---|---|---|---|---|
| 4 | −600 | .595 | .283 | 3.00 |
| | | 4.06 | .463 | 7.20 |
| | | 1.05 | .293 | 3.20 |
| | | 2.02 | .263 | 3.00 |
| | | 1.49 | .243 | 2.50 |
| 5 | +400 | 0 | .205 | 3.58 |
| | | .830 | .174 | 2.60 |
| | | 1.60 | .133 | 1.50 |
| | | 1.83 | .122 | 1.20 |
| | | 2.01 | .105 | .91 |
| | | 2.43 | .071 | .20 |
| | | .404 | .191 | 3.25 |
| | | 1.25 | .152 | 2.05 |
| | | 2.99 | .018 | −.76 |
| 6 | −400 | 0 | .141 | 1.48 |
| | | 1.02 | .113 | 1.00 |
| | | 2.01 | .153 | 2.00 |
| | | 3.00 | .228 | 3.50 |
| | | .60 | .128 | 1.40 |
| | | 1.49 | .118 | 1.30 |
| | | 2.53 | .193 | 2.80 |
| 7 | +200 | 0 | .52 | .79 |
| | | .210 | .52 | .68 |
| | | .411 | .49 | .60 |

TABLE 3-1 Continued.

| Test No. | Propeller RPM | Carriage Speed Ft/Sec | Torque Ft-LBS | Thrust LBS |
|---|---|---|---|---|
| 7 | +200 | .641 | .41 | .42 |
| | | .842 | .33 | .29 |
| | | 1.05 | .27 | .13 |
| | | 1.25 | .22 | –.08 |
| | | 1.41 | .13 | –.21 |
| | | 1.61 | .02 | –.42 |
| | | .51 | .035 | .43 |
| | | 1.14 | .022 | –.02 |
| | | .701 | .040 | .38 |
| | | 1.11 | .026 | .01 |
| 8 | –200 | 0 | .038 | .41 |
| | | .516 | .033 | .35 |
| | | 1.00 | .039 | .52 |
| | | 2.02 | .083 | 1.31 |
| | | .850 | .033 | .40 |
| | | 1.55 | .065 | .95 |
| | | .297 | .034 | .36 |
| | | .69 | .029 | .35 |
| | | 1.66 | .061 | 1.00 |
| 11 | +200 | 0 | .048 | .750 |
| | | .243 | .043 | .740 |
| | | .405 | .048 | .800 |
| | | .610 | .043 | .720 |

TABLE 3-1 Continued.

| Test No. | Propeller RPM | Carriage Speed Ft/Sec | Torque Ft-LBS | Thrust LBS |
|---|---|---|---|---|
| 11 | +200 | .813 | .033 | .600 |
| | | 1.034 | .035 | .700 |
| | | 1.50 | .053 | 1.200 |
| | | 1.996 | .061 | 1.750 |
| | | .911 | .028 | .68 |
| | | .144 | .043 | .80 |
| | | 1.325 | .048 | 1.05 |
| 12 | −200 | 0 | .043 | .41 |
| | | .210 | .042 | .37 |
| | | .61 | .029 | .18 |
| | | 1.03 | .014 | −.10 |
| | | .38 | .038 | .29 |
| 13 | +400 | 1.000 | .183 | 3.30 |
| | | 1.51 | .183 | 3.20 |
| | | 2.01 | .173 | 2.90 |
| | | 2.49 | .203 | 3.85 |
| | | .500 | .183 | 3.40 |
| | | 1.75 | .143 | 2.50 |
| | | 3.00 | .213 | 4.80 |
| | | 0 | .198 | 3.40 |
| 14 | −400 | 0 | .144 | 1.54 |
| | | .414 | .133 | 1.33 |
| | | .820 | .117 | 1.00 |
| | | 1.20 | .095 | .63 |
| | | 1.63 | .072 | .140 |
| | | 1.92 | .063 | −.220 |

TABLE 3-1 Continued.

| Test No. | Propeller RPM | Carriage Speed Ft/Sec | Torque Ft-LBS | Thrust LBS |
|---|---|---|---|---|
| 15 | +600 | 0 | .463 | 8.1 |
| | | 1.00 | .433 | 9.0 |
| | | 2.00 | .423 | 7.4 |
| | | 3.02 | .413 | 7.0 |
| | | 1.02 | .463 | 8.2 |
| | | 2.52 | .333 | |
| | | 2.60 | .363 | 5.4 |
| | | 3.52 | .463 | 8.4 |
| 16 | −600 | 0 | .311 | 3.60 |
| | | 1.032 | .268 | 2.72 |
| | | 2.010 | .189 | 1.170 |
| | | 2.50 | .145 | .310 |
| | | .398 | .303 | 3.33 |
| | | .609 | .297 | 3.30 |
| | | 1.509 | .236 | 1.95 |
| | | 2.71 | .128 | −.150 |
| 17 | +700 | 0 | .643 | 11.4 |
| | | 1.00 | .633 | 11.0 |
| | | 2.00 | .583 | 10.5 |
| | | 3.02 | .483 | 7.4 |
| | | 4.04 | .633 | 11.8 |
| | | 3.52 | .573 | 9.5 |
| | | 4.52 | .663 | 12.8 |
| | | 2.52 | .583 | 10.1 |

TABLE 3-1 Continued.

| Test No. | Propeller RPM | Carriage Speed Ft/Sec | Torque Ft-LBS | Thrust LBS |
|---|---|---|---|---|
| 17 | +700 | 3.81 | .593 | 10.8 |
| | | 2.81 | .553 | 9.4 |
| 18 | −700 | 0 | .421 | 4.72 |
| | | 1.01 | .378 | 4.00 |
| | | 2.01 | .303 | 2.35 |
| | | 3.00 | .190 | .229 |
| 19 | +750 | .50 | .723 | 13.4 |
| | | 1.00 | .683 | 12.6 |
| | | 1.50 | .743 | 12.8 |
| | | 2.00 | .643 | 12.0 |
| | | 2.50 | .683 | 12.2 |
| | | 3.0 | .643 | 11.2 |
| | | 3.0 | .643 | 11.0 |
| | | 3.5 | .613 | 10.2 |
| | | 0 | .743 | 13.1 |
| | | 5.0 | .783 | 16.0 |
| | | 4.3 | .713 | 13.1 |
| | | 3.91 | .683 | 12.0 |
| | | 3.50 | .623 | 10.2 |
| 20 | −750 | 0 | .473 | 5.45 |
| | | 1.00 | .435 | |
| | | 2.00 | .353 | 2.90 |
| | | 3.00 | .235 | .700 |

TABLE 3-1 Continued.

| Test No. | Propeller RPM | Carriage Speed Ft/Sec | Torque Ft-LBS | Thrust LBS |
|---|---|---|---|---|
| 20 | −750 | .725 | .458 | 4.80 |
| | | 1.50 | .403 | 3.51 |
| | | 3.50 | .180 | −.570 |
| | | 0 | .506 | 5.42 |

Notes:

a. In tests numbers 1-8, the Mohole propeller model was moving ahead. In test numbers 11-20, the propeller was moving astern.

b. .017 Ft-LBS has been subtracted to account for hub and bearing friction.

c. For a locked propeller moving ahead.

$$10\ K_Q' = .200$$
$$K_T' = .175$$

For a locked propeller moving astern.

$$10\ K_Q' = .182$$
$$K_T' = .175$$

These data represents tests no. 9 and 10 respectively.

Figures 3.3 to 3.20. The temperature of the towing tank water was 70°F throughout the testing program. ( $\rho$ = 1.9362)

For some applications it is convenient to use torque and thrust coefficients calculated on the basis of speed of advance, i.e. $K_Q' = \frac{Q}{\rho v^2 D^3}$ and $K_T' = \frac{T}{\rho v^2 D^2}$. Figures 3.21 through 3.30 are plots of $K_Q'$ and $K_T'$ coefficients versus inverse advance coefficients ($J' = \frac{1}{J} = \frac{nD}{V}$). Each figure has four curves, all representing the same RPM but different testing conditions according to the directions of speed of advance and porpeller rotation. The linear scale of the $K_Q'$ and $K_T'$ is the square root of the calculated numerical values.

Results of additional open water propeller tests which were run to determine the effect of pitch-diameter ratio on the performance characteristics of the main propulsion propeller are given in the appendix.

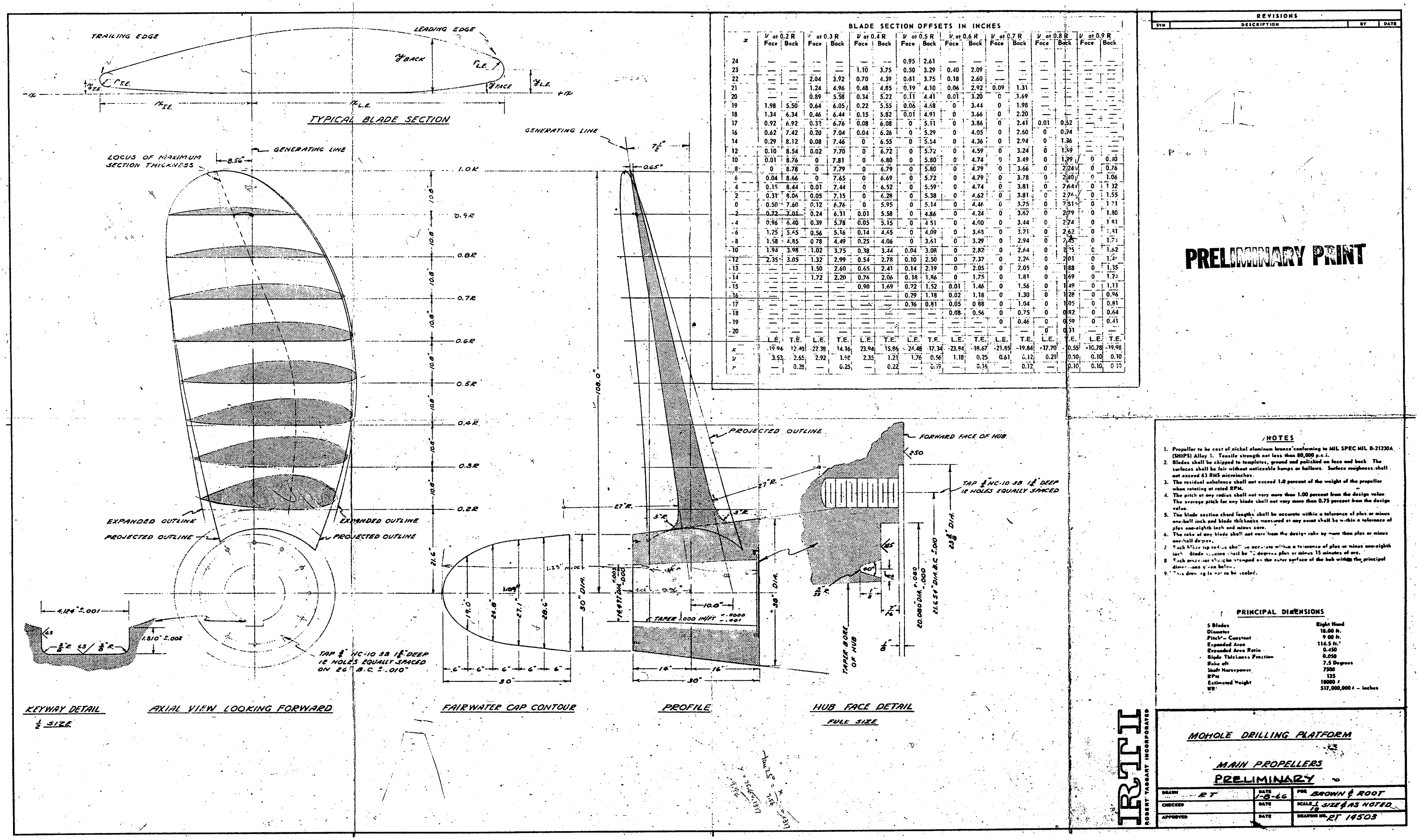


Figure 3.1
Project Mohole Main Propulsion
Propeller Characteristics.

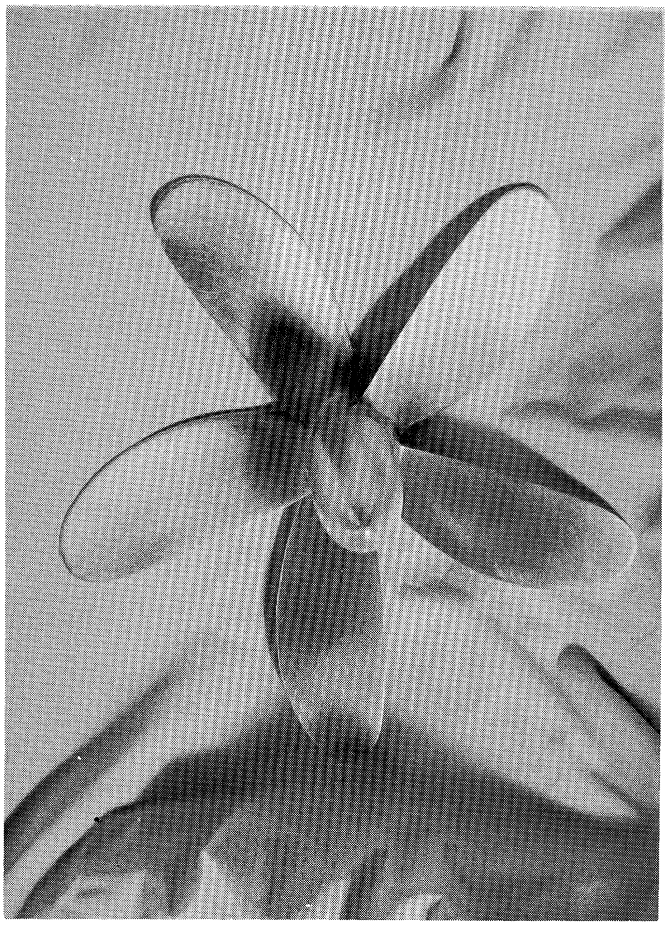

Figure 3.2
Project Mohole Main Propulsion
Propeller Model.

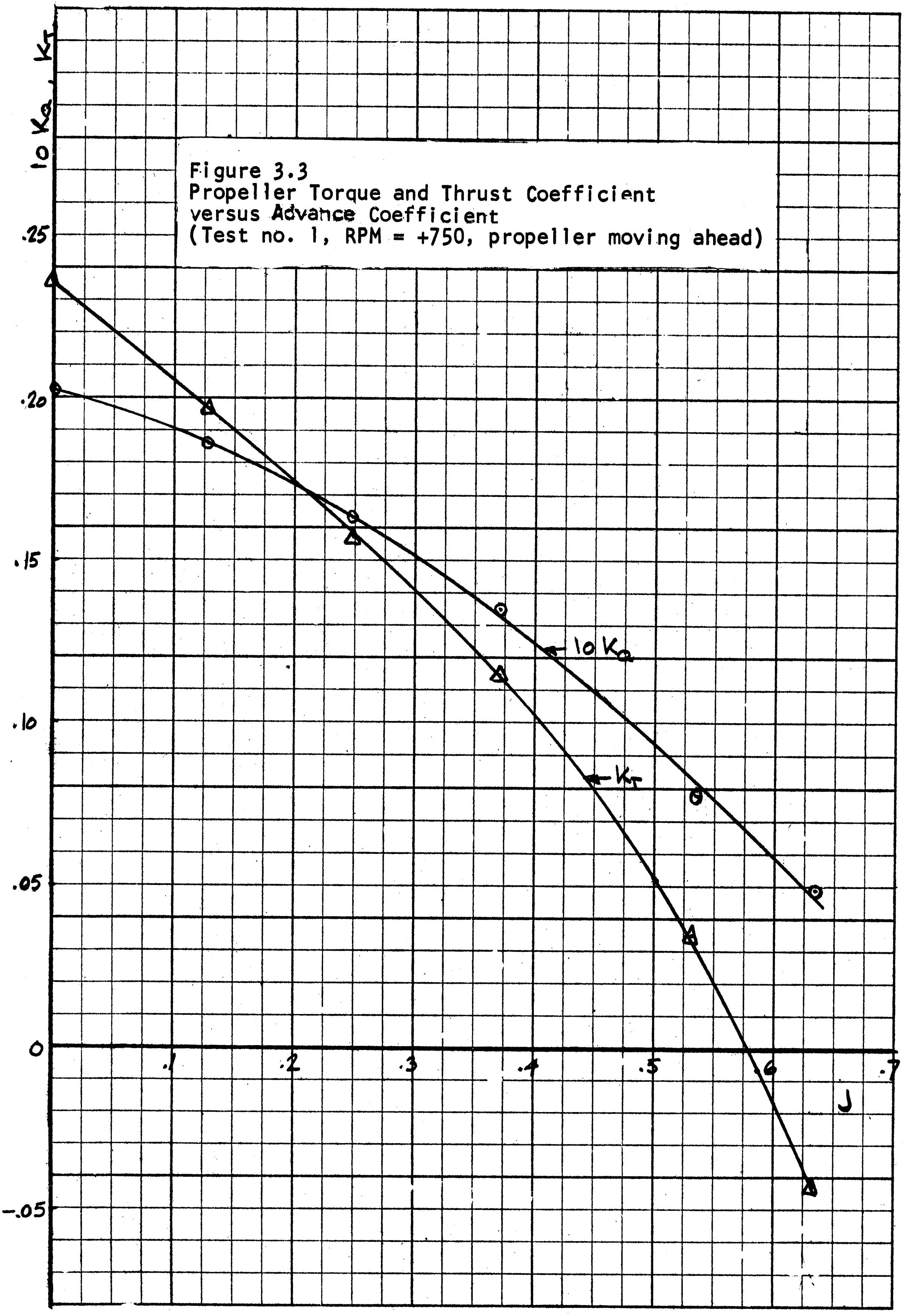


Figure 3.3
Propeller Torque and Thrust Coefficient versus Advance Coefficient
(Test no. 1, RPM = +750, propeller moving ahead)

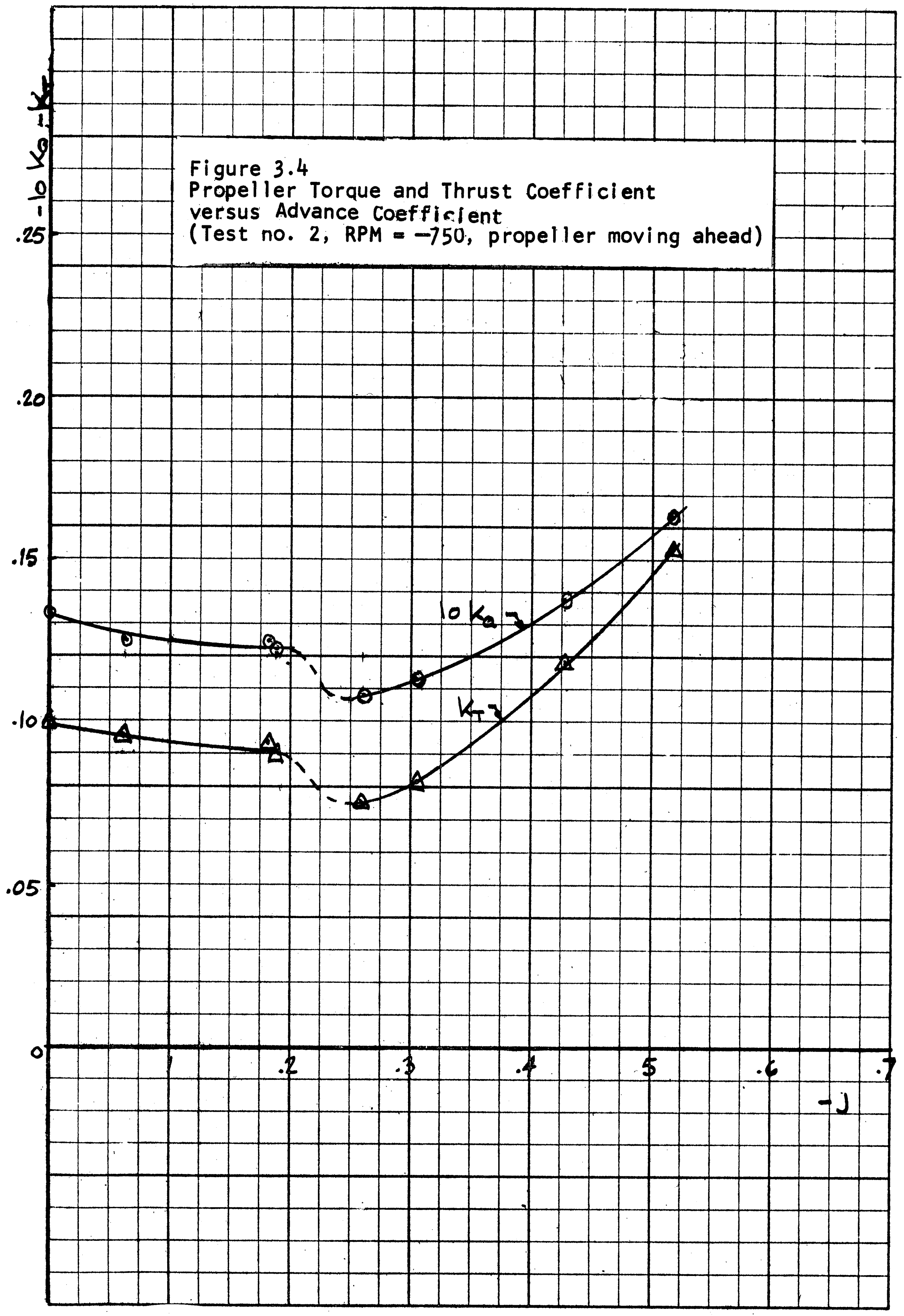


Figure 3.4
Propeller Torque and Thrust Coefficient
versus Advance Coefficient
(Test no. 2, RPM = -750, propeller moving ahead)

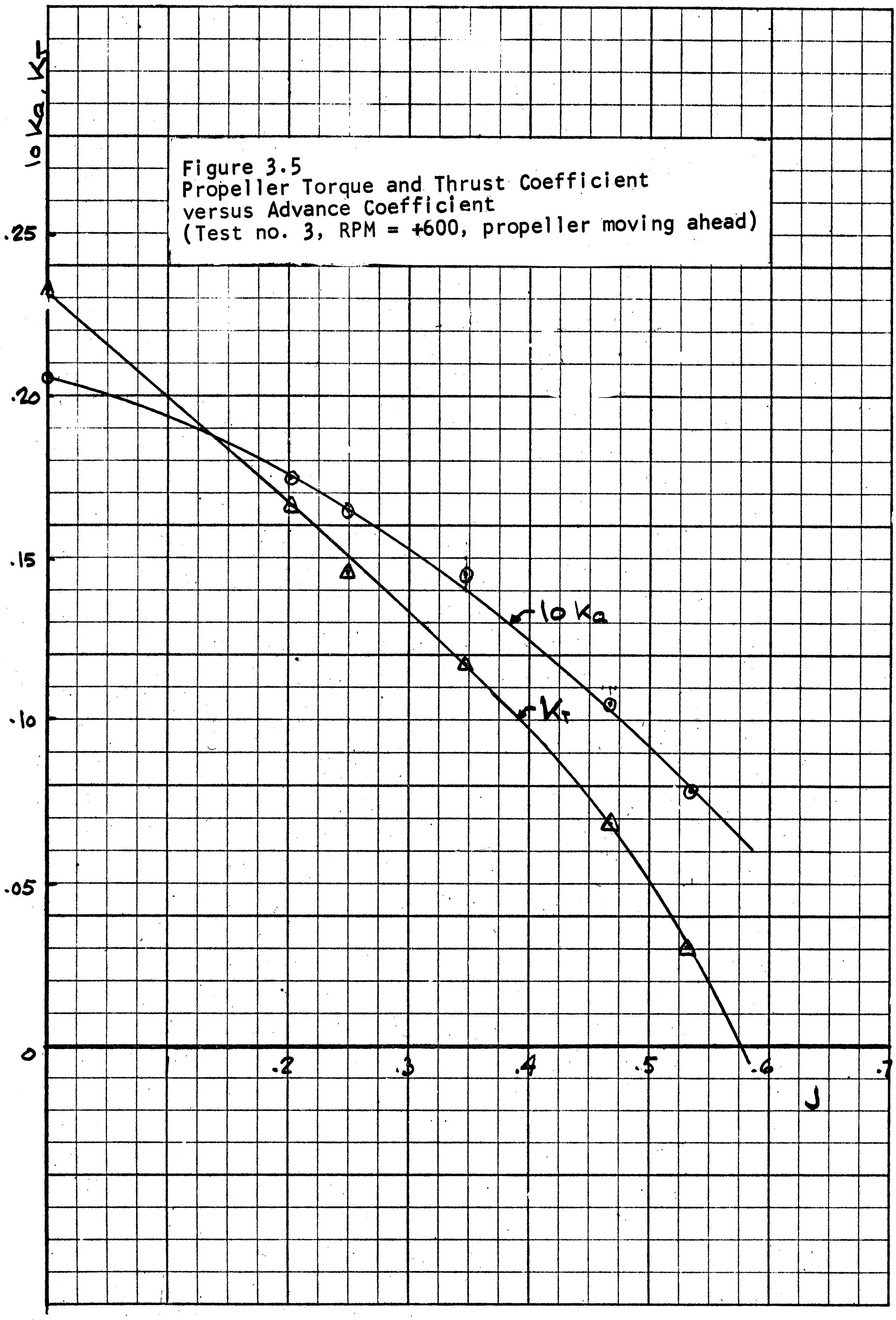

Figure 3.5
Propeller Torque and Thrust Coefficient
versus Advance Coefficient
(Test no. 3, RPM = +600, propeller moving ahead)
10 Kq, Kt
.25
.20
.15
.10
.05
0
.2
.3
.4
.5
.6
.7
J
10 Kq
Kt

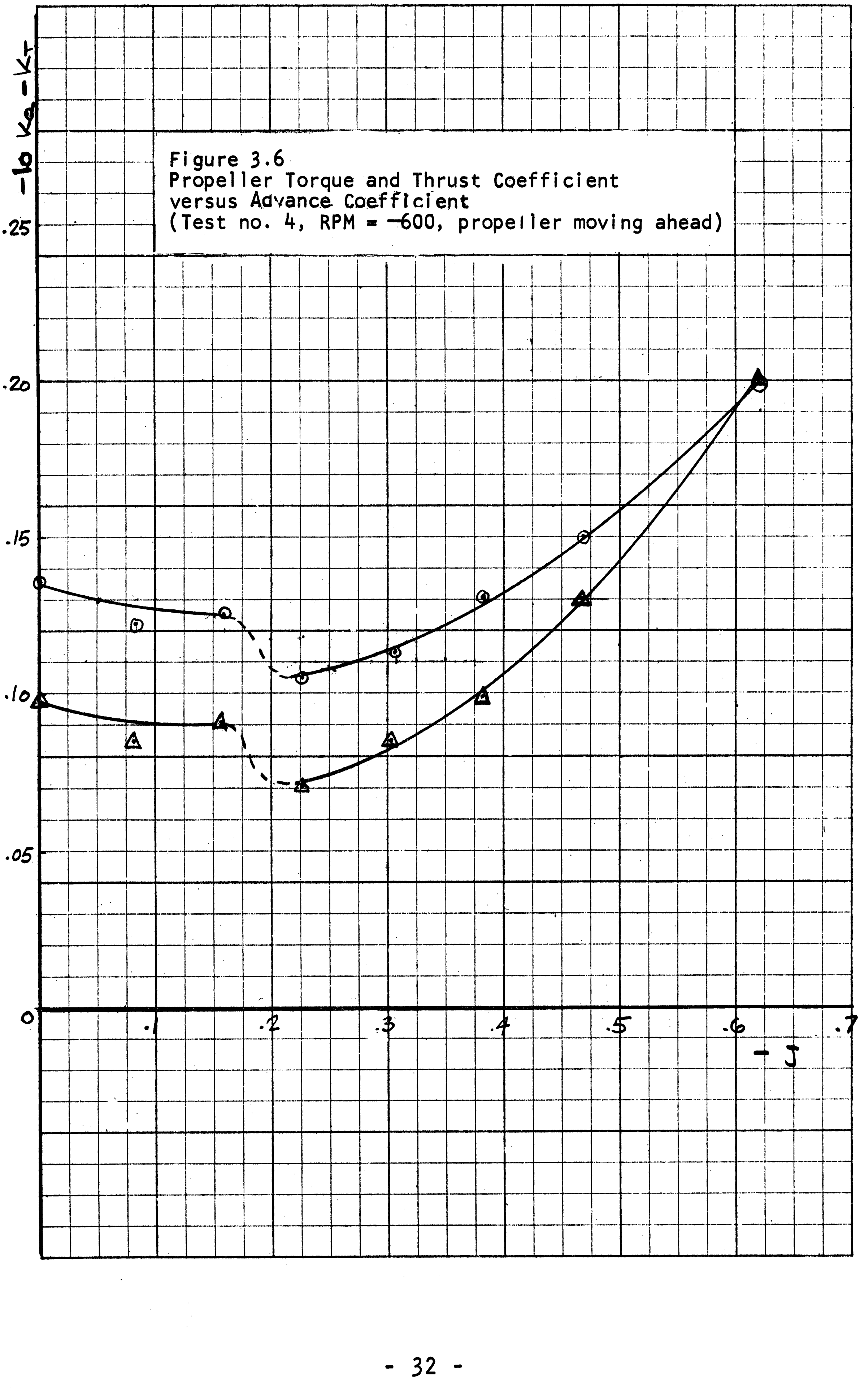

Figure 3.6
Propeller Torque and Thrust Coefficient
versus Advance Coefficient
(Test no. 4, RPM = −600, propeller moving ahead)

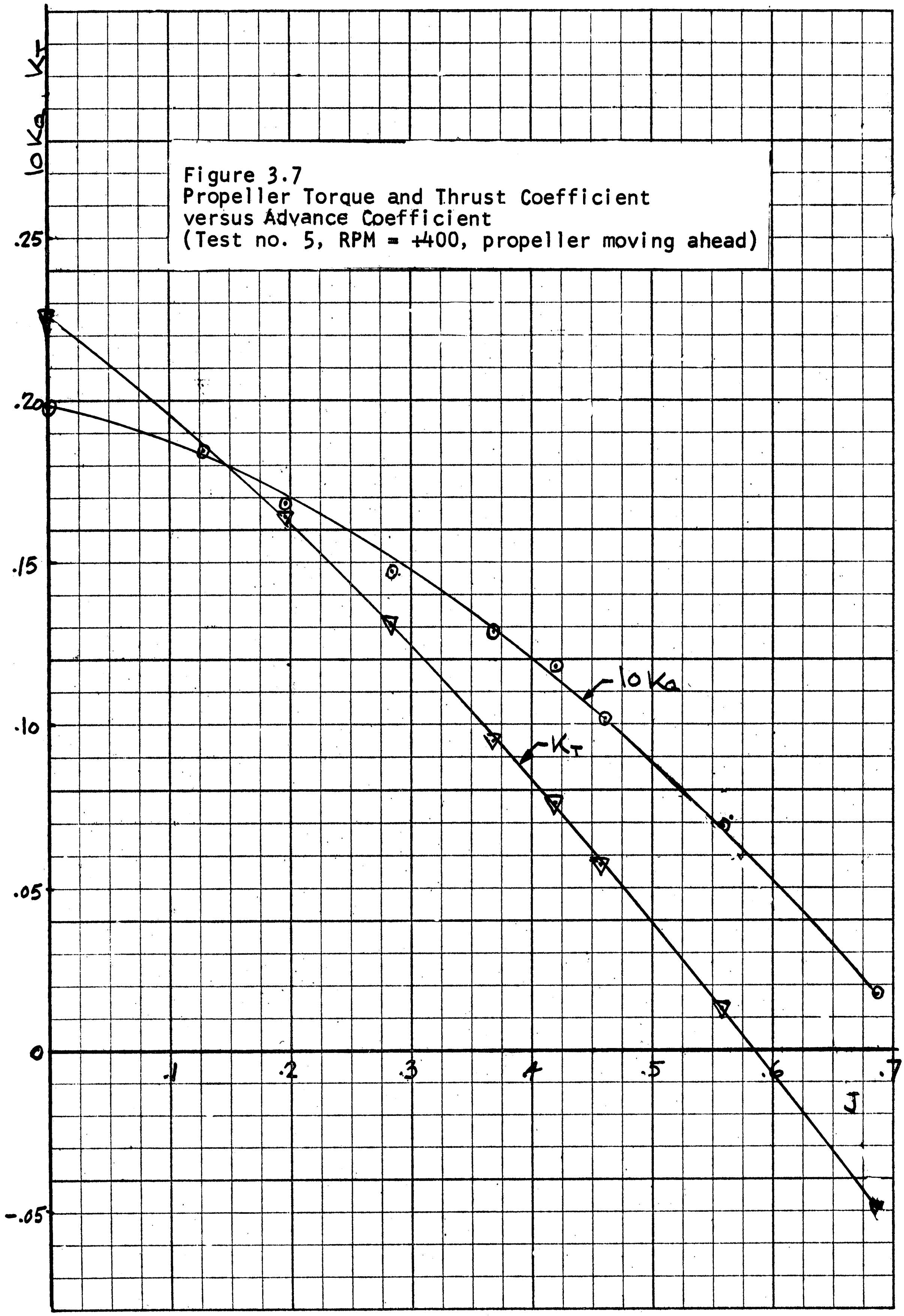
10Kq, KT
Figure 3.7
Propeller Torque and Thrust Coefficient
versus Advance Coefficient
(Test no. 5, RPM = +400, propeller moving ahead)
.25
.20
.15
.10
.05
0
-.05
.1
.2
.3
.4
.5
.6
.7
J
10Kq
KT

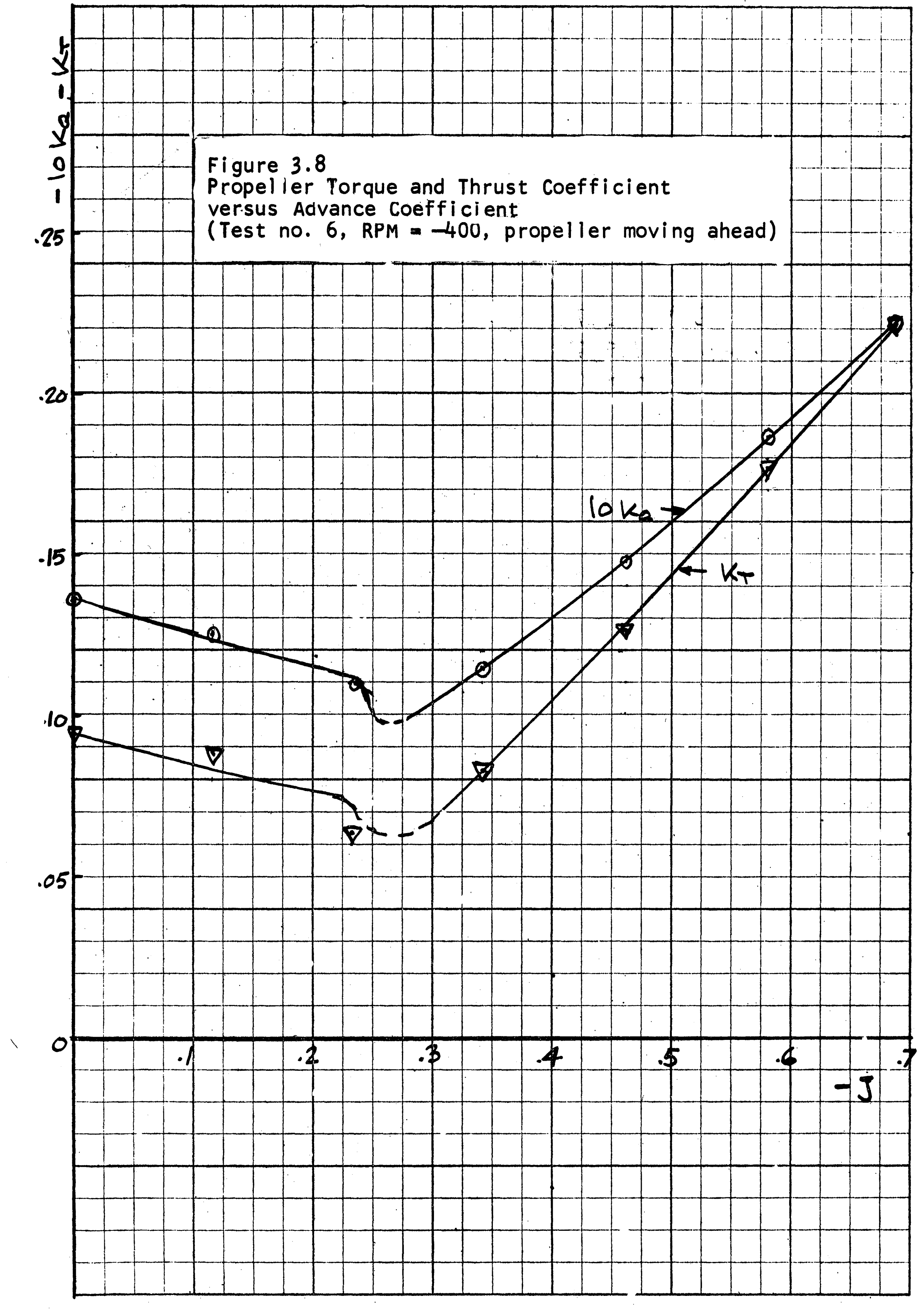


Figure 3.8
Propeller Torque and Thrust Coefficient
versus Advance Coefficient
(Test no. 6, RPM = -400, propeller moving ahead)

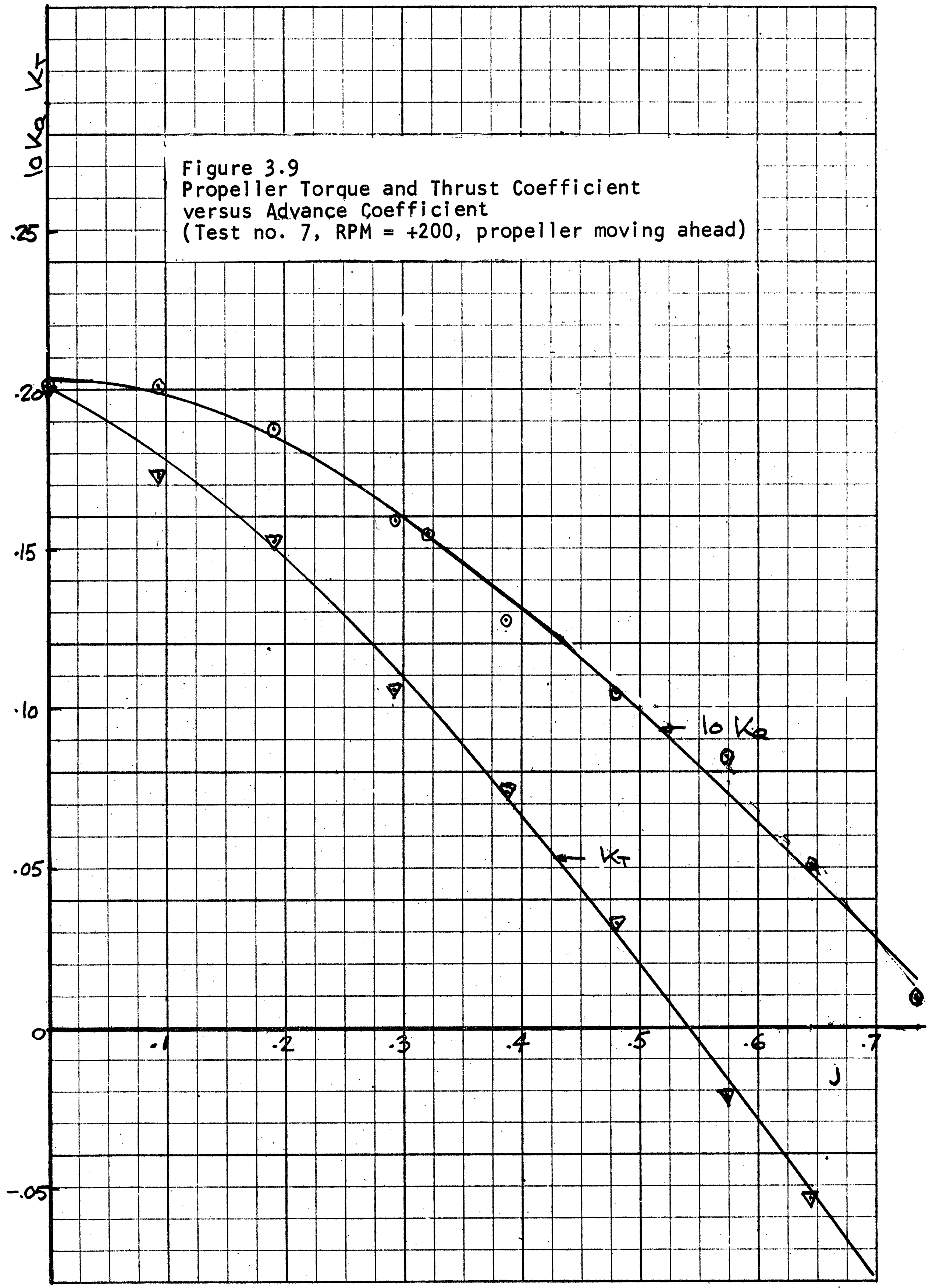

Figure 3.9
Propeller Torque and Thrust Coefficient versus Advance Coefficient
(Test no. 7, RPM = +200, propeller moving ahead)

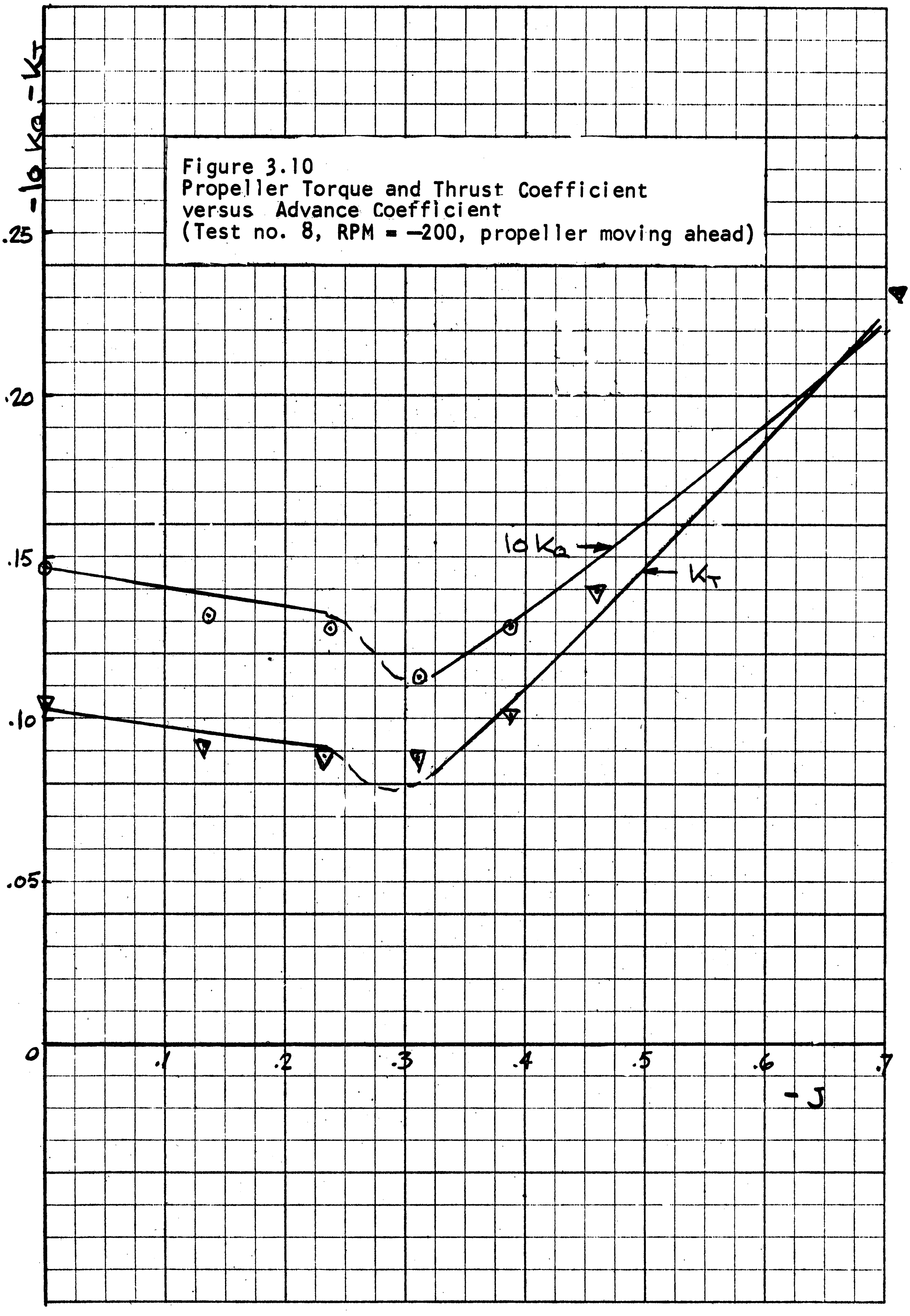


Figure 3.10
Propeller Torque and Thrust Coefficient versus Advance Coefficient
(Test no. 8, RPM = −200, propeller moving ahead)

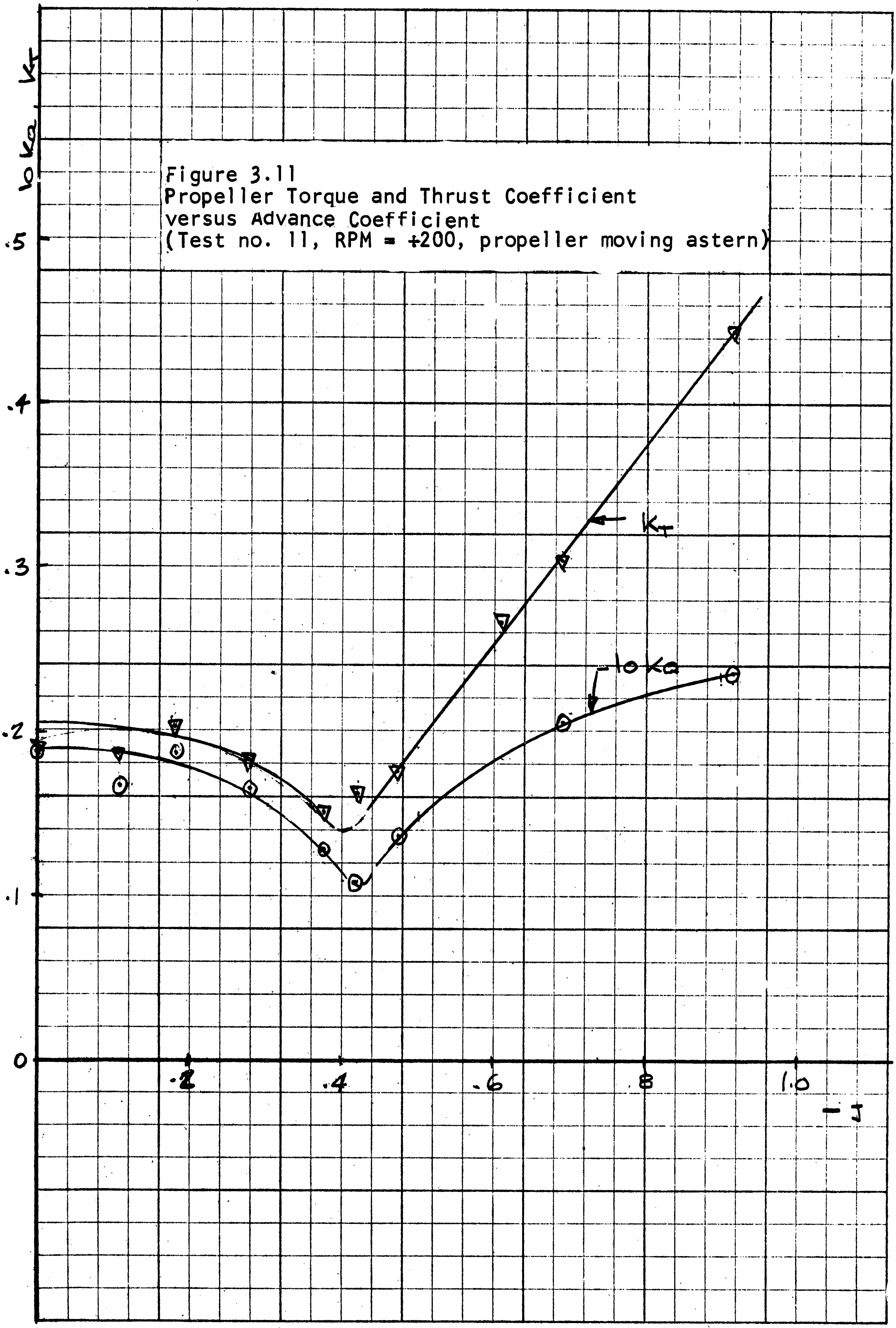


Figure 3.11
Propeller Torque and Thrust Coefficient
versus Advance Coefficient
(Test no. 11, RPM = +200, propeller moving astern)

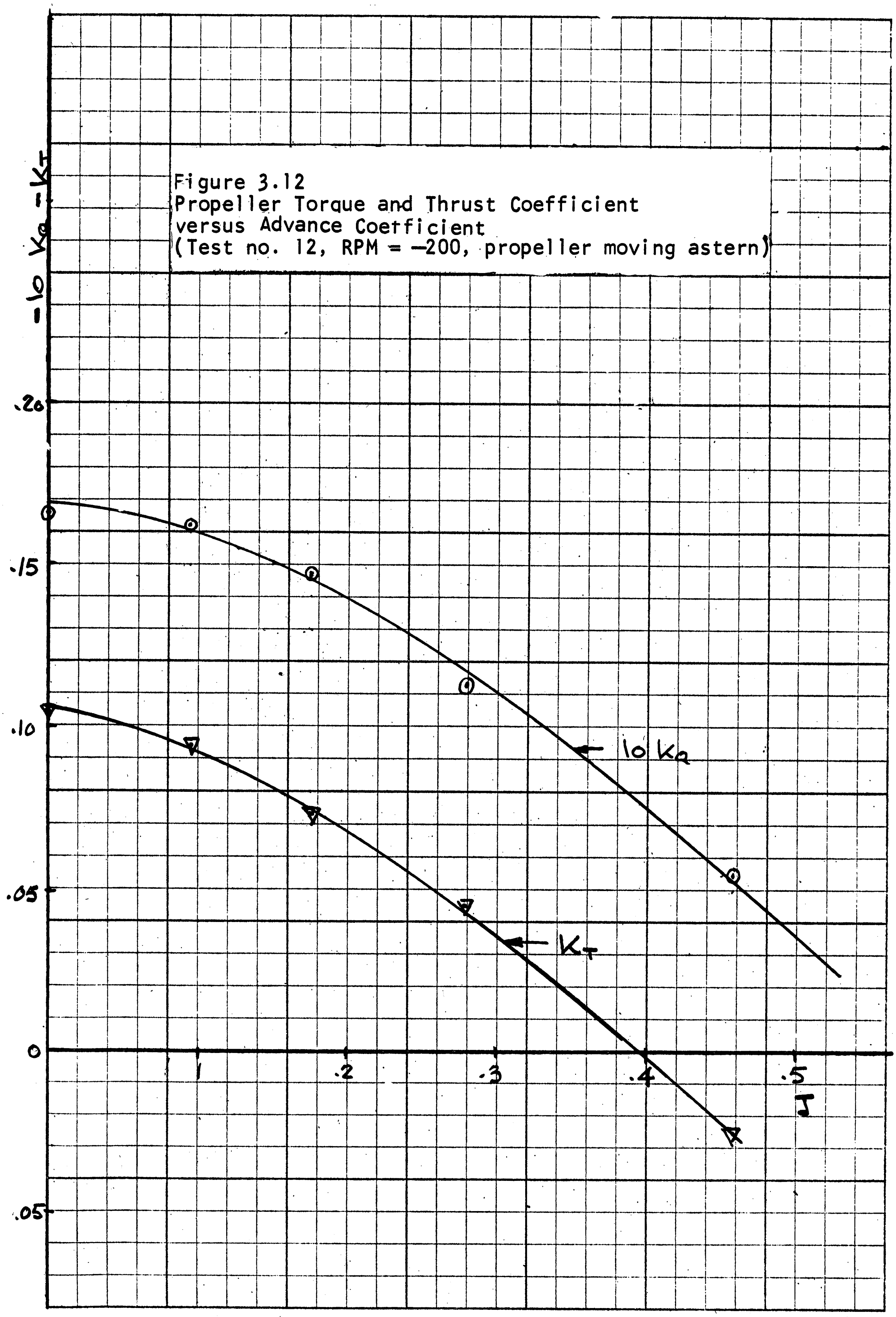


Figure 3.12
Propeller Torque and Thrust Coefficient
versus Advance Coefficient
(Test no. 12, RPM = –200, propeller moving astern)

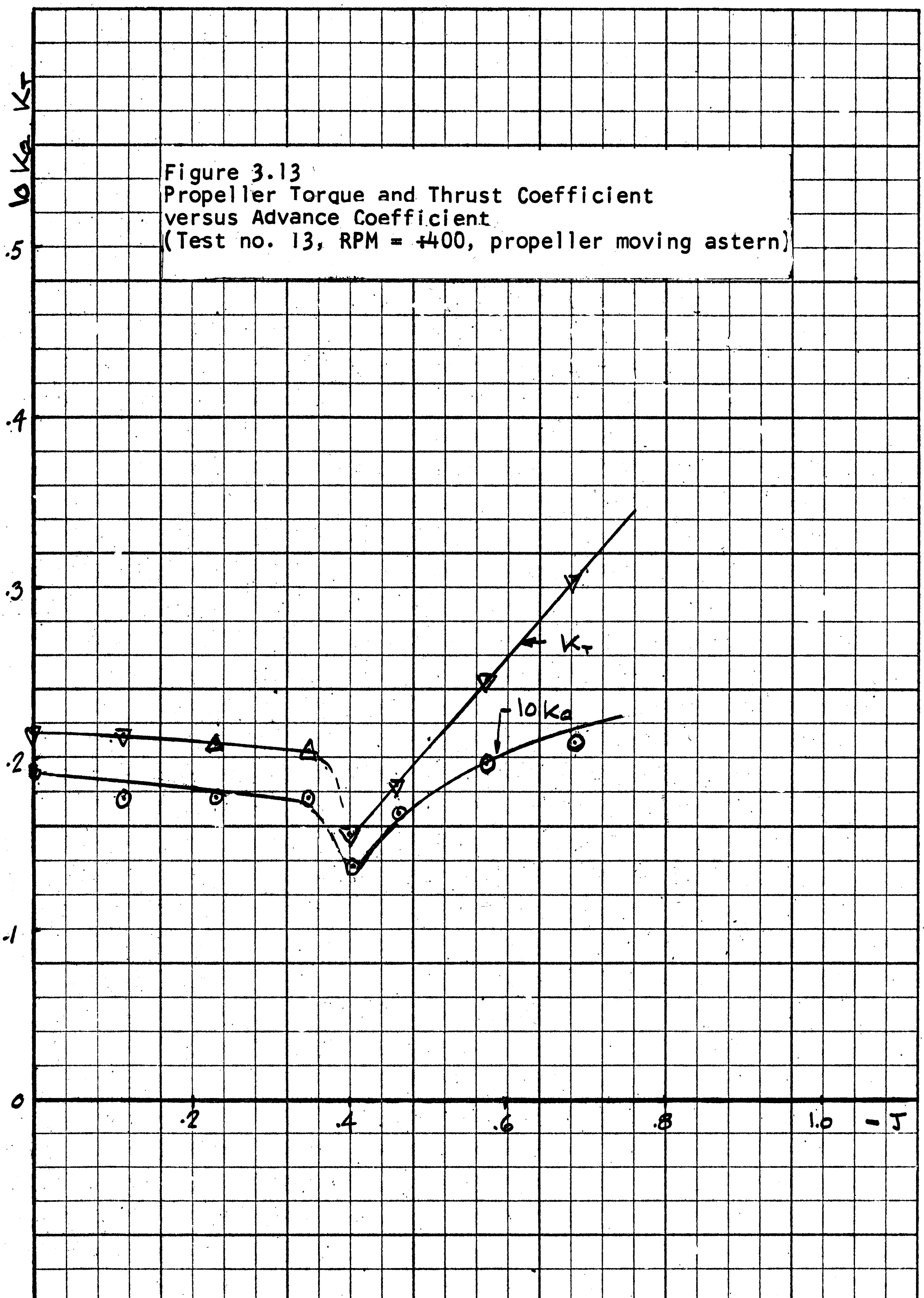


Figure 3.13
Propeller Torque and Thrust Coefficient
versus Advance Coefficient
(Test no. 13, RPM = +400, propeller moving astern)

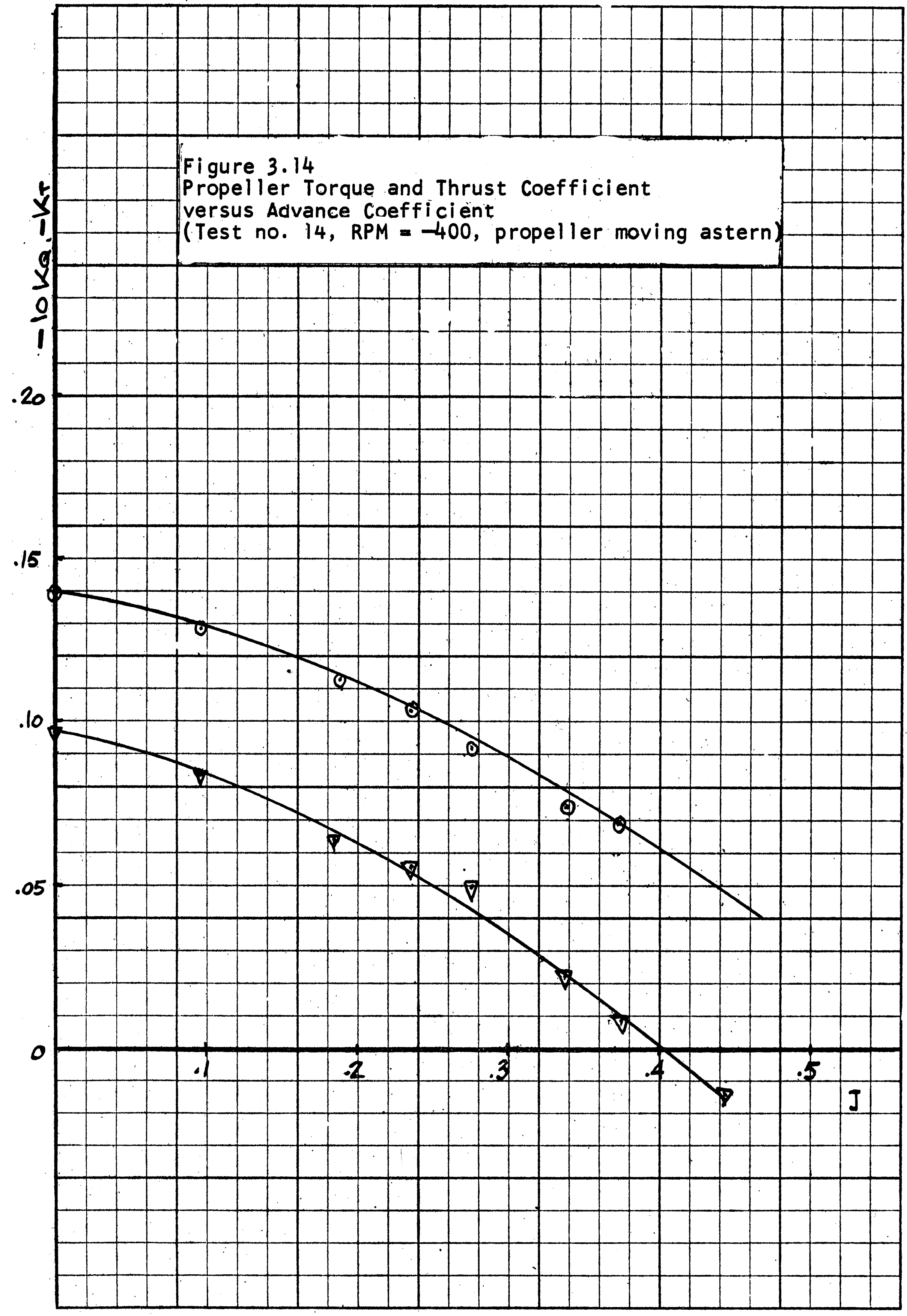

Figure 3.14
Propeller Torque and Thrust Coefficient
versus Advance Coefficient
(Test no. 14, RPM = -400, propeller moving astern)
-10Kq, -Kт
.20
.15
.10
.05
0
.1
.2
.3
.4
.5
J

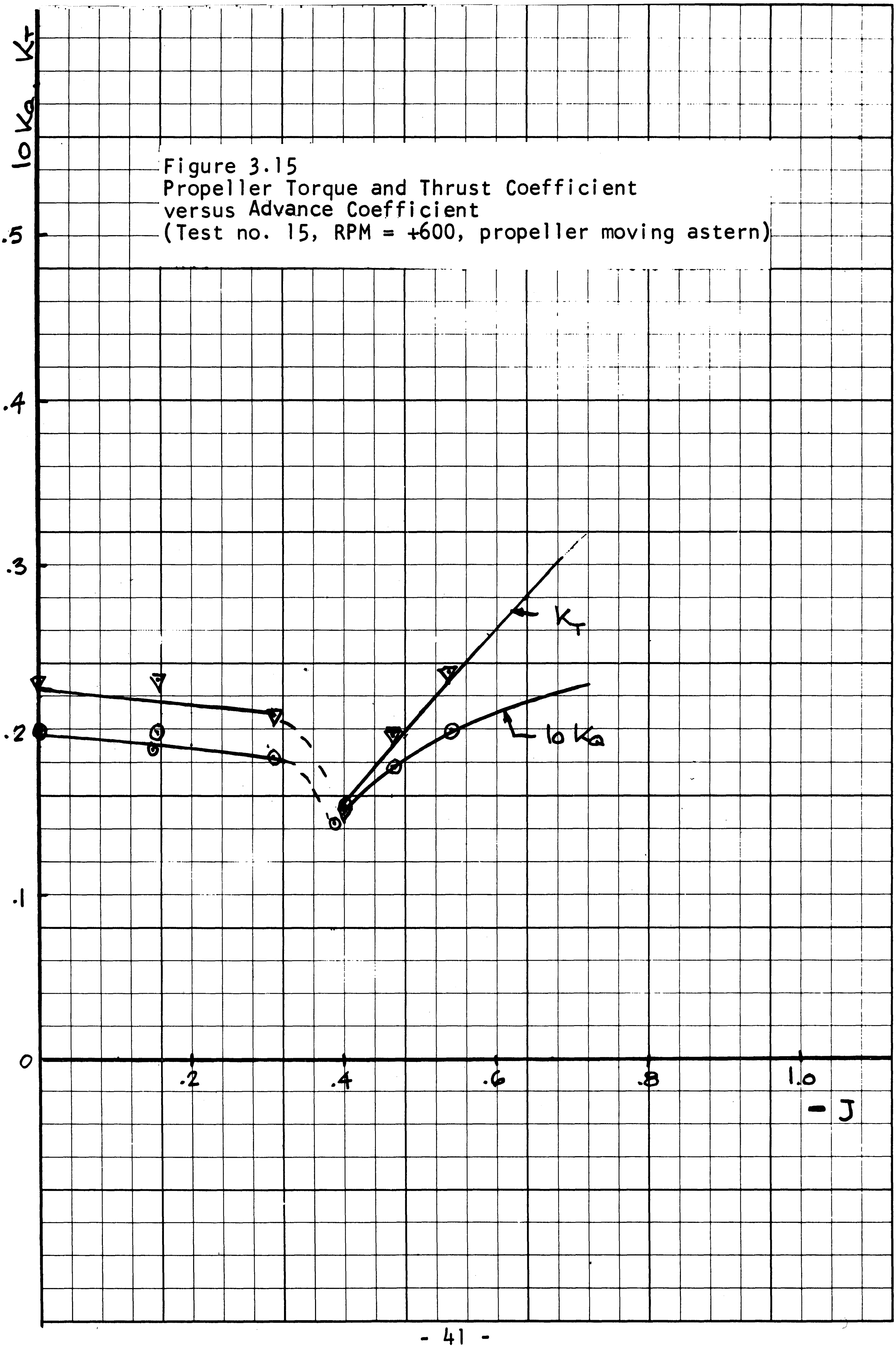


Figure 3.15
Propeller Torque and Thrust Coefficient
versus Advance Coefficient
(Test no. 15, RPM = +600, propeller moving astern)

Figure 3.16
Propeller Torque and Thrust Coefficient
versus Advance Coefficient
(Test no. 16, RPM = -600, propeller moving astern)

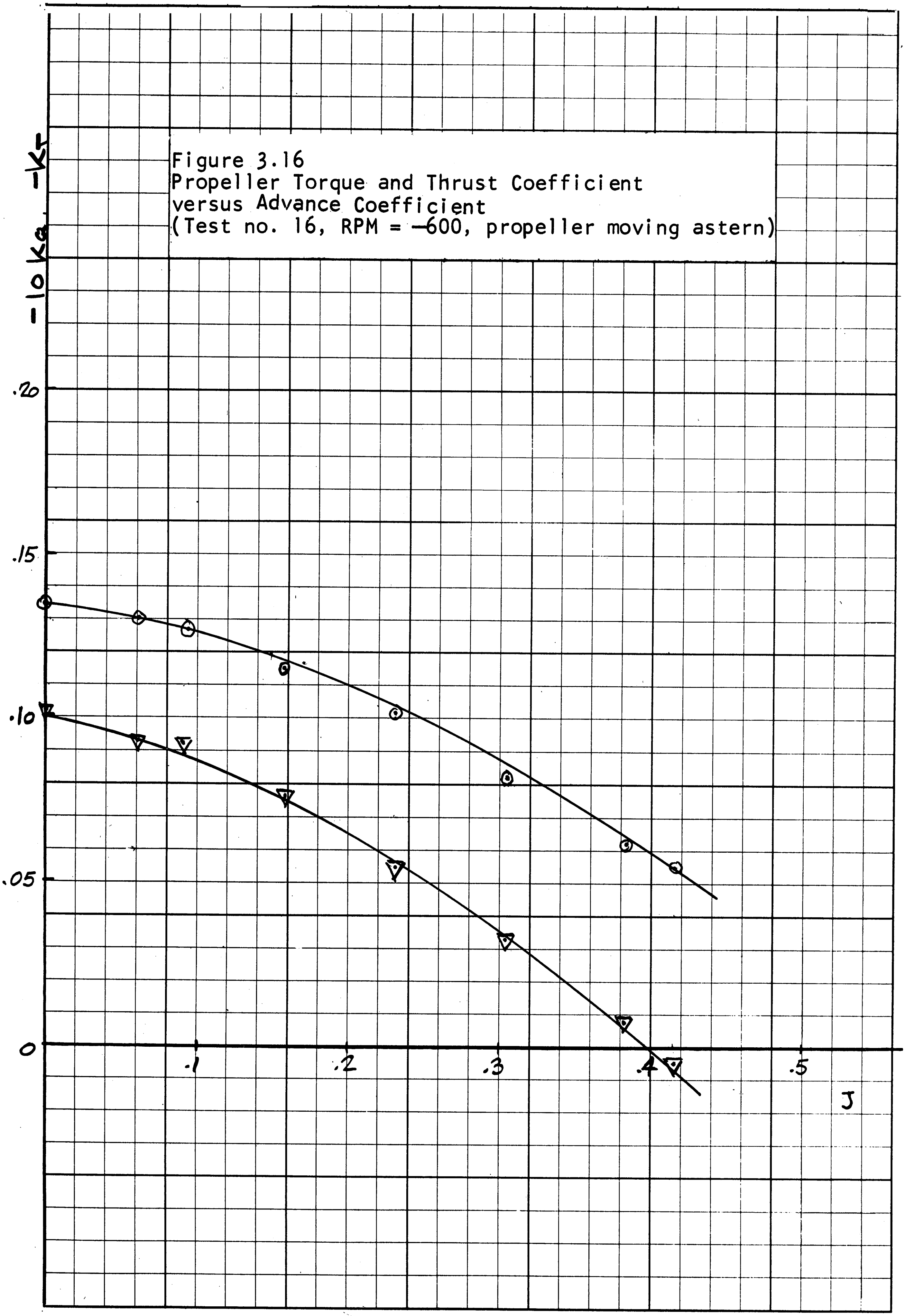

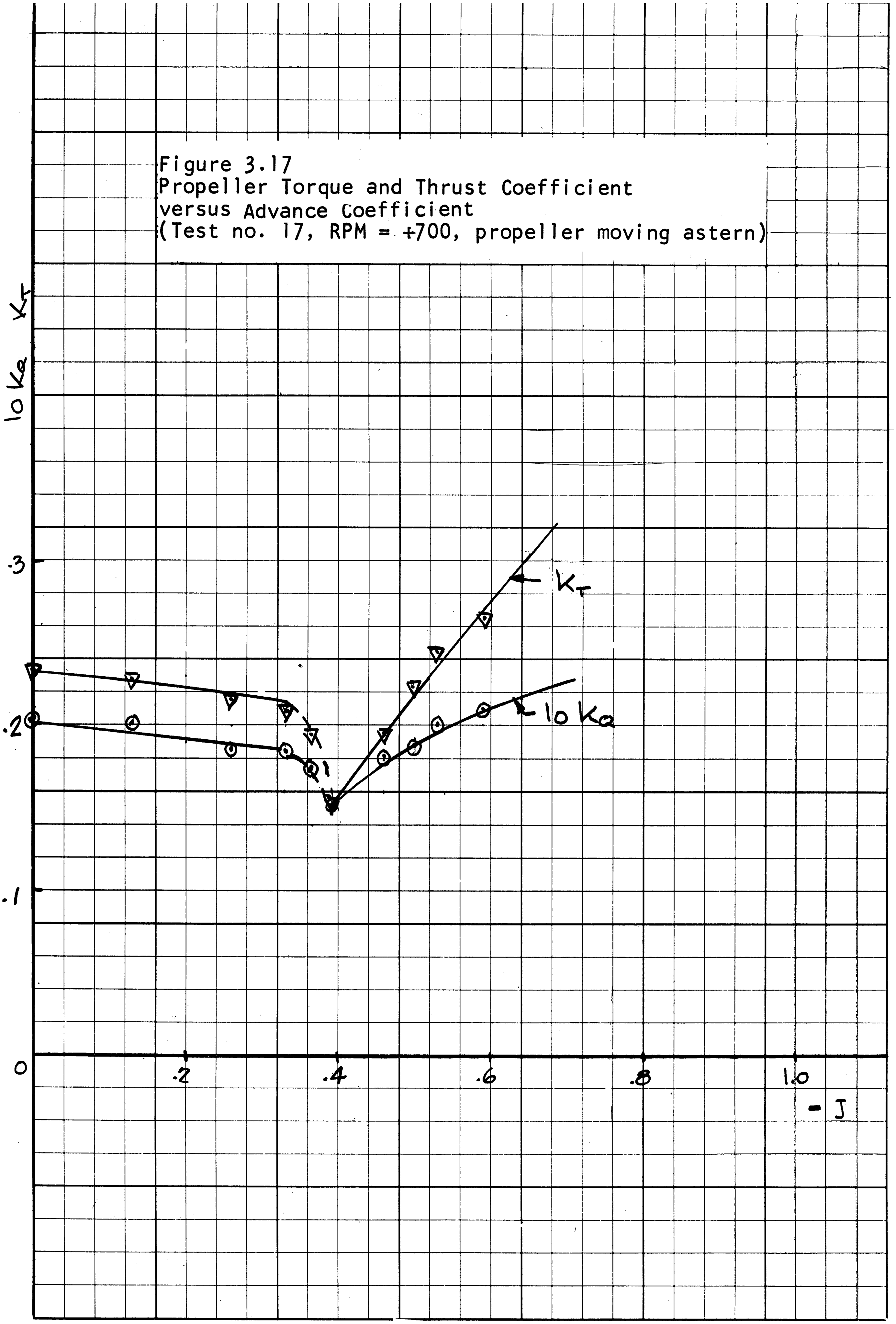

Figure 3.17
Propeller Torque and Thrust Coefficient
versus Advance Coefficient
(Test no. 17, RPM = +700, propeller moving astern)
10 Kq  KT
·3
·2
·1
0
·2
·4
·6
·8
1.0
- J
KT
10 Kq

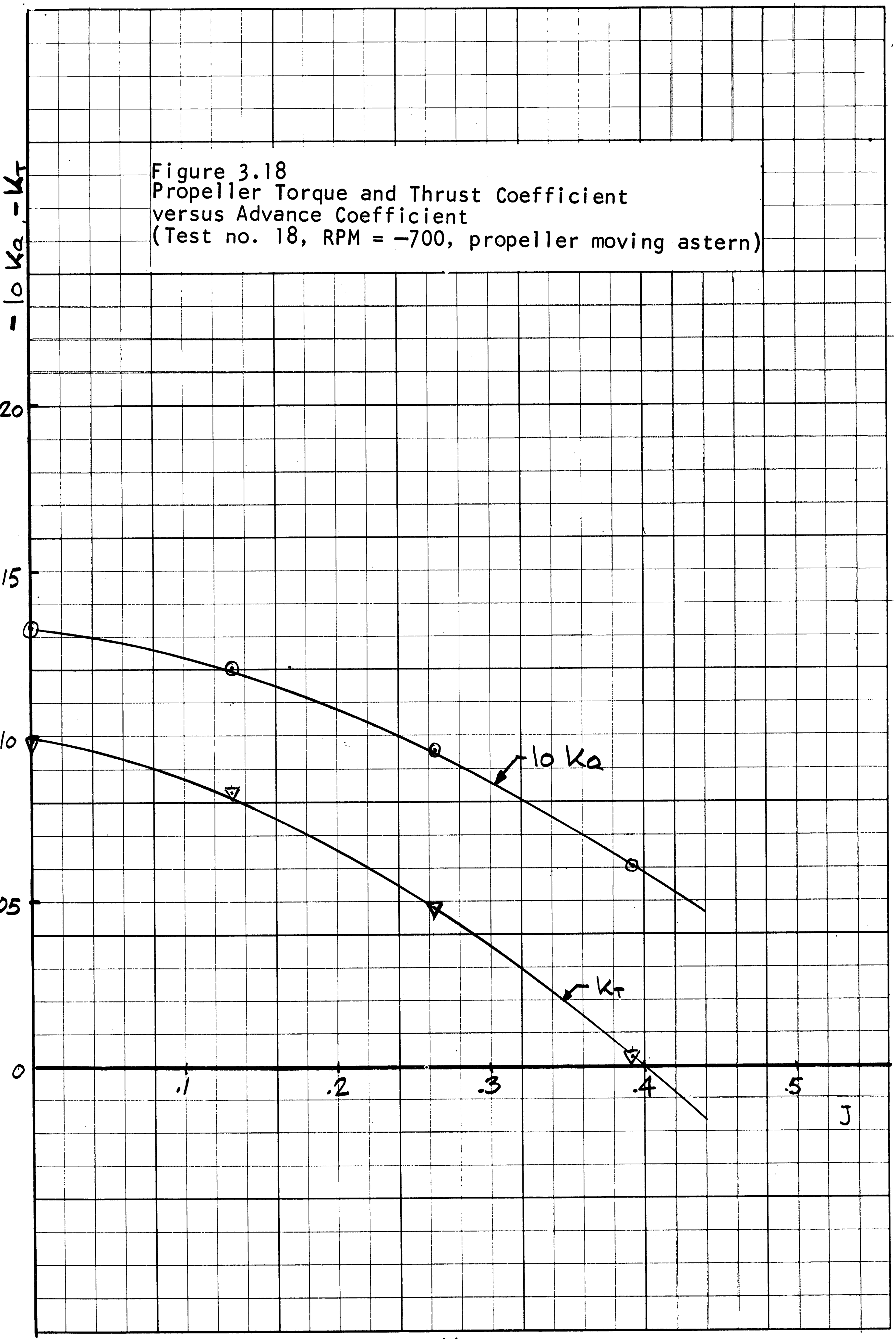


Figure 3.18
Propeller Torque and Thrust Coefficient
versus Advance Coefficient
(Test no. 18, RPM = −700, propeller moving astern)

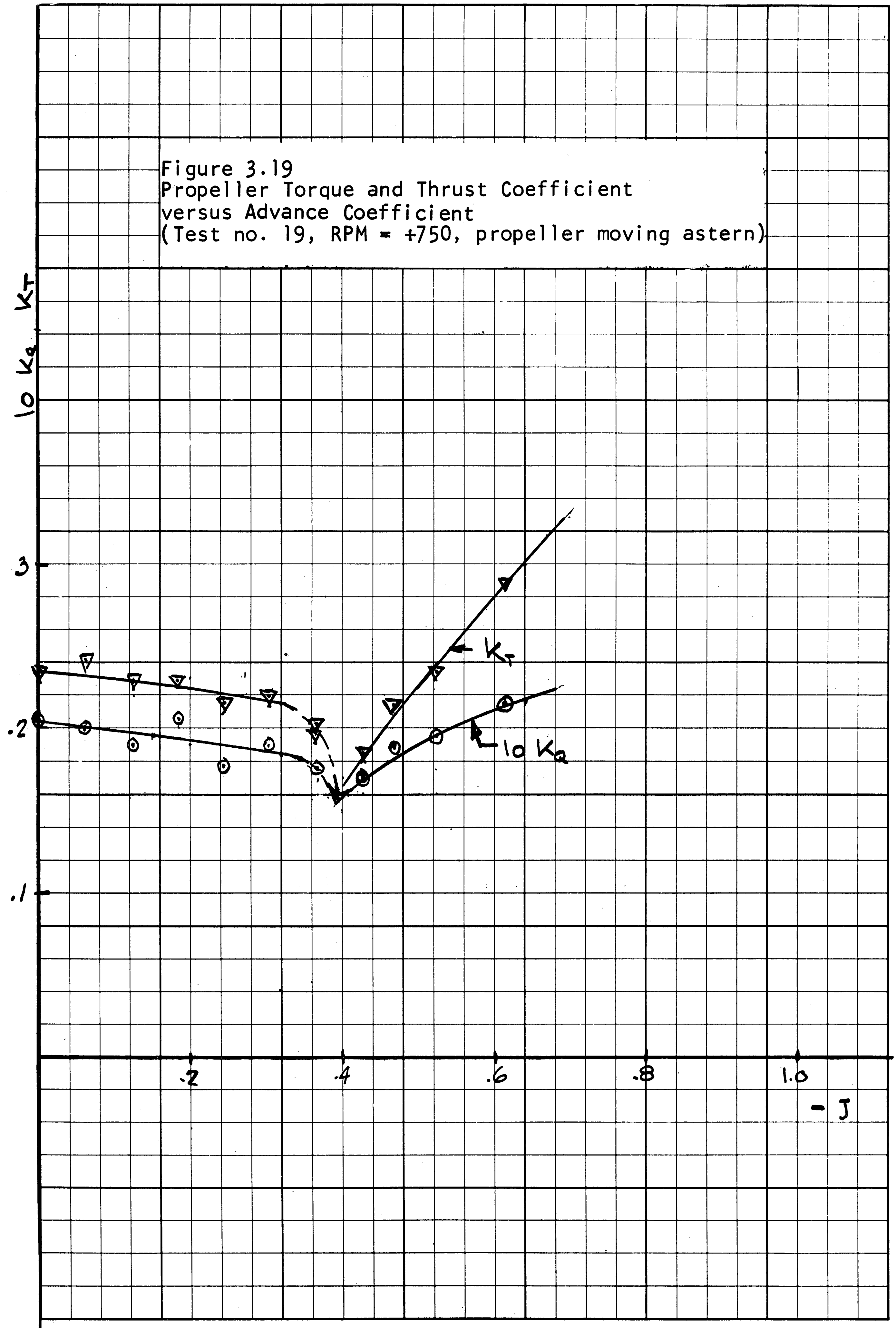

Figure 3.19
Propeller Torque and Thrust Coefficient
versus Advance Coefficient
(Test no. 19, RPM = +750, propeller moving astern)

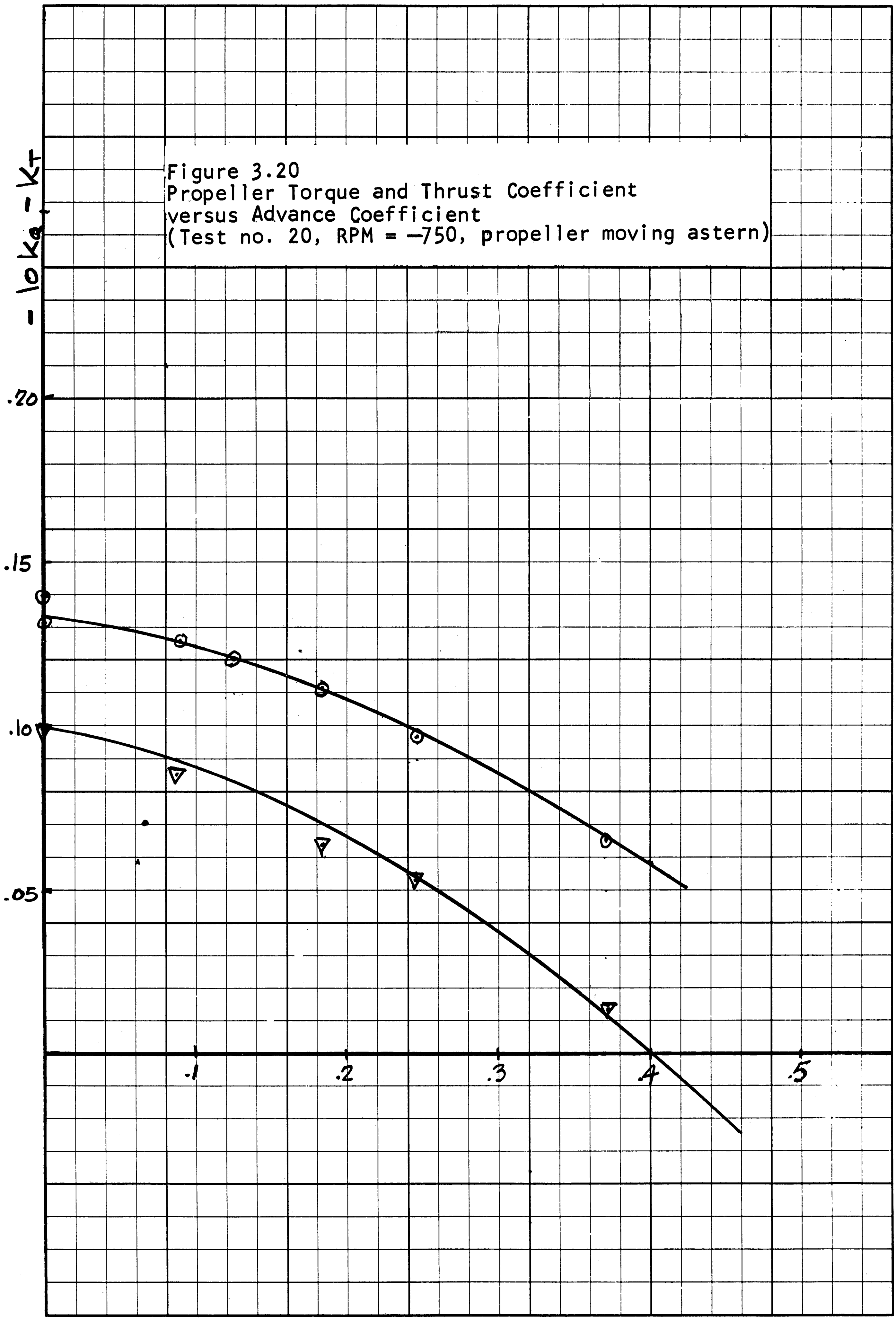


Figure 3.20
Propeller Torque and Thrust Coefficient
versus Advance Coefficient
(Test no. 20, RPM = −750, propeller moving astern)

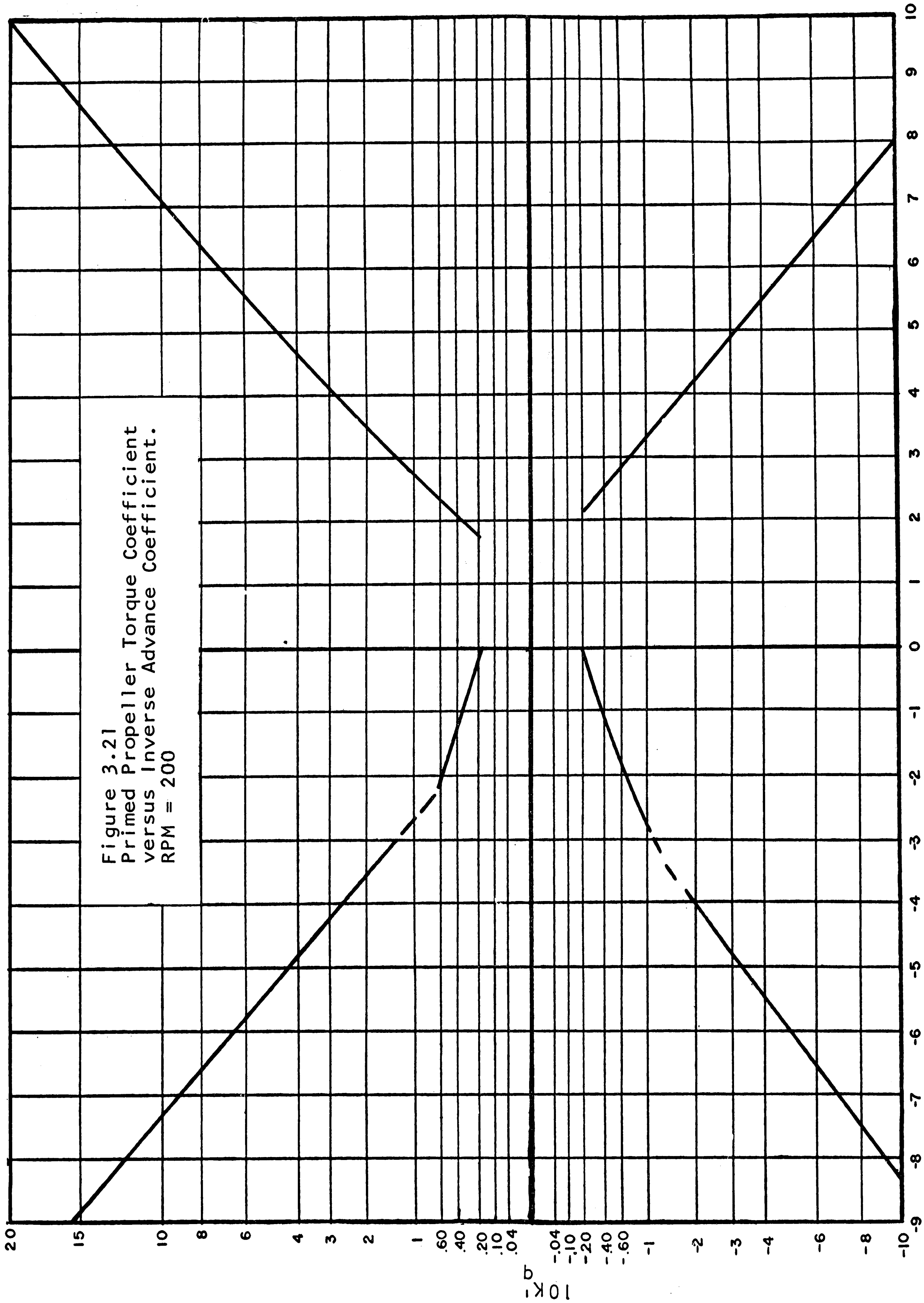


Figure 3.21
Primed Propeller Torque Coefficient
versus Inverse Advance Coefficient.
RPM = 200

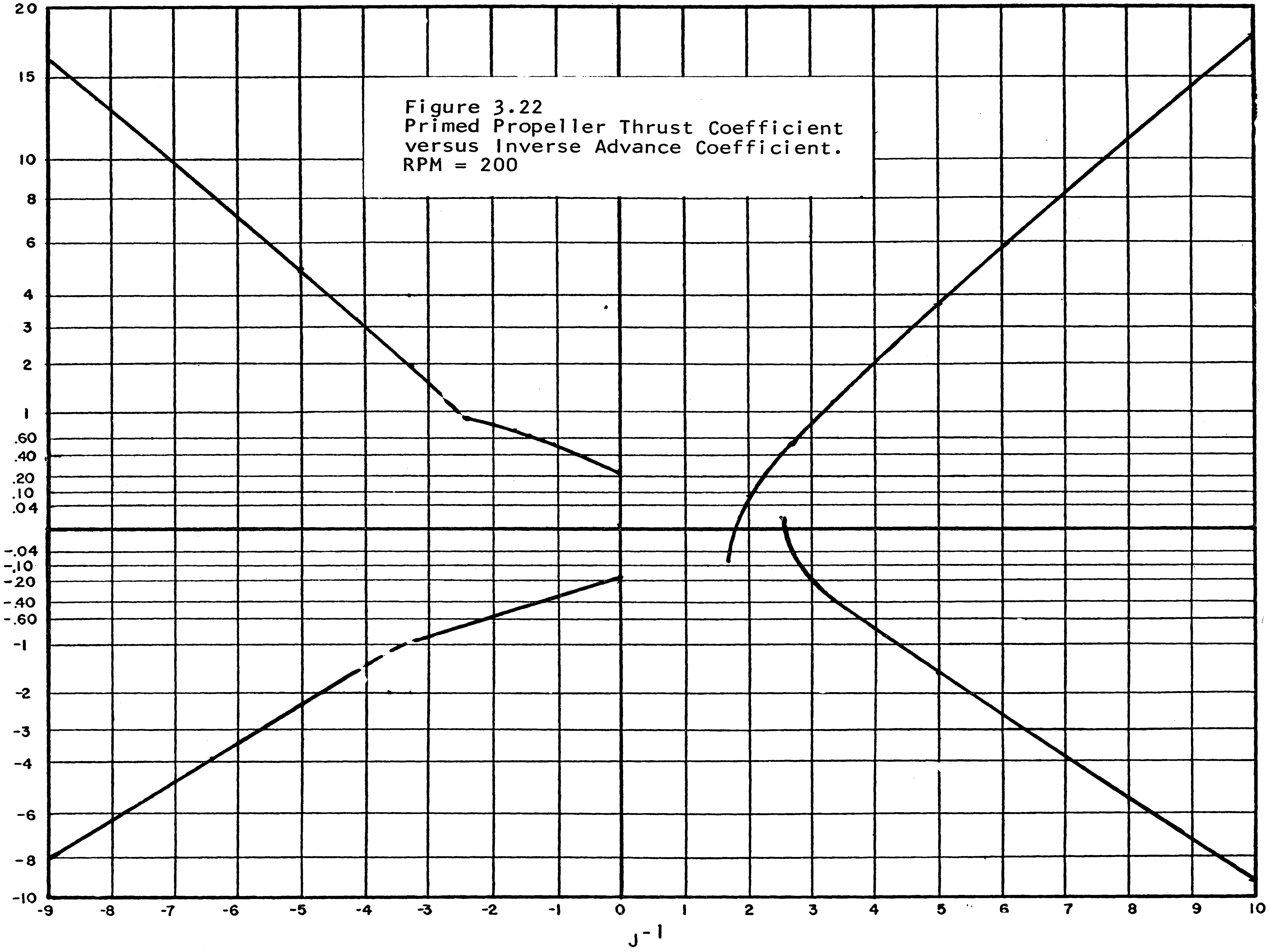


Figure 3.22
Primed Propeller Thrust Coefficient
versus Inverse Advance Coefficient.
RPM = 200

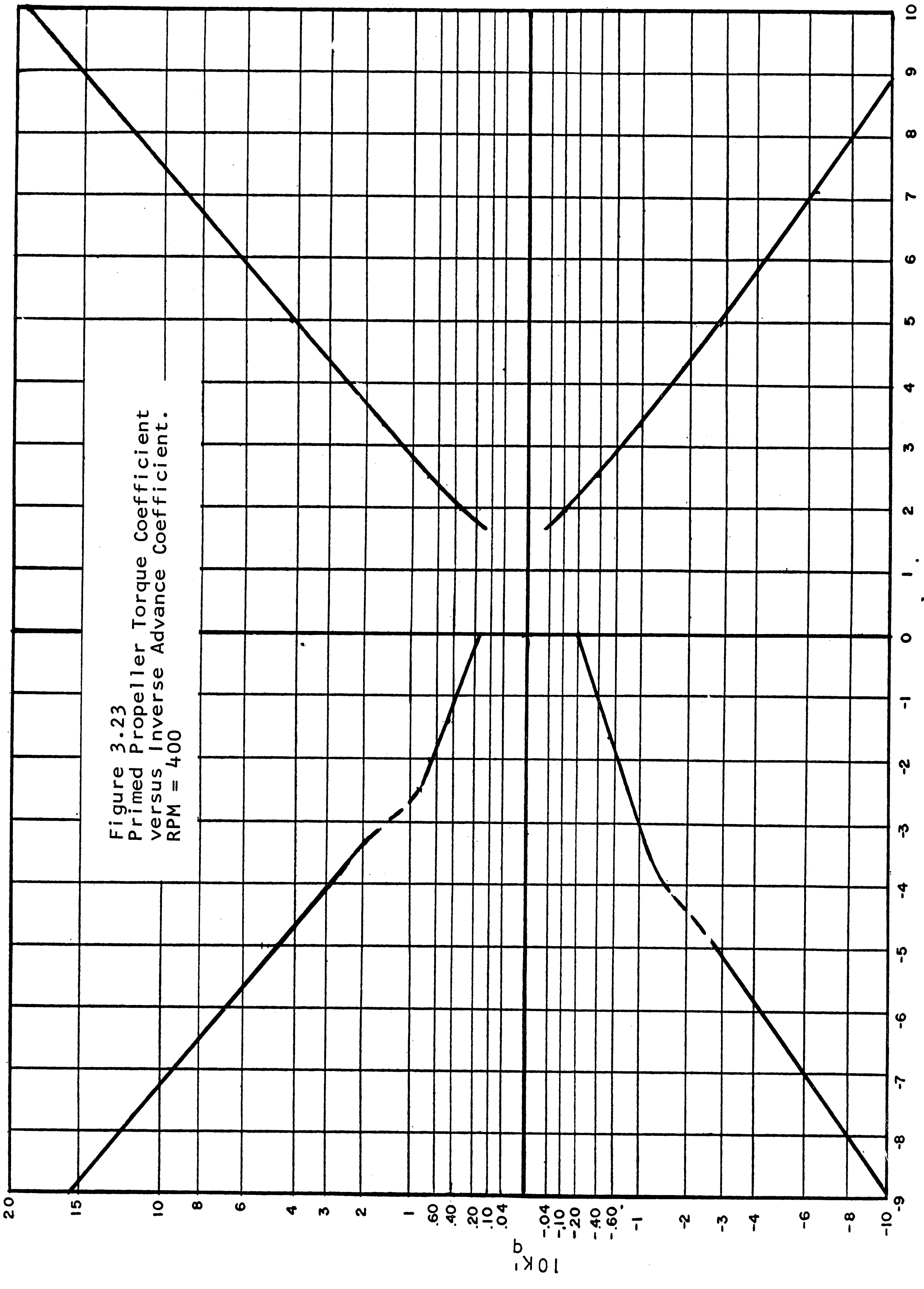


Figure 3.23
Primed Propeller Torque Coefficient versus Inverse Advance Coefficient.
RPM = 400

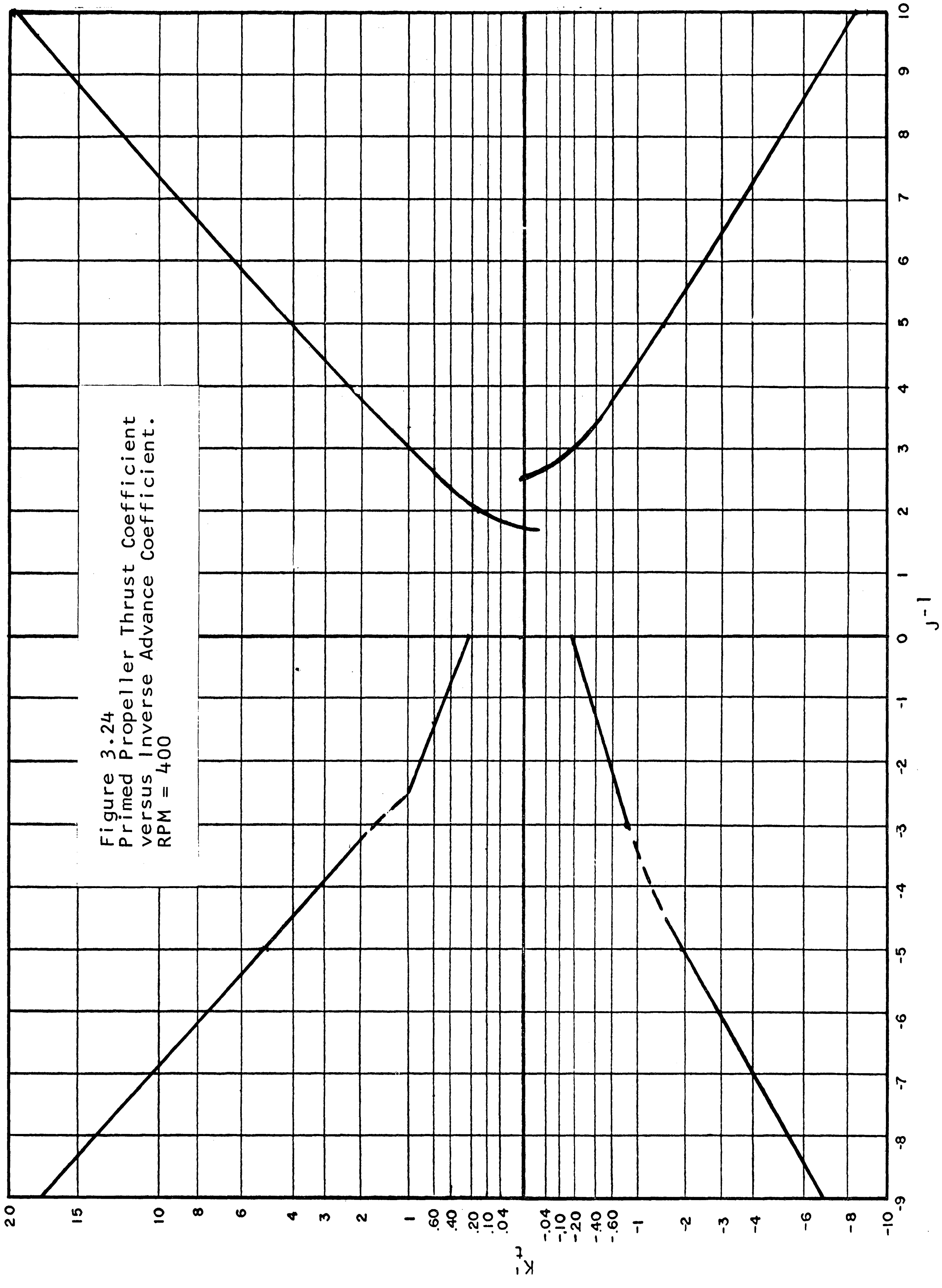


Figure 3.24
Primed Propeller Thrust Coefficient
versus Inverse Advance Coefficient.
RPM = 400

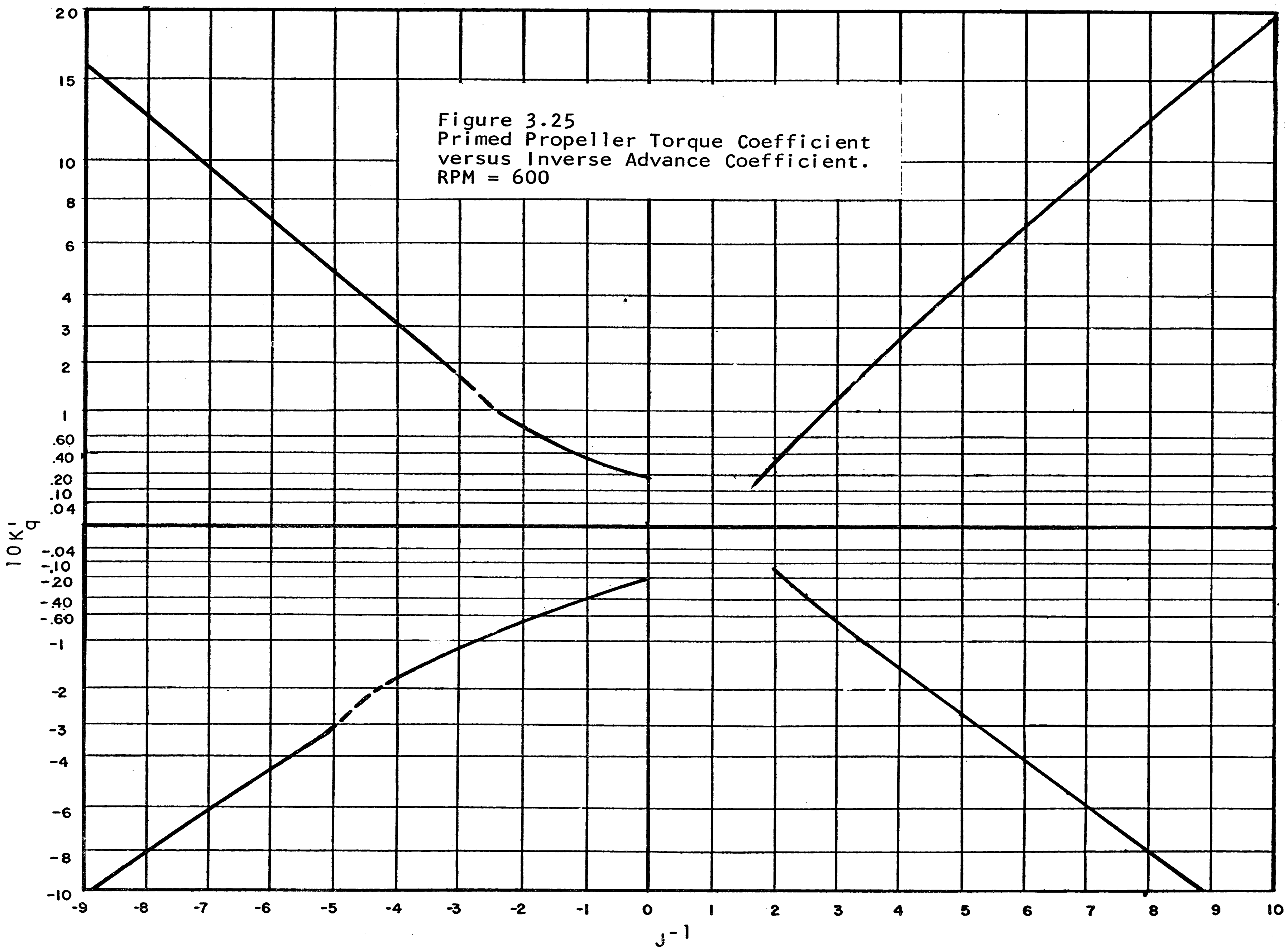


Figure 3.25
Primed Propeller Torque Coefficient versus Inverse Advance Coefficient.
RPM = 600

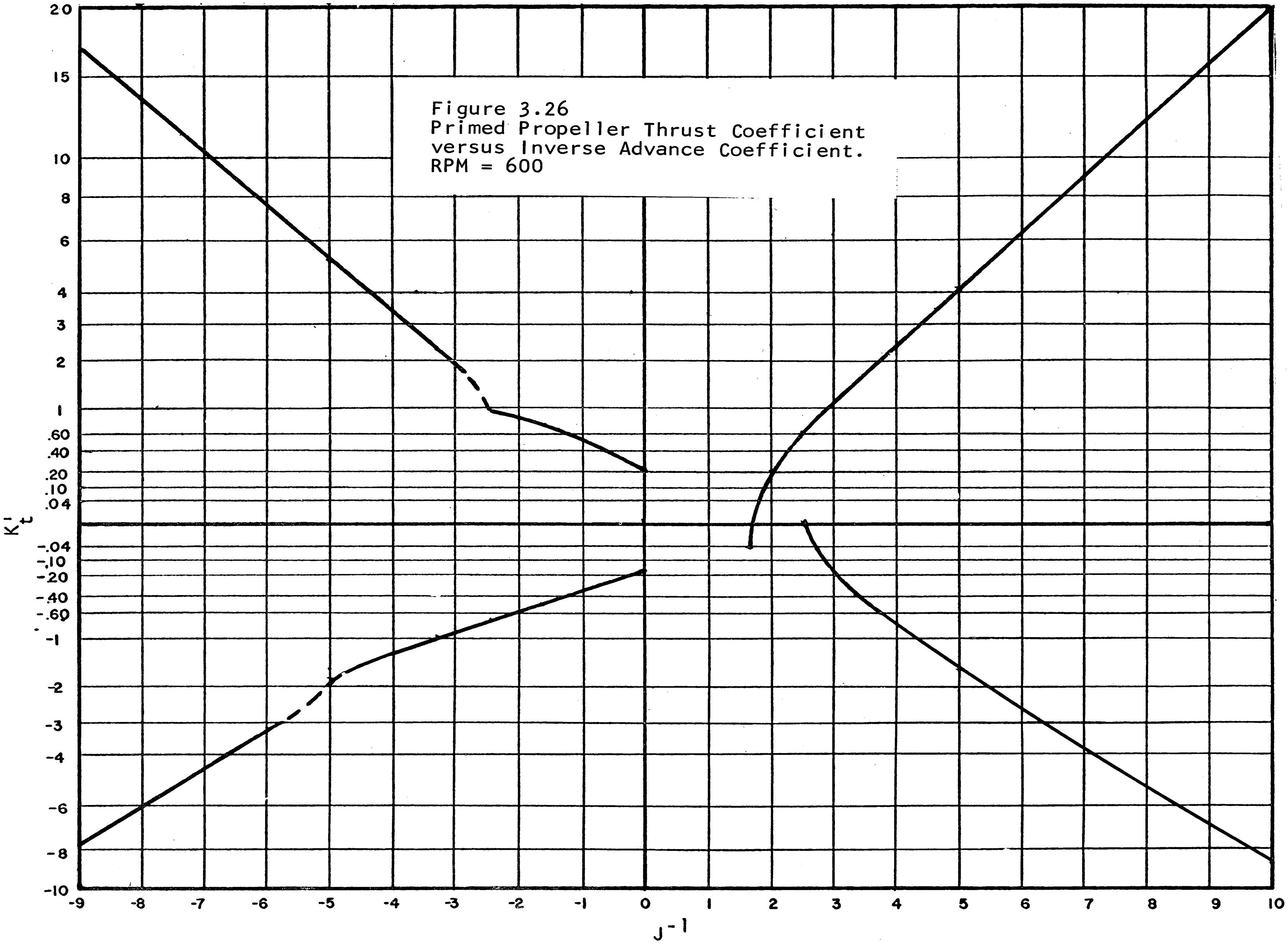


Figure 3.26
Primed Propeller Thrust Coefficient
versus Inverse Advance Coefficient.
RPM = 600

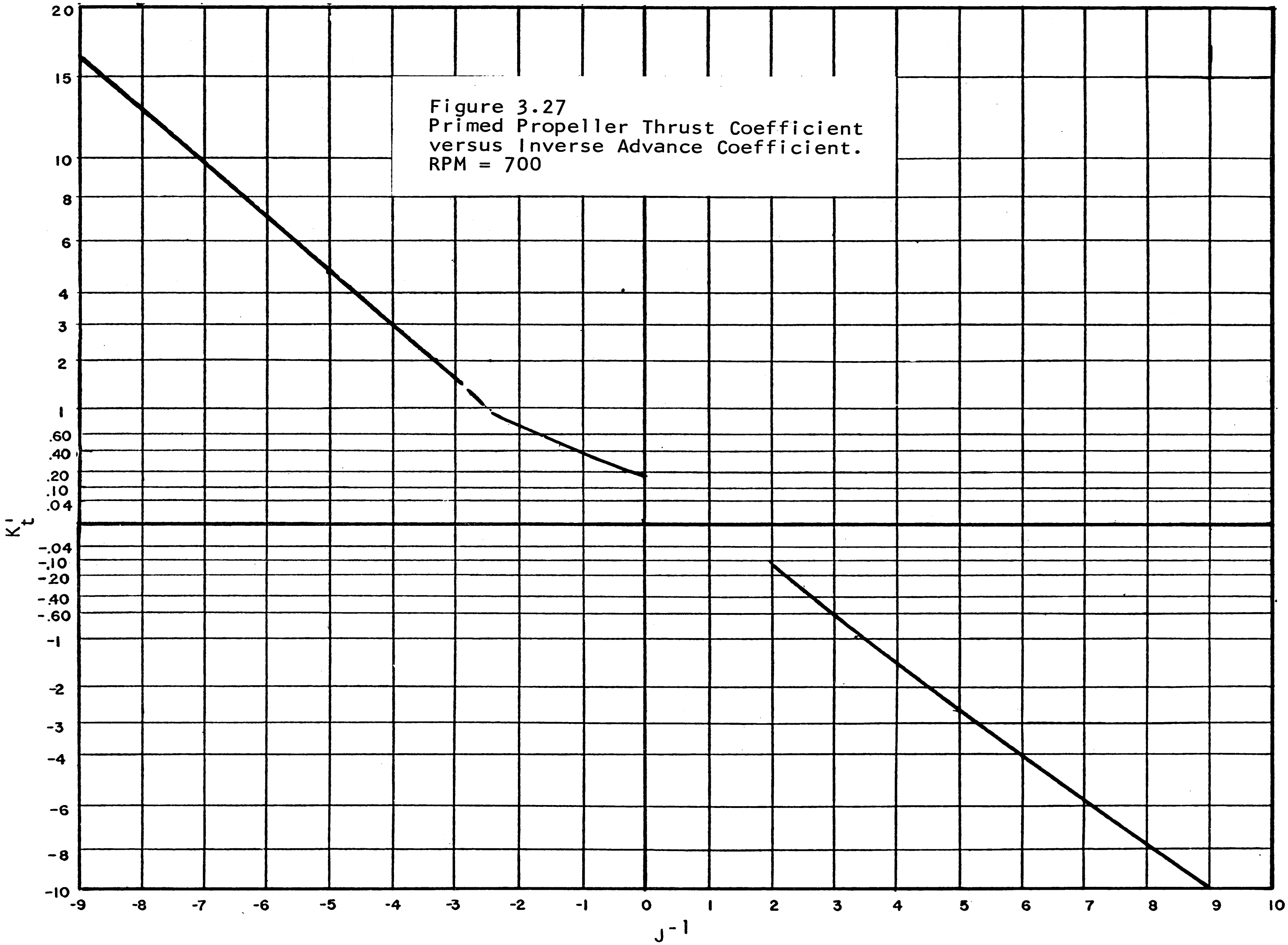


Figure 3.27
Primed Propeller Thrust Coefficient
versus Inverse Advance Coefficient.
RPM = 700

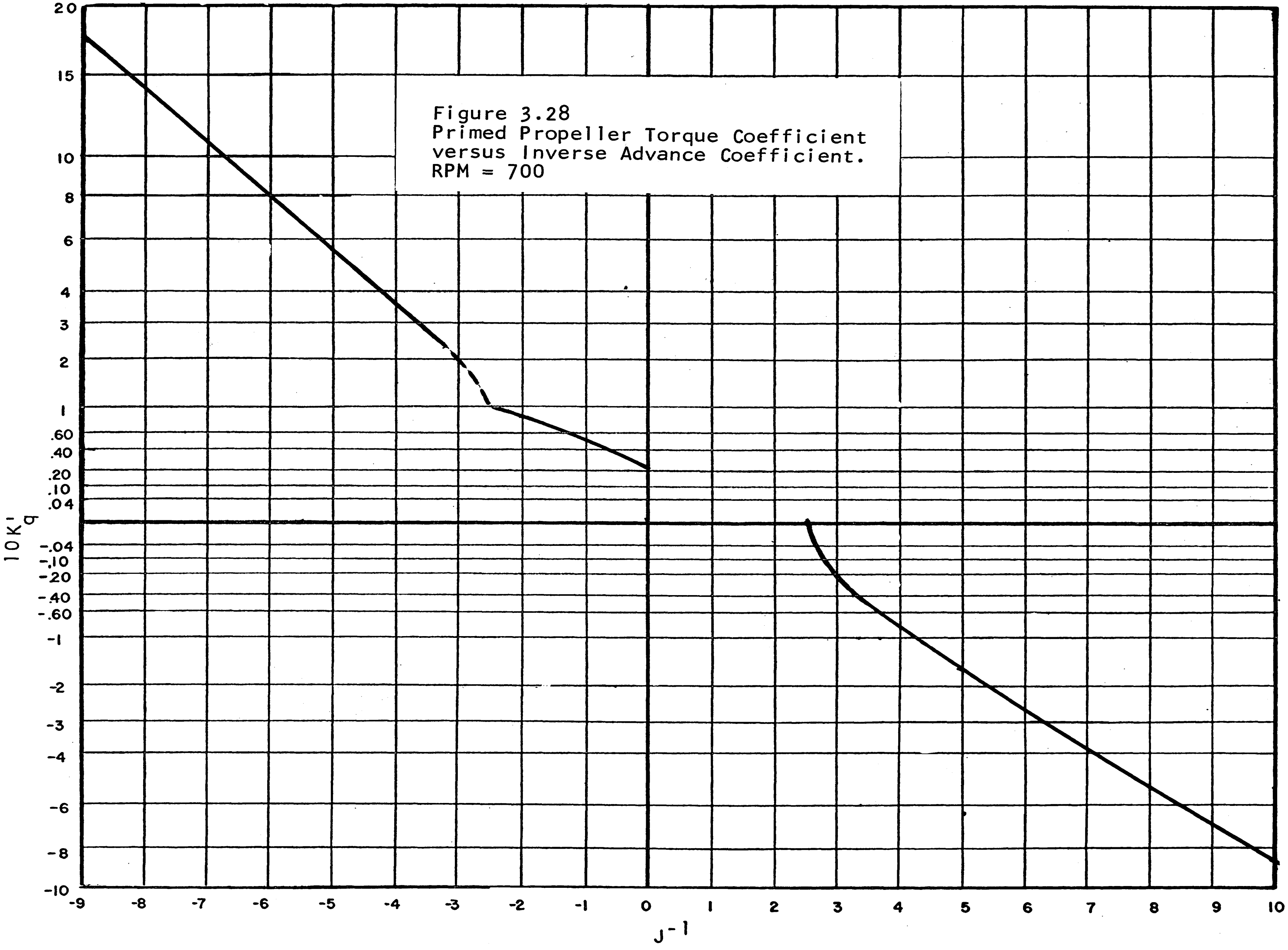


Figure 3.28
Primed Propeller Torque Coefficient
versus Inverse Advance Coefficient.
RPM = 700

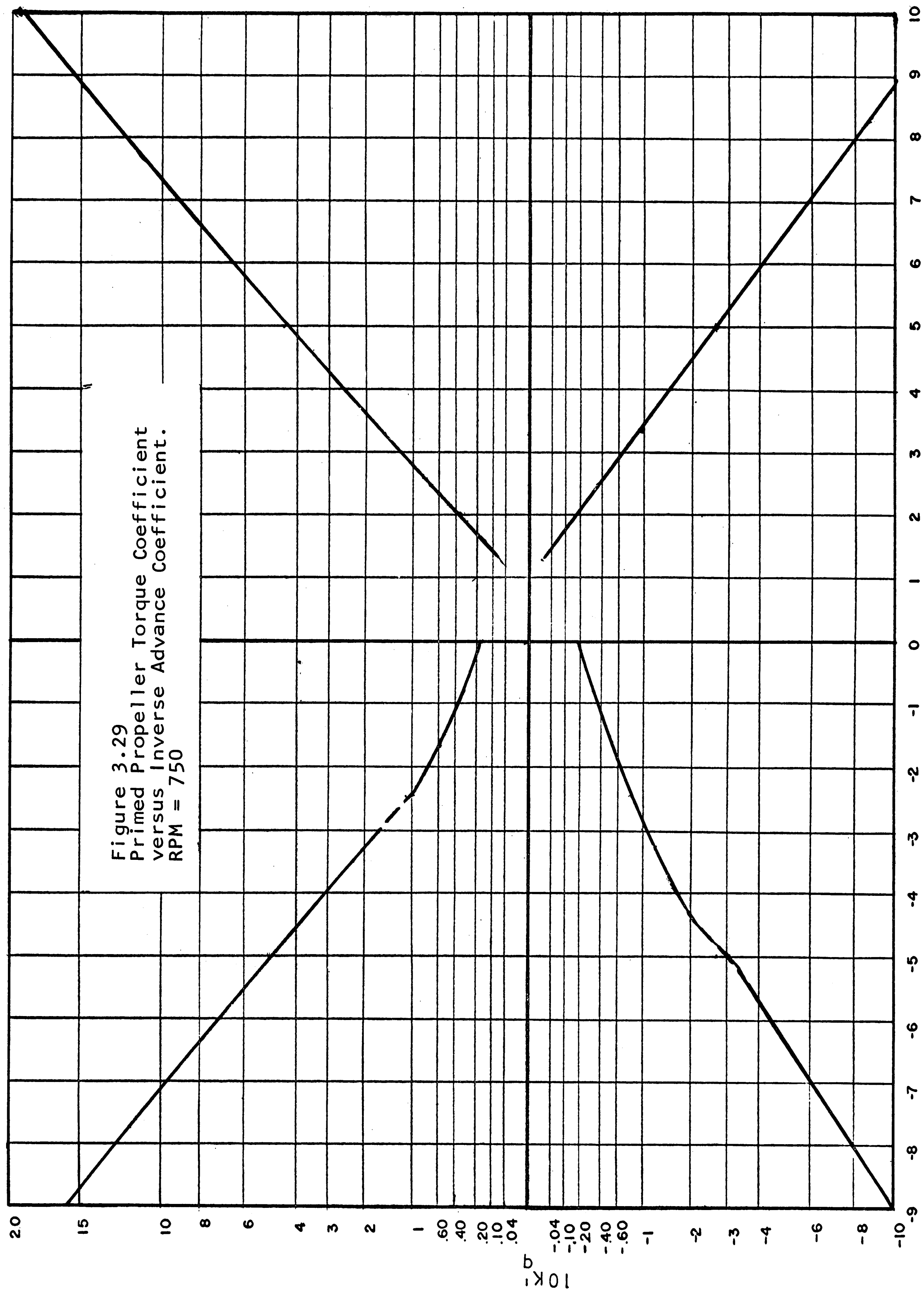


Figure 3.29
Primed Propeller Torque Coefficient
versus Inverse Advance Coefficient.
RPM = 750

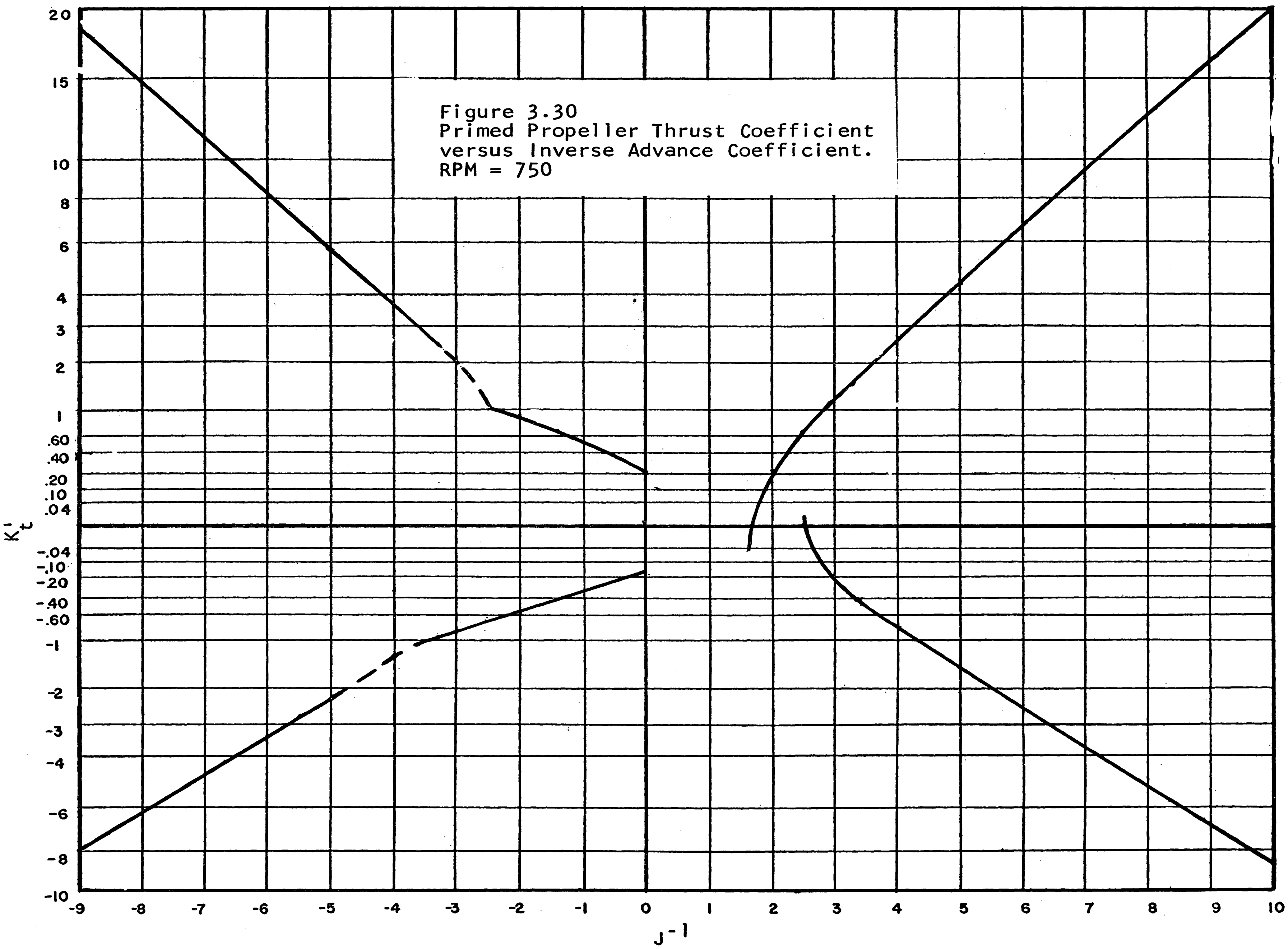


Figure 3.30
Primed Propeller Thrust Coefficient
versus Inverse Advance Coefficient.
RPM = 750

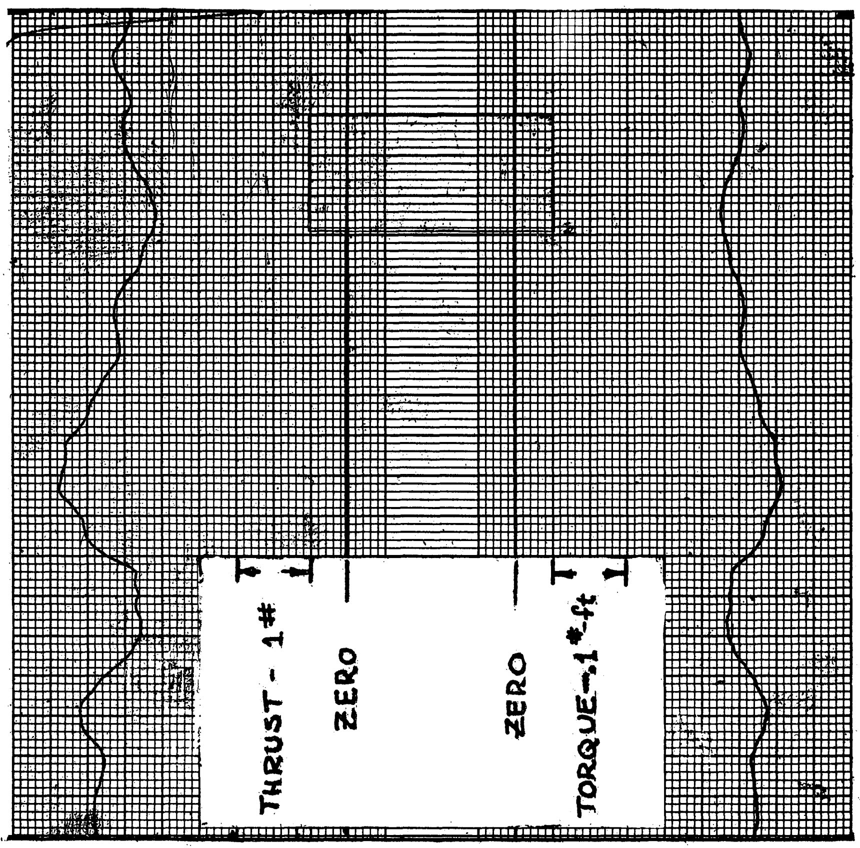


Figure 3.31
Typical Propeller Test Record from Test No. 4;
RPM = -600, Carriage Speed 1.05 Ft/Sec.

## 4. FLOW STUDIES

To observe more closely the large scale separations and eddy flows around the stern of the model, tufts were cemented to the model and movies as well as still pictures were taken under various operating conditions. A 16mm movie film entitled "Project Mohole: Flow Observations on the Starboard Hull" should be considered part of this report. The movie shows the flow around the stern of the model, in both transit and drilling conditions, with and without the propeller operating, at various angles to the flow, with and without the vertical fins. They also show the irregular motion of the wake wheels in the drilling condition. In some runs a wax chip of neutral buoyancy is allowed to move in the flow field near the stern, illustrating in a qualitative sense the large temporal and spatial velocity variations present in the flow.

The still pictures, Figures 4.1 through 4.10 need little explanation in addition to their captions except to note that the propeller appears to have little effect on the flow around the stern. The separated regions, which in the transit condition are clearly caused by the presence of the free surface, remain largely the same size regardless of whether the propeller is operating or not. The propeller in all cases, is operating at an RPM sufficient to propel the hull straight ahead at 10 knots. However, all pictures were taken with the model rigidly clamped at a fixed heading angle.

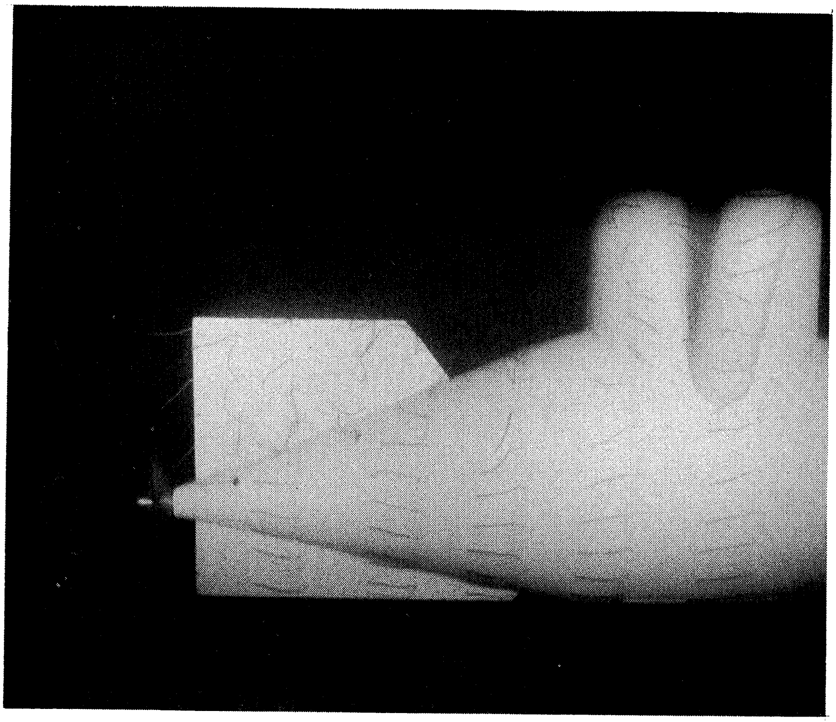

Figure 4.1
65' Draft; 0° Heading; Self-Propelled;
Fins on.

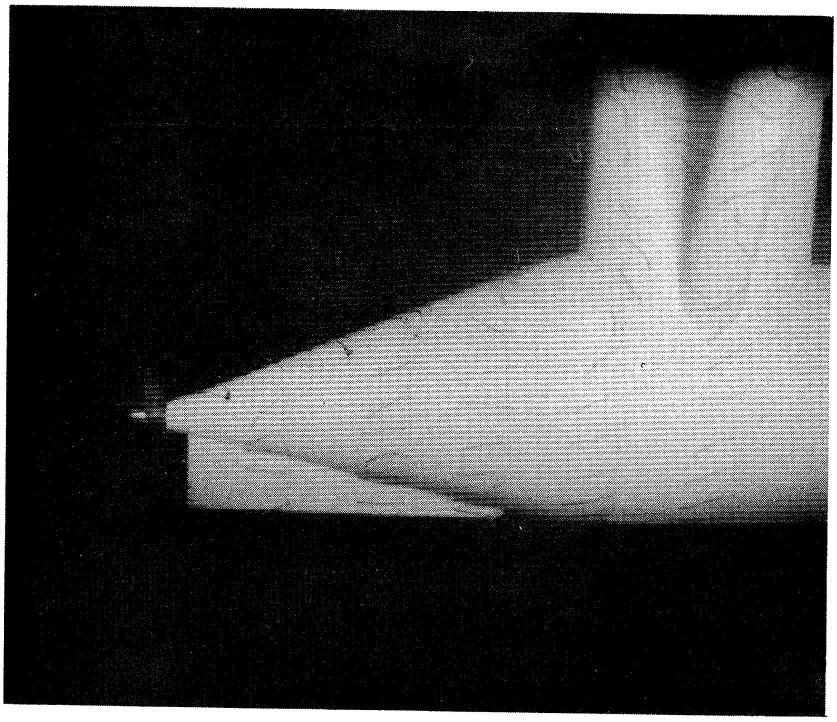

Figure 4.2
65' Draft; 0° Heading; Ship Speed 10 Knots;
Tom Fin Removed.

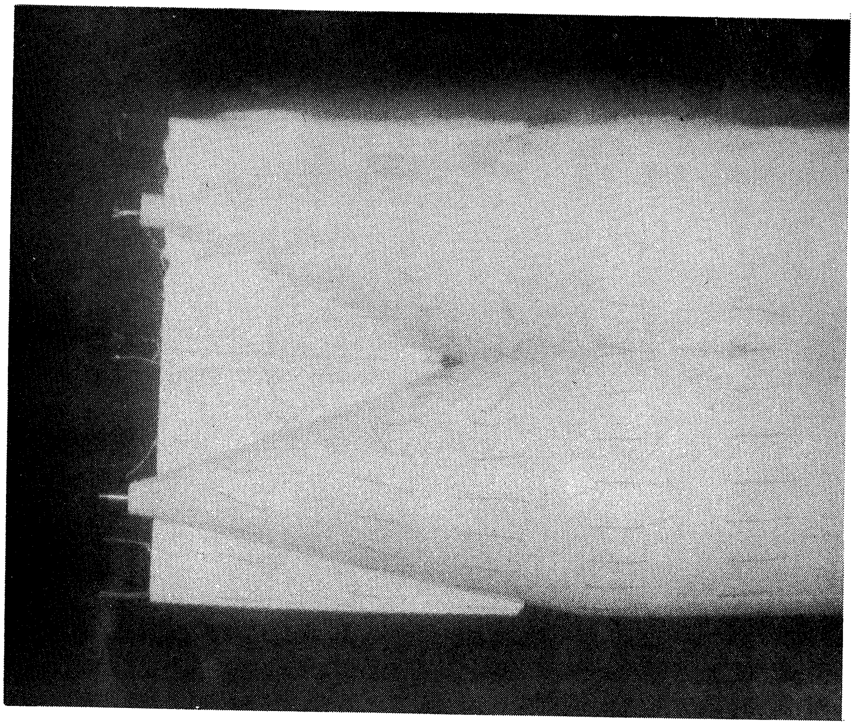

Figure 4.3
29' Draft; $0^{o}$ Heading; Ship Speed 10 Knots;
No Propeller; Fins On.

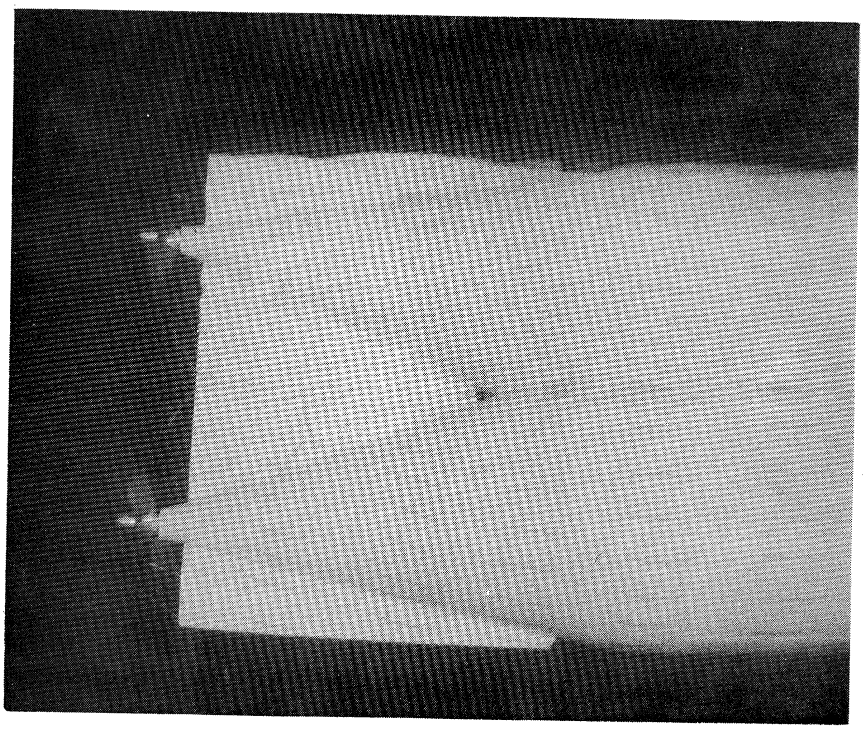

Figure 4.4
29' Draft; $0^{o}$ Heading; Ship Speed 10 Knots;
Self-Propelled; Fins On.

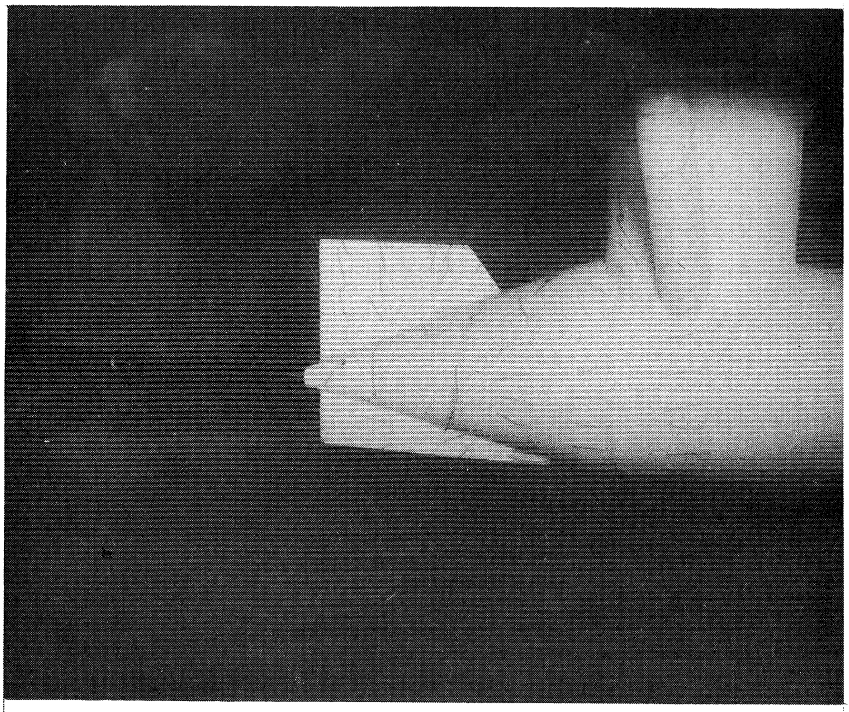

Figure 4.5
65' Draft; 20$^{o}$ Heading; Downstream Side;
Ship Speed 10 Knots; No Propeller; Fins On.

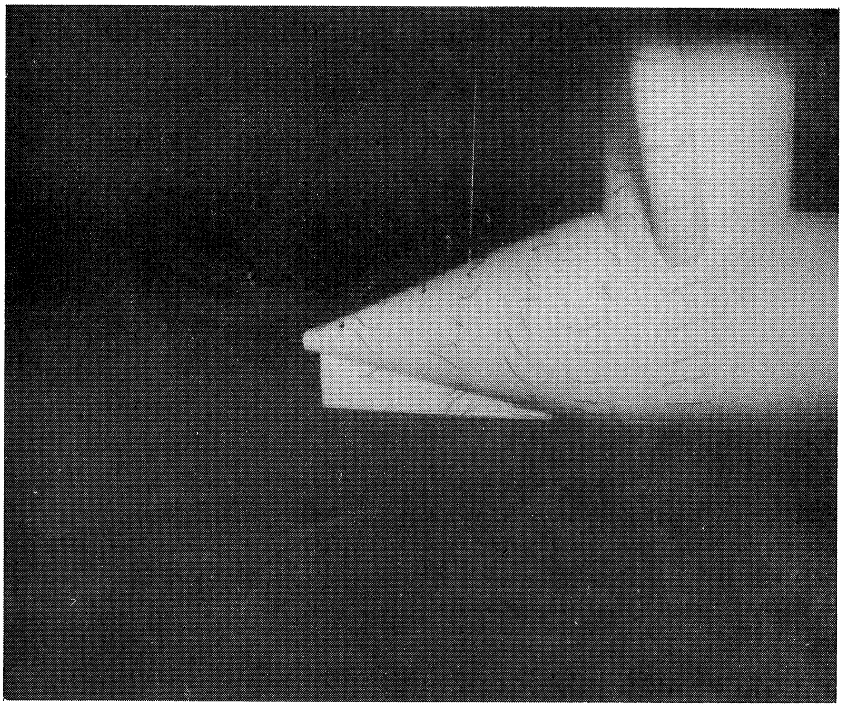

Figure 4.6
65' Draft; 20$^{o}$ Heading; Downstream Side;
Ship Speed 10 Knots; No Propeller;
Top Fin Removed.

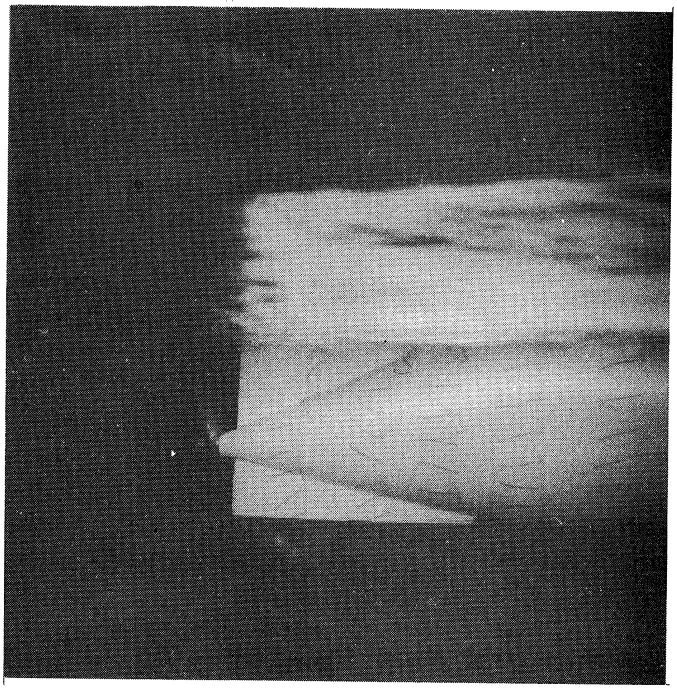

Figure 4.7
29' Draft; $20^{o}$ Heading; Downstream Side;
Ship Speed 10 Knots; Self-Propelled;
Fins on.

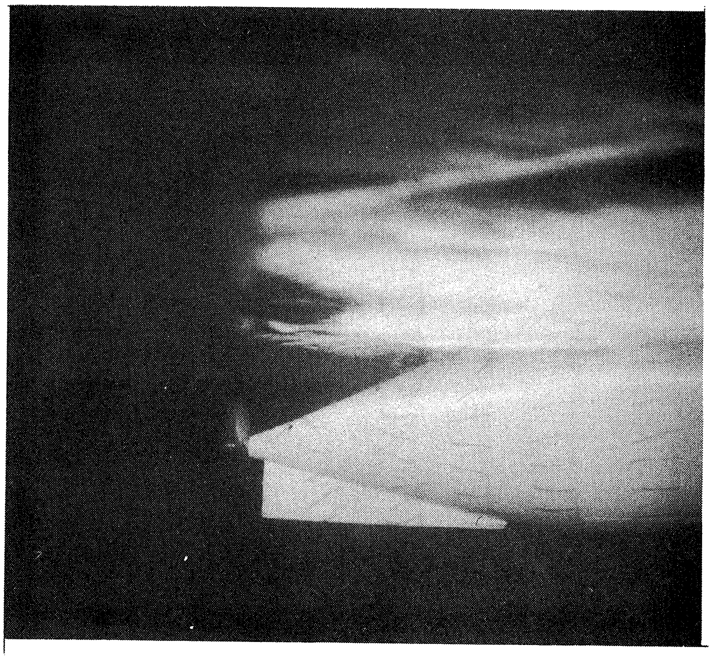

Figure 4.8
29' Draft; $20^{o}$ Heading; Downstream Side;
Ship Speed 10 Knots; Self-Propelled;
Top Fin Removed.

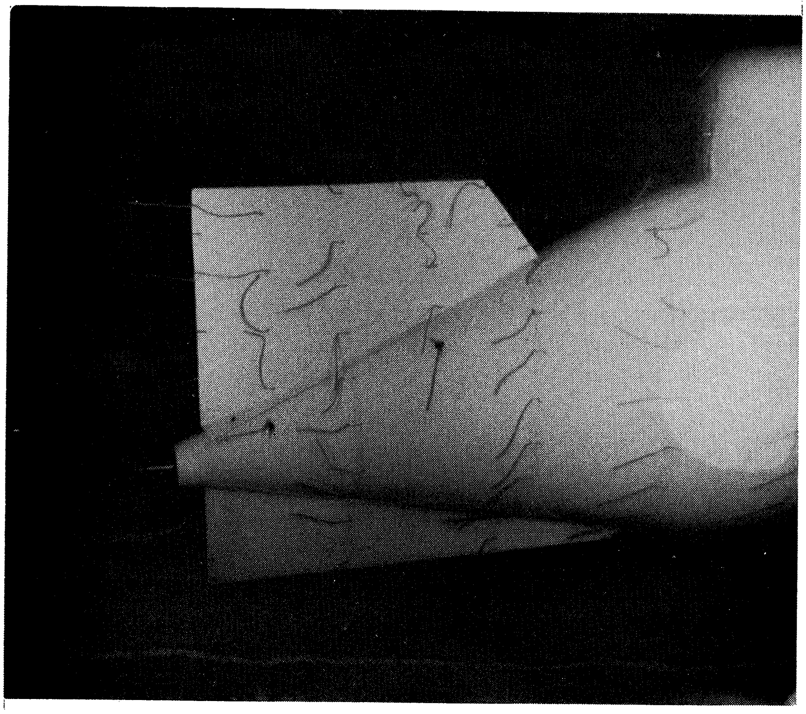

Figure 4.9
65' Draft; 20° Heading; Upstream Side;
Ship Speed 10 Knots; No Propeller;
Fins On.

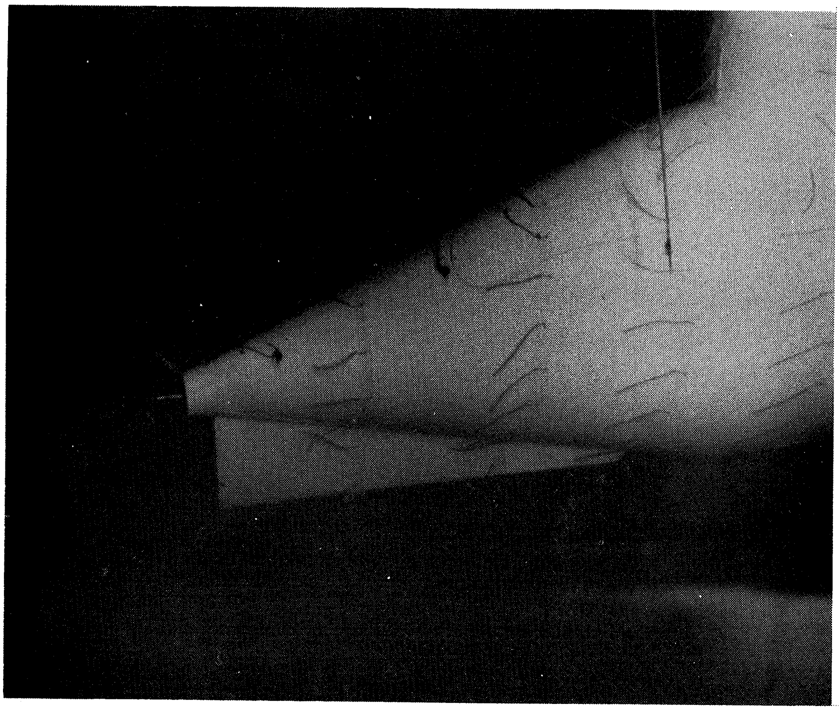

Figure 4.10
65' Draft; 20° Heading; Upstream Side;
Ship Speed 10 Knots; No Propeller;
Top Fin Removed.

BIBLIOGRAPHY

1. Michelsen, F. C. and Rabe, N., "Model Tests of Project Mohole Drilling Platform," University of Michigan, Department of Naval Architecture and Marine Engineering, Report No. 06333-1-F, August 1964.

2. Gebhardt, J. C. and Michelsen, F. C., "High Response Pitot Tube Techniques for Measurements of Time and Space Variations of the Velocity Distribution in the Wake of a Ship Model," Paper presented at the United States--Japan Seminar on Instrumentation for Hydraulic Research, Tokyo, Japan, April 7-15, 1965.

3. Gebhardt, J. C., "The Direct Conversion of Analog Data to a Form Usable by the IBM 7090 Computer," University of Michigan, Department of Naval Architecture and Marine Engineering, Report, May 1966.

# APPENDIX

## Additional Propeller Tests

To investigate the dependence of pitch-diameter ratio on the performance of the Mohole main propulsion propellers, additional propeller tests were run on a white metal casting of the same dimensions as the original model propeller. The pitch-diameter ratio at the .7 radius was .509 for the casting compared with .505 for the original. The two models were remarkably alike in all respects except that the blades of the casting were a maximum of 5% thinner than those of the original near the leading edges.

The pitch-diameter ratio was varied by merely cutting off the blade tips at a constant radius thereby decreasing d and increasing P/d. Five different diameters were tested after the original casting was tested. Figures A-1 through A-6 show the results of these tests. The torque and thrust coefficients which are plotted were calculated using the actual diameter of the propeller, not the original diameter. In Figure A-7 the thrust and torque coefficients obtained with the propeller turning backwards and moving astern are plotted. The pitch-diameter was .539 during this test. Figures A-8 and A-9 show the relationship between the torque and thrust coefficients and pitch diameter ratio at zero speed of advance.

The limited data taken at large advance coefficients made it difficult to judge the influence of diameter on the peak efficiency. However, it appears that the peak efficiency increases slightly as the diameter advances.

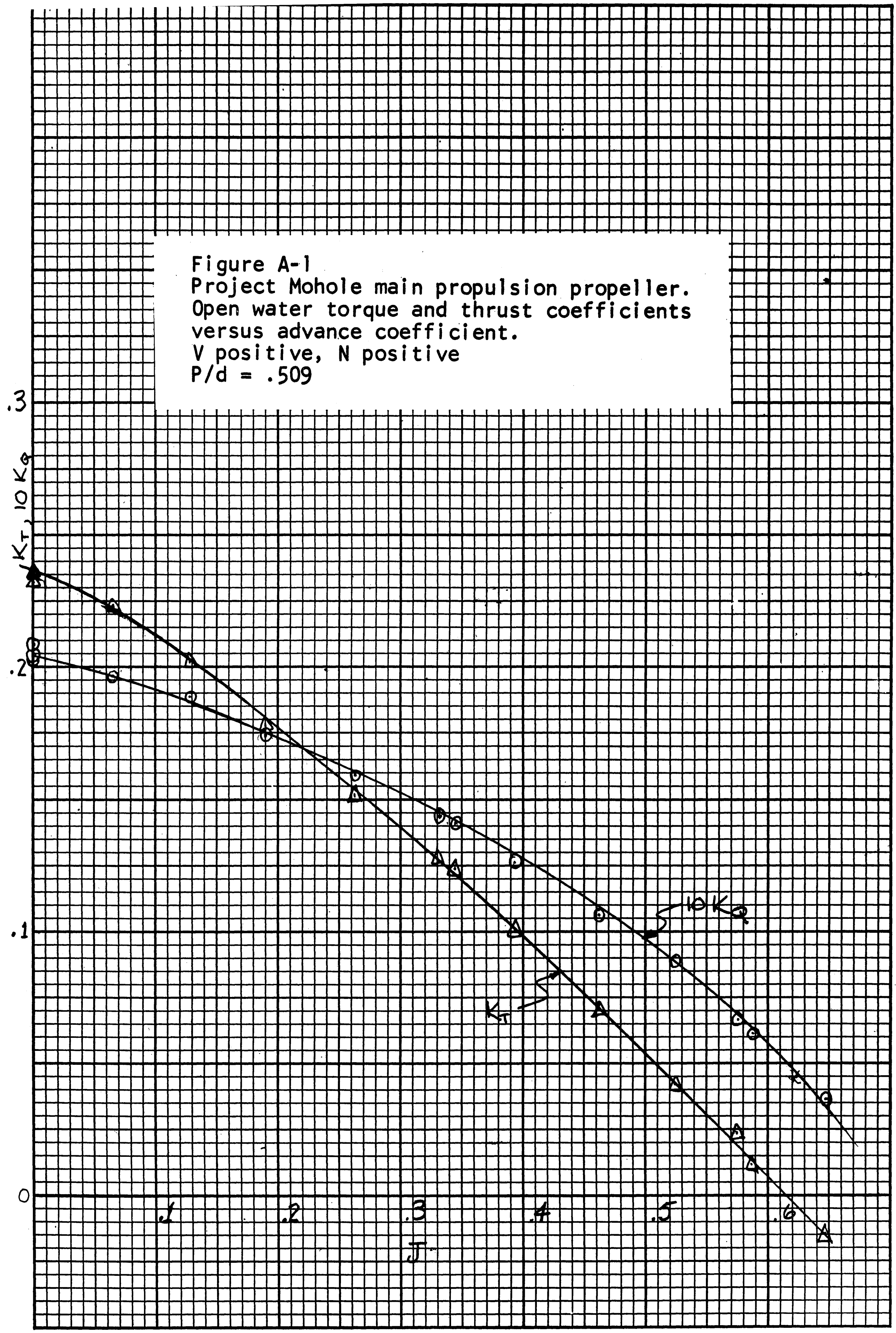


Figure A-1
Project Mohole main propulsion propeller.
Open water torque and thrust coefficients
versus advance coefficient.
V positive, N positive
P/d = .509

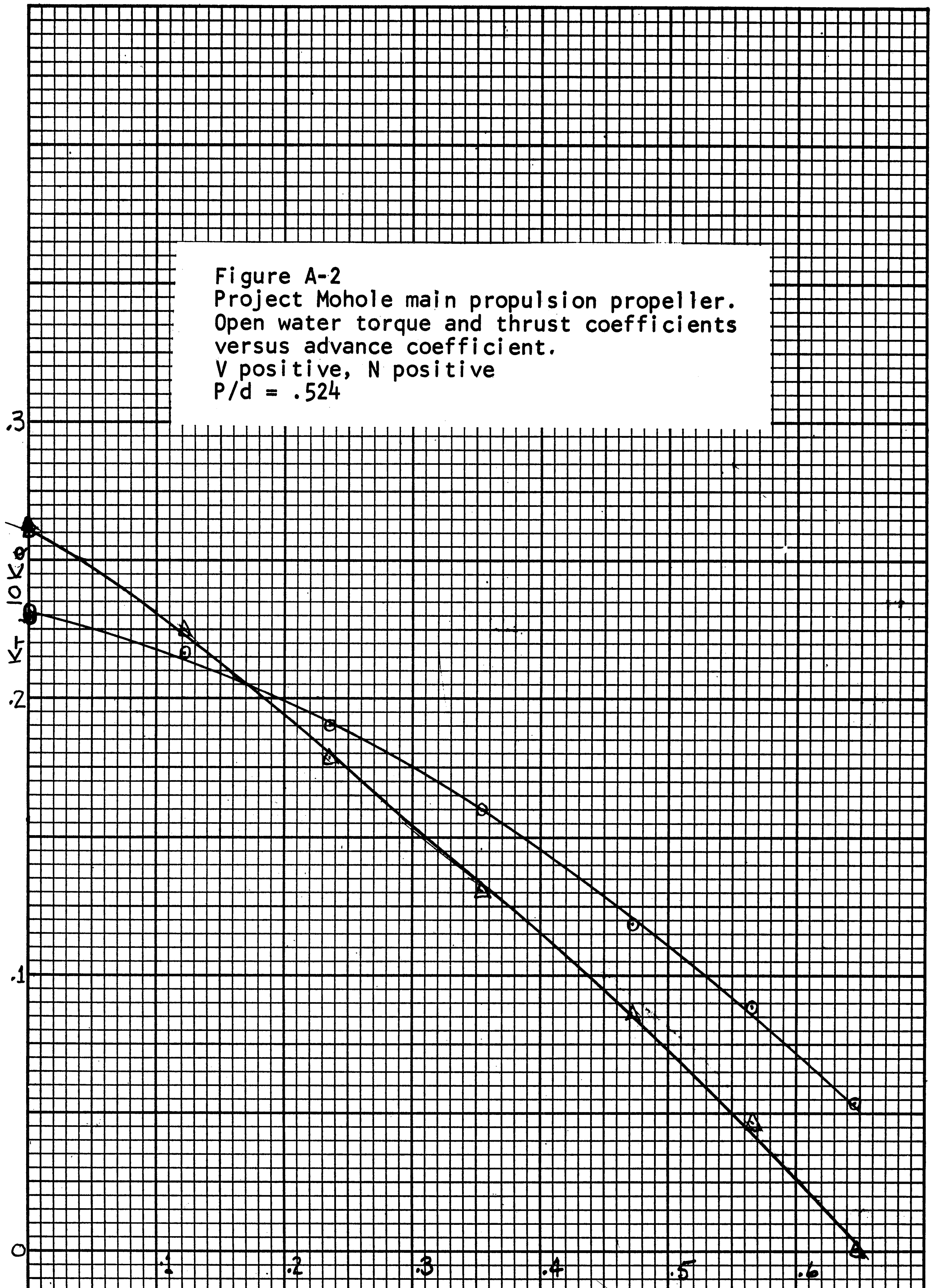


Figure A-2
Project Mohole main propulsion propeller.
Open water torque and thrust coefficients
versus advance coefficient.
V positive, N positive
P/d = .524

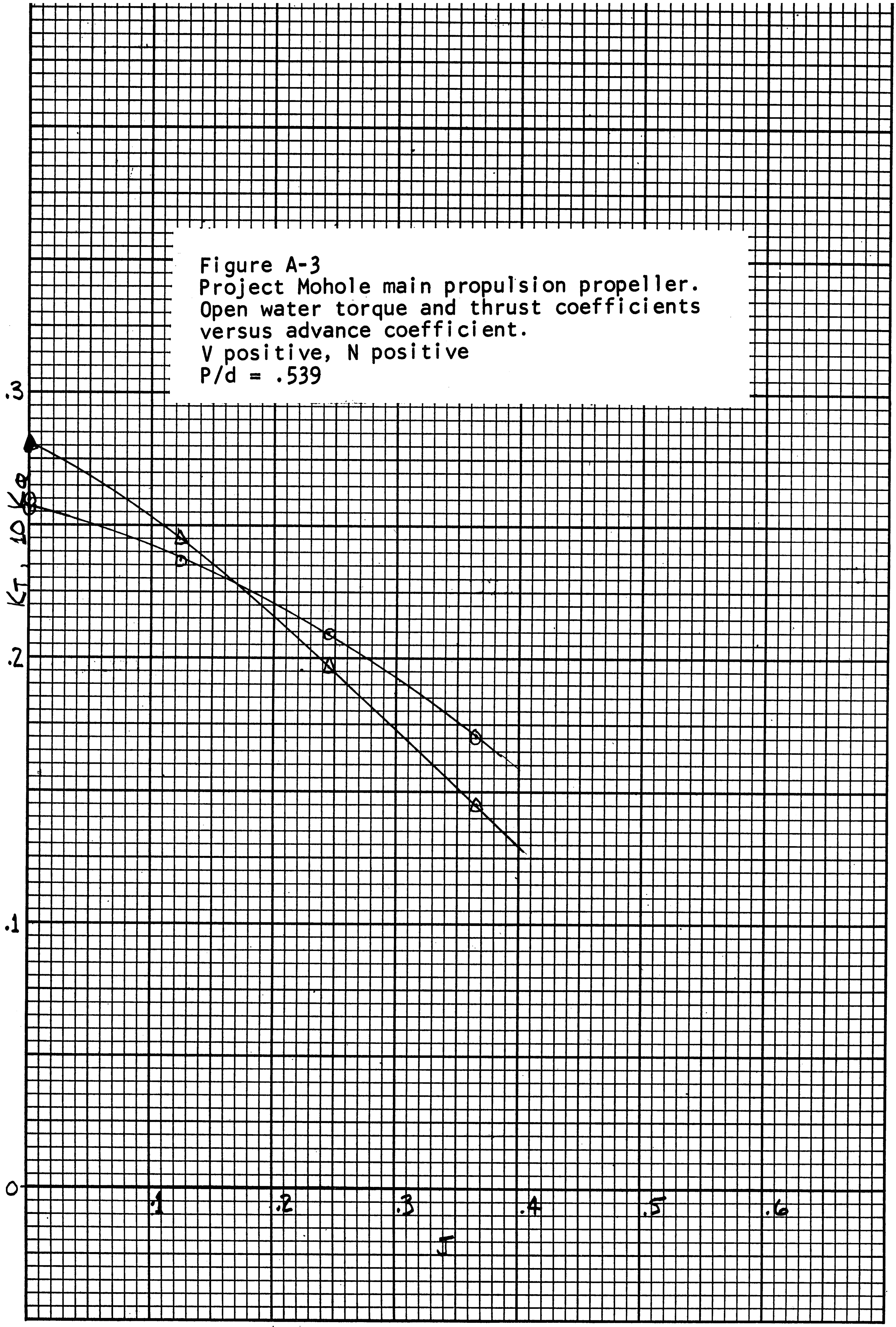


Figure A-3
Project Mohole main propulsion propeller.
Open water torque and thrust coefficients
versus advance coefficient.
V positive, N positive
P/d = .539

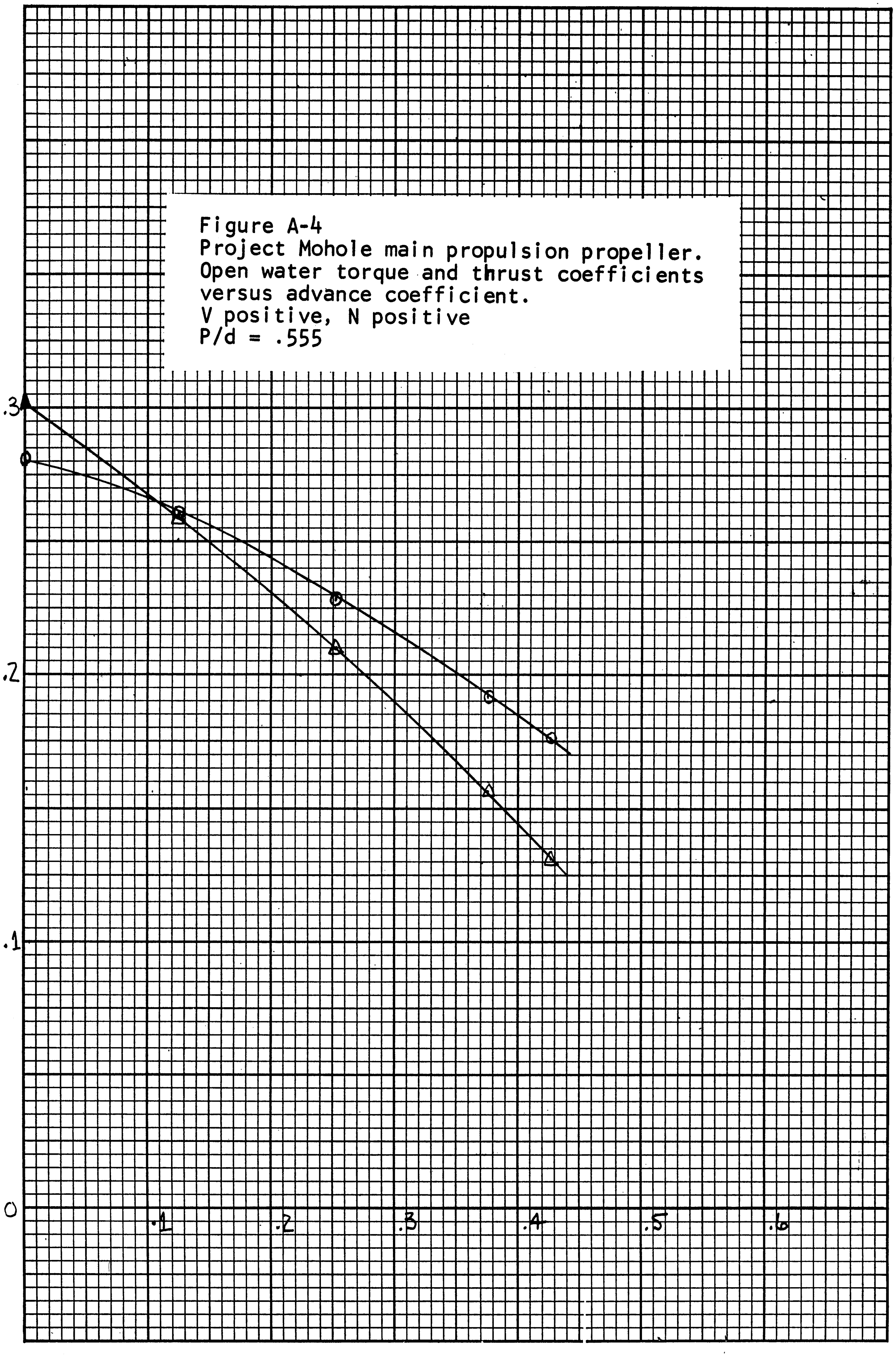


Figure A-4
Project Mohole main propulsion propeller.
Open water torque and thrust coefficients versus advance coefficient.
V positive, N positive
P/d = .555

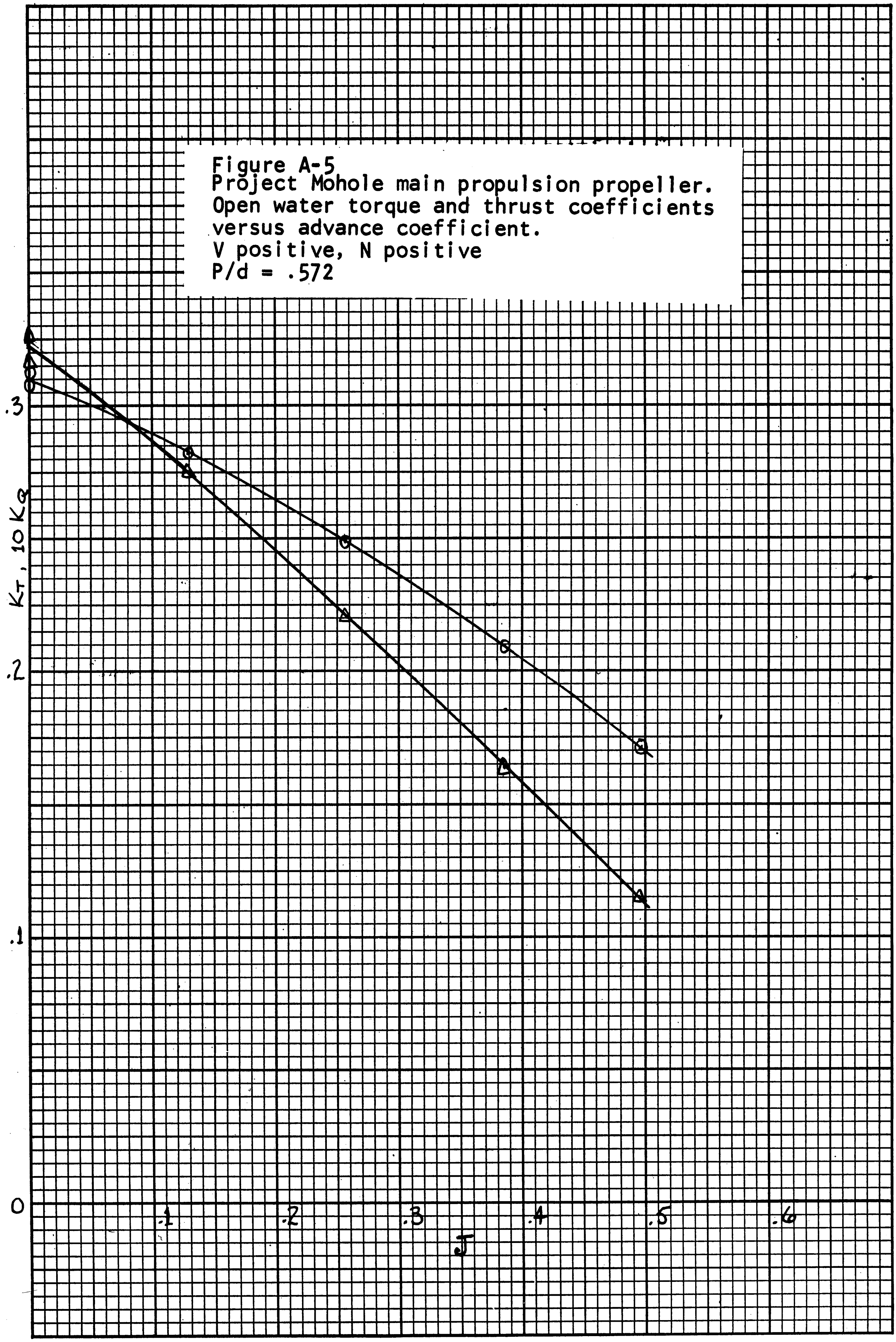
Figure A-5
Project Mohole main propulsion propeller.
Open water torque and thrust coefficients
versus advance coefficient.
V positive, N positive
P/d = .572
$K_T$, $10K_Q$
.3
.2
.1
0
.1
.2
.3
.4
.5
.6
J

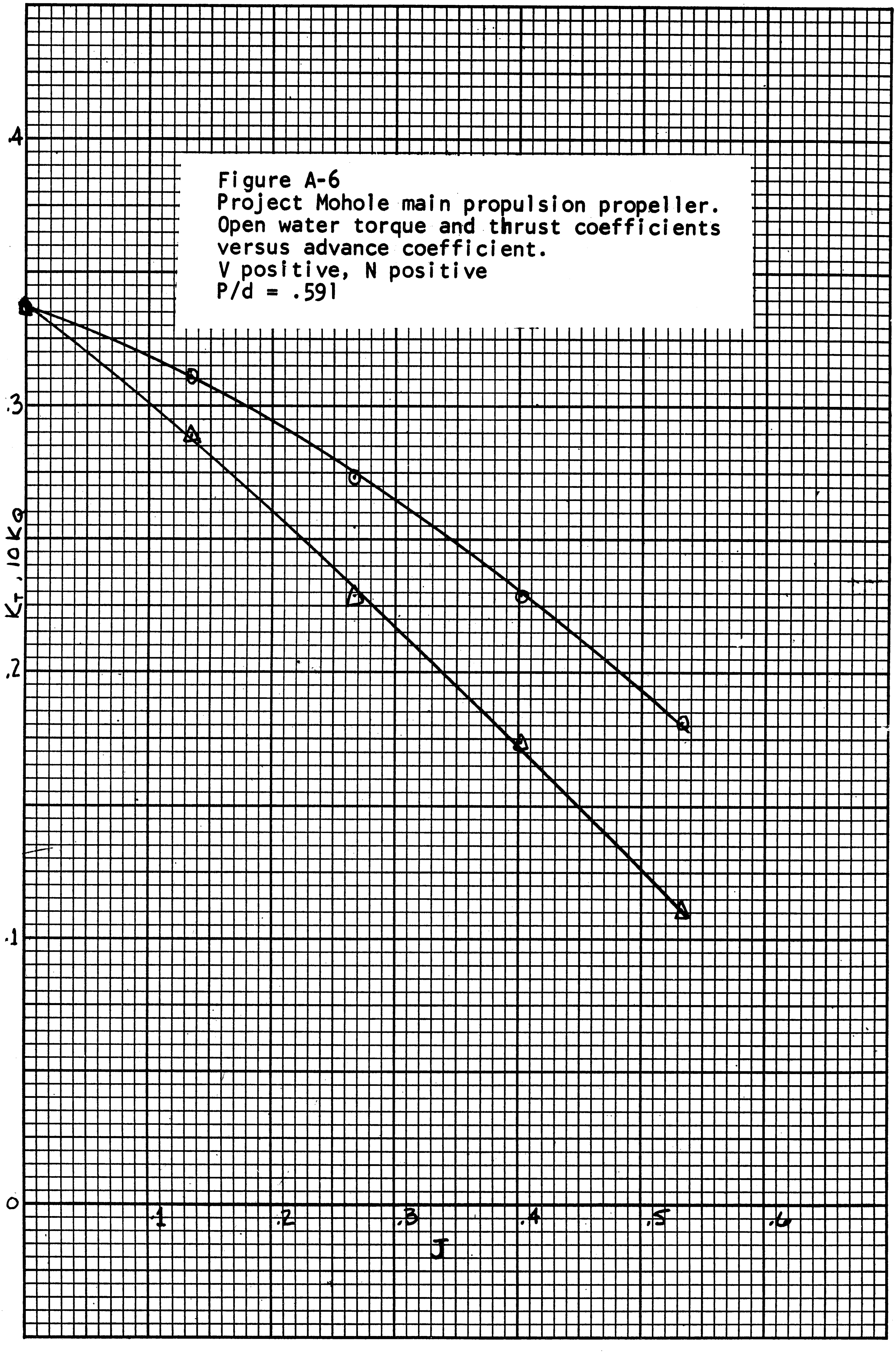


Figure A-6
Project Mohole main propulsion propeller.
Open water torque and thrust coefficients
versus advance coefficient.
V positive, N positive
P/d = .591

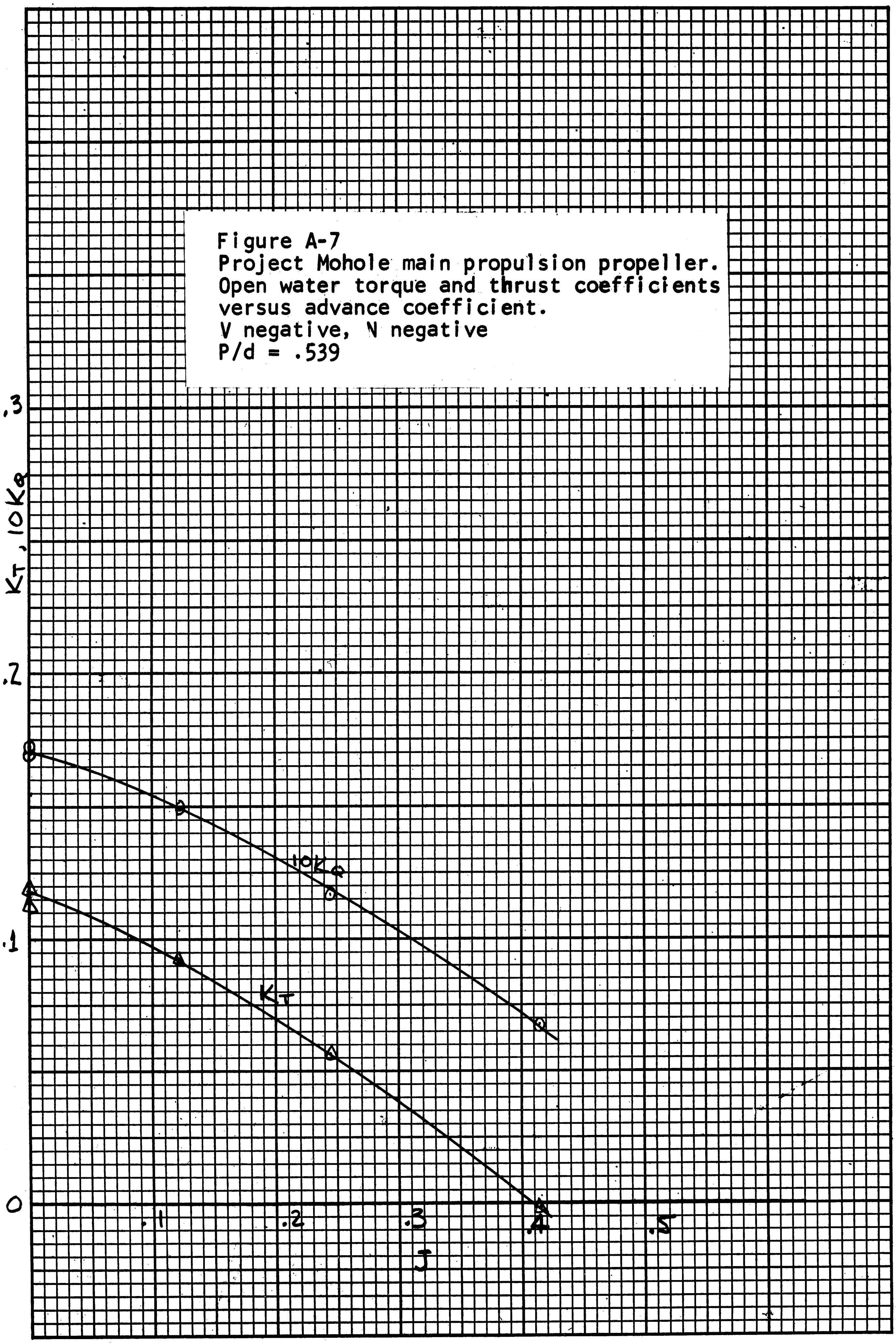


Figure A-7
Project Mohole main propulsion propeller.
Open water torque and thrust coefficients versus advance coefficient.
V negative, N negative
P/d = .539

Figure A-8
Project Mohole main propulsion propellers.
Open water bollard pull torque and thrust coefficients versus P/d.
V positive, N positive

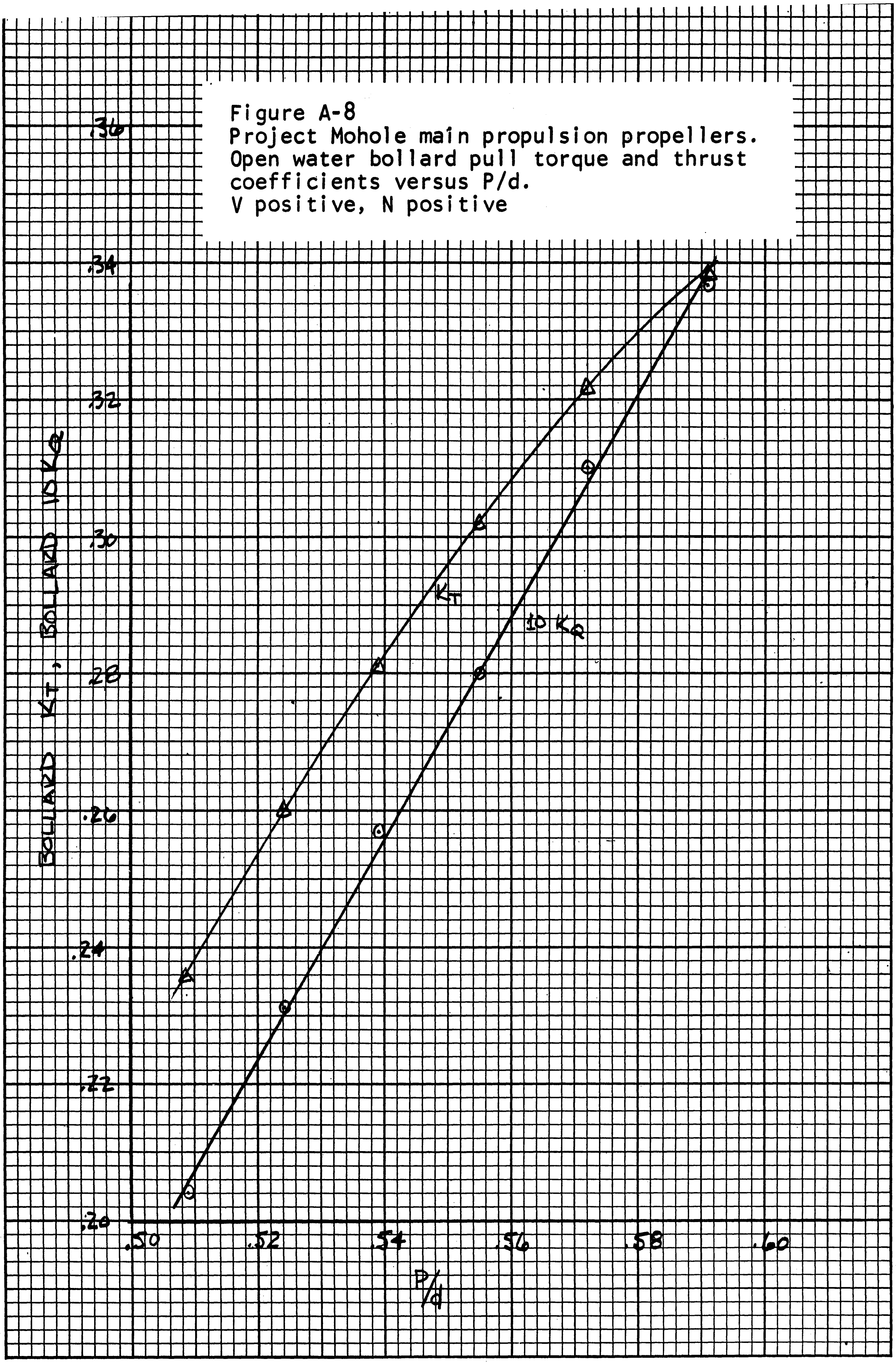

Figure A-9
Project Mohole main propulsion propellers.
Open water bollard pull torque and thrust coefficients versus P/d.
V negative, N negative

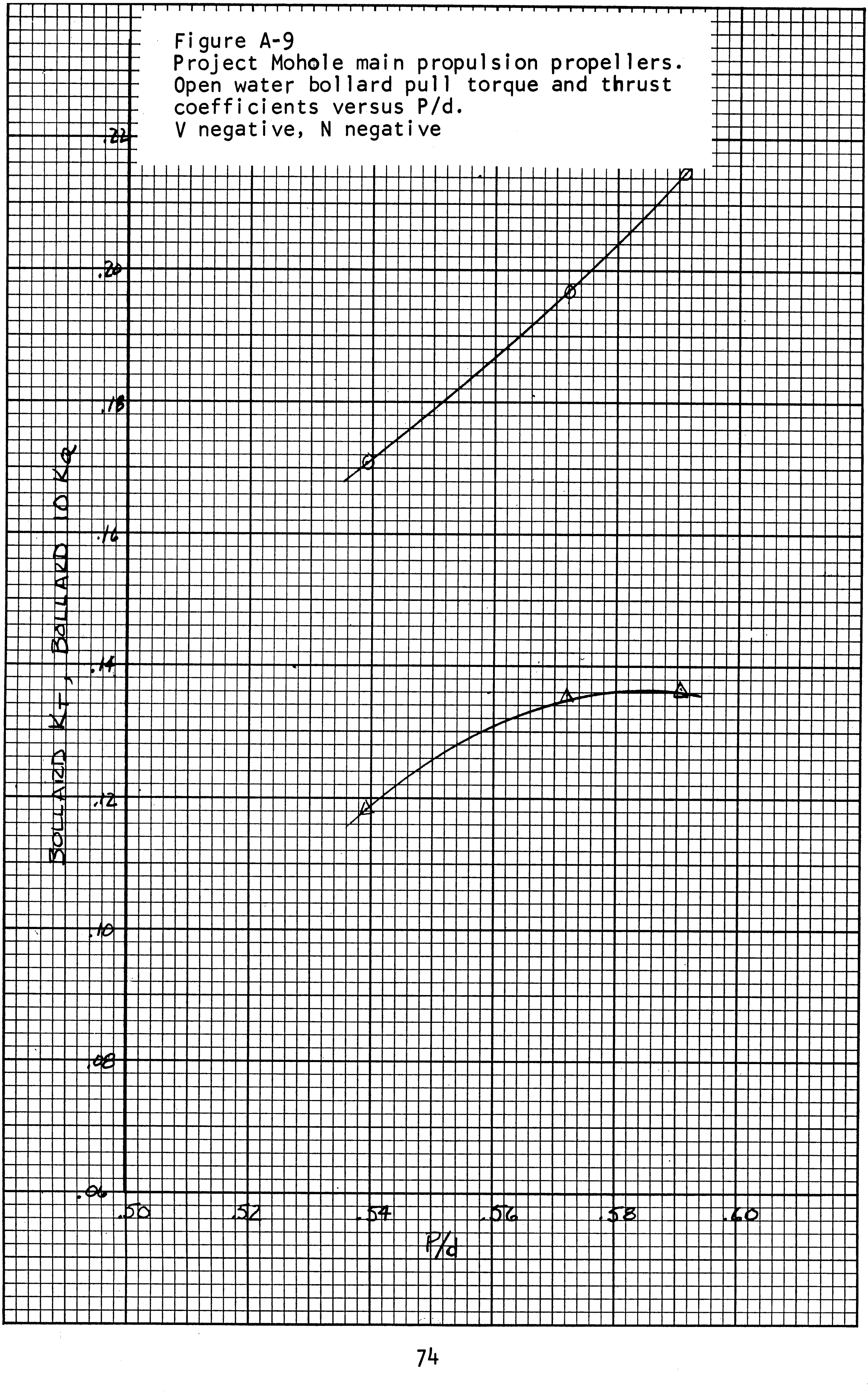

UNIVERSITY OF MICHIGAN
3 9015 02826 0795